THERMODYNAMIC STUDIES ON BIPHENYL AND RELATED SUBSTANCES

by

Kazuya Saito
M.S., Osaka University, 1983

Dissertation
submitted to the Graduate School of
Faculty of Science, Osaka University
in partial fulfilment of the requirements for
the Degree of Doctor of Science

1986

Doctoral Committee:
Professor Hideaki Chihara, Chairman,
Professor Hiroshi Suga,
Professor Fumikazu Kanamaru.

Acknowledgments

I wish to express sincere thanks to Professor Hideaki Chihara and Associate Professor Tooru Atake for their kind guidance, encouragement and stimulative discussions filled with deep insight into science, and also for their critical reading of this manuscript.

I would like to thank Professor Yasutoshi Saito for his heartful encouragement.

Thanks are also due to all the members of Chihara Laboratory and of Saito and Atake Laboratory for their useful discussions and encouragement.

I also thank all my friends for their valuable suggestions and encouragement.

contents

Abstract

Thermodynamic studies were carried out on biphenyl and its related substances; biphenyl, biphenyl-d_{10}, p-terphenyl, p-terphenyl-d_{14}, p-quaterphenyl, 4,4'-difluorobiphenyl, p,p'-biphenol, p-phenylphenol, perfluorobiphenyl, and perchlorobiphenyl. The heat capacities were measured by adiabatic calorimetry between 4 and 300 K and some thermodynamic functions were determined. The special attention was paid to correlating the intramolecular twisting degree(s) of freedom with the macroscopic properties.

Thermodynamic properties of the phase transitions associated with molecular conformation change in p-polyphenylenes (biphenyl, biphenyl-d_{10}, p-terphenyl, p-terphenyl-d_{14}, and p-quaterphenyl) were determined. The values of the transition temperatures and of the entropies of transition were in the order of the molecular size, i.e. biphenyl < p-terphenyl < p-quaterphenyl. The entropies of transition of biphenyl and p-terphenyl are unchanged by deuteration, while the transition temperatures shift to the lower temperatures by deuteration except for the lock-in transition of biphenyl.

The properties of the phase transitions of p-polyphenylenes were compared with one another and discussed in relation to the internal flexibility. The Ising type theory of the transition was developed for

p-terphenyl and compared well with the experimental results.

As the temperature decreased, the heat capacity of biphenyl decreased less steeply than those of p-terphenyl and p-quaterphenyl, and the crossover of the heat capacities occured. The crossover was attributed to the greater twisting flexibility of phenyl rings in biphenyl from lattice dynamics calculation. The role of the incommensurability in the crossover phenomena was pointed out by comparing the low temperature heat capacities of biphenyl with those of 4,4'-difluorobiphenyl.

No phase transition was detected by the heat capacity measurements for 4,4'-difluorobiphenyl, p,p'-biphenol and p-phenylphenol. The reason for the absence of any phase transition was ascertained by comparing their intramolecular potential curves with that of biphenyl, and by calculating the static lattice energies.

The twisting flexibilities of perfluorobiphenyl and perchlorobiphenyl molecules were compared through analyzing their low temperature heat capacities.

Chapter I Introduction

Properties of molecular crystals have been investigated extensively.[1] There are two limiting types of crystalline phase of interest; plastic crystal[2] and liquid crystal.[3] These two phases are regarded as the extreme cases in which melting of crystal takes place in a step-wise manner. In plastic crystals, which generally consist of a globular molecule, the orientational order melts before the translational one. On the other hand, the translational order melts before the orientational in liquid crystals, which generally consist of an elongated rod-like molecule. The studies on the thermodynamic nature and the molecular dynamics of these mesophases give us well-resolved informations on the successive excitation of the two types of motional modes in molecular crystals.

In addition to the rotational and the translational degrees of freedom, a molecule has the internal degree(s) of freedom, e.g. intramolecular vibration, internal rotation, inversion, etc. Generally, since internal degrees of freedom have rather large excitation energy compared with lattice modes, they are hardly perturbed by the intermolecular interactions. However, they will be perturbed strongly and coupled with lattice modes, if their excitation

energies lie in the region of low energy comparable to those of lattice modes. In such molecules as ethane and as biphenyl, strong coupling is expected between the intramolecular twisting motion and lattice modes because the intramolecular barrier hindering rotation is of some $kJ \cdot mol^{-1}$ and the reduced moment of inertia for the twisting motion amounts to a quarter of that of the whole molecule about the molecular figure axis. If a phase is characterized by melting of only a kind of internal degrees of freedom, it may be regarded as the third phase specific to molecular crystals. It is the purpose of this research to study the thermodynamic property of a group of molecular crystals, p-polyphenylenes and their derivatives, in connection with their intramolecular degrees of freedom. The effects of molecular symmetry and nature of intramolecular potential on the crystal packing, on molecular motion, and on heat capacity will be discussed.

The samples we have chosen are biphenyl and its homologous and substituted molecules; biphenyl($C_{12}H_{10}$), biphenyl-d_{10} ($C_{12}D_{10}$), p-terphenyl ($C_{18}H_{14}$), p-terphenyl-d_{14} ($C_{18}D_{14}$), p-quaterphenyl ($C_{24}H_{18}$), 4,4'-difluorobiphenyl ($C_{12}H_8F_2$), p,p'-biphenol ($C_{12}H_{10}O_2$), p-phenylphenol ($C_{12}H_{10}O$), perfluorobiphenyl ($C_{12}F_{10}$), and perchlorobiphenyl ($C_{12}Cl_{10}$). They all have the internal twisting degree(s) of freedom with

rather low excitation energies. The first five molecules belong to a family of compounds so-called p-polyphenylene. They are twisted in the gaseous and the liquid states, and of planar conformation in crystal at room temperature. On cooling, however, they resume a twisted conformation below the phase transition temperature. Although the crystals of the other five compounds do not show any phase transition, studies on them are interesting from the point of view of the relation between thermodynamic properties and the internal twisting degree of freedom.

This thesis is organized as follows. Chapter II describes a simple group theoretical consideration and the classification of the intramolecular twisting modes of the molecules treated in this study. The calculation of the intramolecular potential curves for each twisting motion is also described.

Chapter III describes the results of heat capacity measurements on p-polyphenylenes. The qualitative and the semi-quantitative interpretations of their phase transitions are presented.

Chapter IV describes the lattice dynamics calculation on biphenyl and p-terphenyl crystals. The crossover between their low temperature heat capacities is interpreted.

Chapter V describes the experimental results on 4,4'-difluorobiphenyl, p,p'-biphenol and p-phenylphenol. The calculation of the static lattice energies

of two possible types of crystal structure throws light on the reason why no phase transition occurs in 4,4'-difluorobiphenyl and p,p'-biphenol crystals.

Chapter VI describes the results of heat capacity measurements on perfluorobiphenyl and perchlorobiphenyl. The relative molecular stiffness for the twisting motion is deduced from their low temperature heat capacities.

The summary of this research is given in Chapter VII.

The program for the heat capacity measurements is given in Appendix.

References to Chapter I

1. A. I. Kitaigorodsky, "Molecular Crystals and Molecules", Academic Press, New York and London, 1973.
2. J. N. Sherwood (ed.), "The Plastically Crystalline State", John Wiley & Sons, Ltd., Chichester, 1979.
3. P. G. de Gennes, "The Physics of Liquid Crystals", Clarendon Press, Oxford, 1974.

Chapter II Molecular symmetry and intramolecular potential for twisting motion

II-1 Molecular symmetry and twisting motion

On considering the intramolecular twisting motion, we must pay some attention to molecular symmetries because a molecule has not only one but some degrees of freedom with respect to twisting motion. In biphenyl and biphenyls substituted with structure-less substituents, there exists only one twisting degree of freedom. On the other hand, p-terphenyl has two twisting degrees of freedom and p-quaterphenyl has three such degrees of freedom.

The classification of twisting motions in p-polyphenylenes is given after group theoretical consideration as follows. Suppose that phenyl rings are rigid and the molecular symmetry is of planar molecule, i.e. D_{2h}, for simplicity. Characters of the representations of symmetry D_{2h} using twist angle of each phenyl ring as basis are tabulated in Table II-1. They are reduced to the irreducible representations by using a character table of irreducible representations of D_{2h} (Table II-2). Modes of A_u symmetry are antisymmetric and those of B_{1g} symmetry are symmetric with respect to the center of the molecule. They are schematically shown in Figure II-1 for p-terphenyl and

Table II-1. Representations of D_{2h} by using the twisting angles as a basis set.

	E	C_{2z}	C_{2y}	C_{2x}	I	σ_z	σ_y	σ_x	
biphenyl	2	2	0	0	0	0	-2	-2	A_u+B_{1g}
p-terphenyl	3	3	-1	-1	1	1	-3	-3	A_u+2B_{1g}
p-quaterphenyl	4	4	0	0	0	0	-4	-4	$2A_u+2B_{1g}$

Table II-2. Characters of irreducible representations of D_{2h}.

	E	C_{2z}	C_{2y}	C_{2x}	I	σ_z	σ_y	σ_x
A_g	1	1	1	1	1	1	1	1
B_{1g}	1	1	-1	-1	1	1	-1	-1
B_{2g}	1	-1	1	-1	1	-1	1	-1
B_{3g}	1	-1	-1	1	1	-1	-1	1
A_u	1	1	1	1	-1	-1	-1	-1
B_{1u}	1	1	-1	-1	-1	-1	1	1
B_{2u}	1	-1	1	-1	-1	1	-1	1
B_{3u}	1	-1	-1	1	-1	1	1	-1

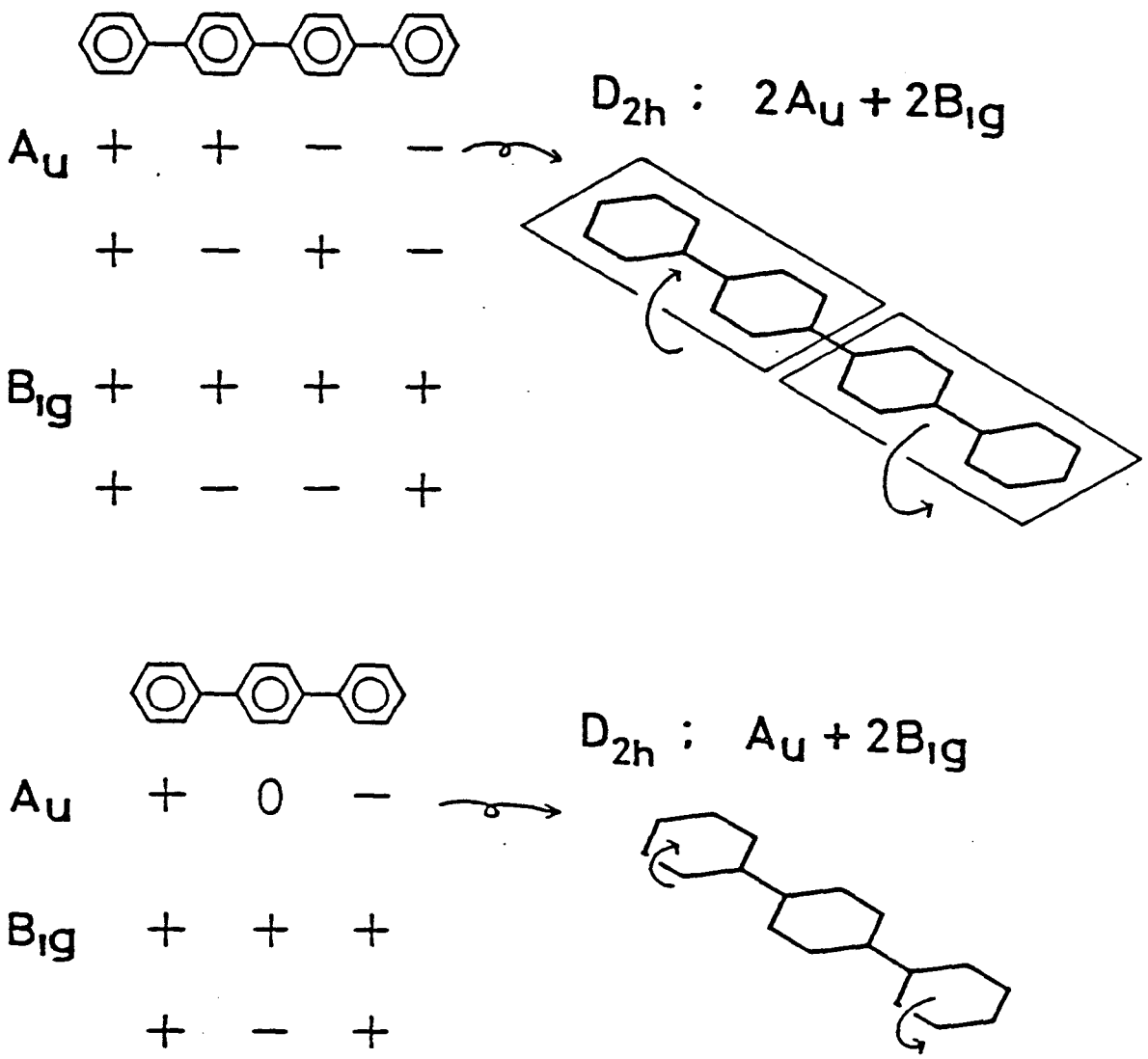

Figure II-1. Possible normal modes of twisting motion, assuming phenyl rings to be rigid and molecular symmetry to be of planar conformation (D_{2h}).

p-quaterphenyl; only one mode in biphenyl is obvious and not shown there. It is natural to expect that a mode with a small number of nodes has a less steep intramolecular potential in the isolated molecule; this will be confirmed in Section II-2 by a simple model calculation. The upper A_u mode of p-quaterphenyl in Figure II-1 should have rather small force constant. On the other hand, the two modes of p-terphenyl must oscillate in a steeper potential because of a large number of pairs of interacting ortho-hydrogens and change in π-conjugation with the twist angle.

The consideration described above is easily extended to the other p-polyphenylenes. p-Polyphenylene consists of an even number of phenyl rings has the A_u mode with only one node; its force constant is small. On the other hand, p-polyphenylene with odd number of phenyl rings does not have such a soft mode.

II-2 Intramolecular potential

It is now in order that we examine the intramolecular potential for each twisting mode. The potential for the twisting mode of the isolated molecule is a resultant of two opposite effects; the π-conjugation favors the planar molecular conformation and the repulsion between ortho atoms prefers the

twisted one. These two effects were treated separately and the overall potential was obtained as the sum of them.

For the calculation of the contribution from π-conjugation, the simple Hückel molecular orbital method was used. All the resonance integrals between two adjacent carbon atoms was the same as β, but it was assumed to change as $\beta\cos\theta$[1] between the central C-C bond, where θ is the twisting angle between the adjacent two phenyl rings. The effects of substituents (F or OH) were taken into account by using the following parameters; the Coulomb integral, $\alpha+3\beta$ (F), $\alpha+2\beta$ (O) where α is the Coulomb integral of carbon atom, and the resonance integral 0.7β (C-F)and 0.8β (C-O).[2] By comparing the result of Hückel method with those of experiments of benzene, the magnitude of β was deduced to be -89 $kJ\cdot mol^{-1}$.[3]

In calculation of the contribution from the ortho atom repulsion, the molecular geometry was fixed: The phenyl rings were assumed as a normal hexagon with the C-C bond length of 0.140 nm. The bond length of the central C-C combining the two phenyl rings was 0.150 nm and the length of C-H bond was 0.110 nm. The atom-atom potential of Buckingham type was summed over all atom pairs within the molecule except for the pairs whose interatomic distances do not depend on the twisting angle. The atom-atom parameters of Williams[4] were used for the calculation. They are tabulated in Table

Table II-3. Atom-atom parameters used for calculation.

$$E = -A/r^6 + B \cdot \exp(-C \cdot r).$$

	A / kJ·mol^{-1}·Å^6	B / kJ·mol^{-1}	C / Å^{-1}
C-C	$2.380 \cdot 10^3$	$3.499 \cdot 10^5$	3.60
C-H	$5.230 \cdot 10^2$	$3.668 \cdot 10^4$	3.67
H-H	$1.140 \cdot 10^2$	$1.110 \cdot 10^4$	3.74

II-3.

The intramolecular potential curves calculated as a function of the twist angle about the central C-C bond are shown in Figure II-2 for the p-polyphenylenes. For biphenyl, the location of the minimum at about 40° and the potential barrier height of order 10 $kJ \cdot mol^{-1}$ at $\theta = 0°$ are in good agreement with the results of experiments.[5-8] Two twisting modes of p-terphenyl degenerate in this treatment, but both the modes show steeper gradient than for biphenyl. The upper A_u mode of p-quaterphenyl in Figure II-2, which is the upper A_u mode shown in Figure II-1, shows a potential curve quite similar to that of biphenyl. This similarity comes from the fact that there are the same number of nodes for the two modes. On the other hand, the potential curve of the lower A_u mode of p-quaterphenyl is the steepest in the three substances. Thus, the consideration in Section II-1 is now clarified; the harder mode appears in larger molecules as the number of phenyl rings within a molecule increases. However, there still exists the "soft" mode similar to that of biphenyl if the number of phenyl rings is even.

Figure II-3 shows the calculated potential curves for biphenyl, 4,4'-difluorobiphenyl, and p,p'-biphenol. The location of the minimum at about 40° for 4,4'-difluorobiphenyl is also in good agreement with the experiment.[9] In spite of the difference in

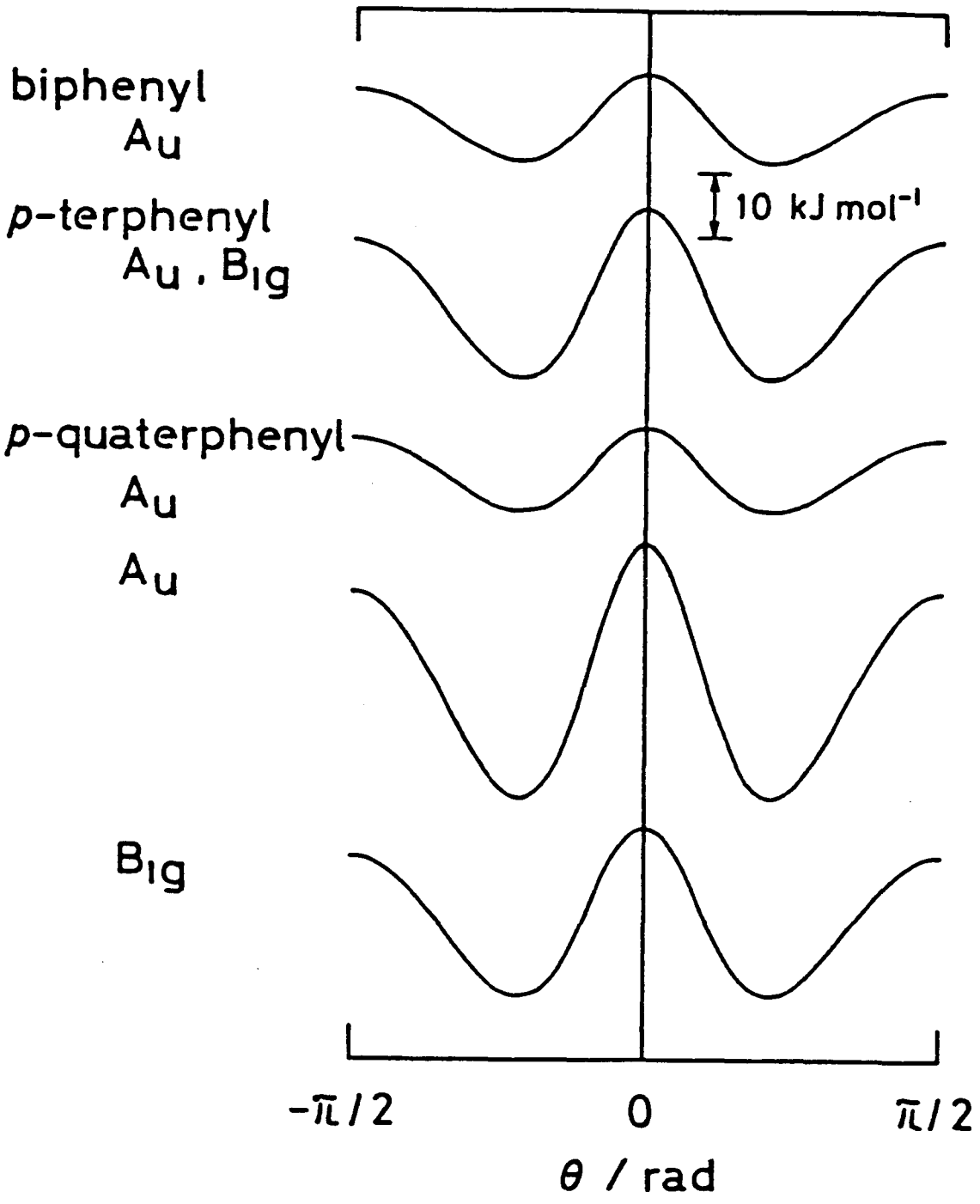

Figure II-2. Calculated intramolecular potential curves for the twisting modes of biphenyl, p-terphenyl and p-quaterphenyl.

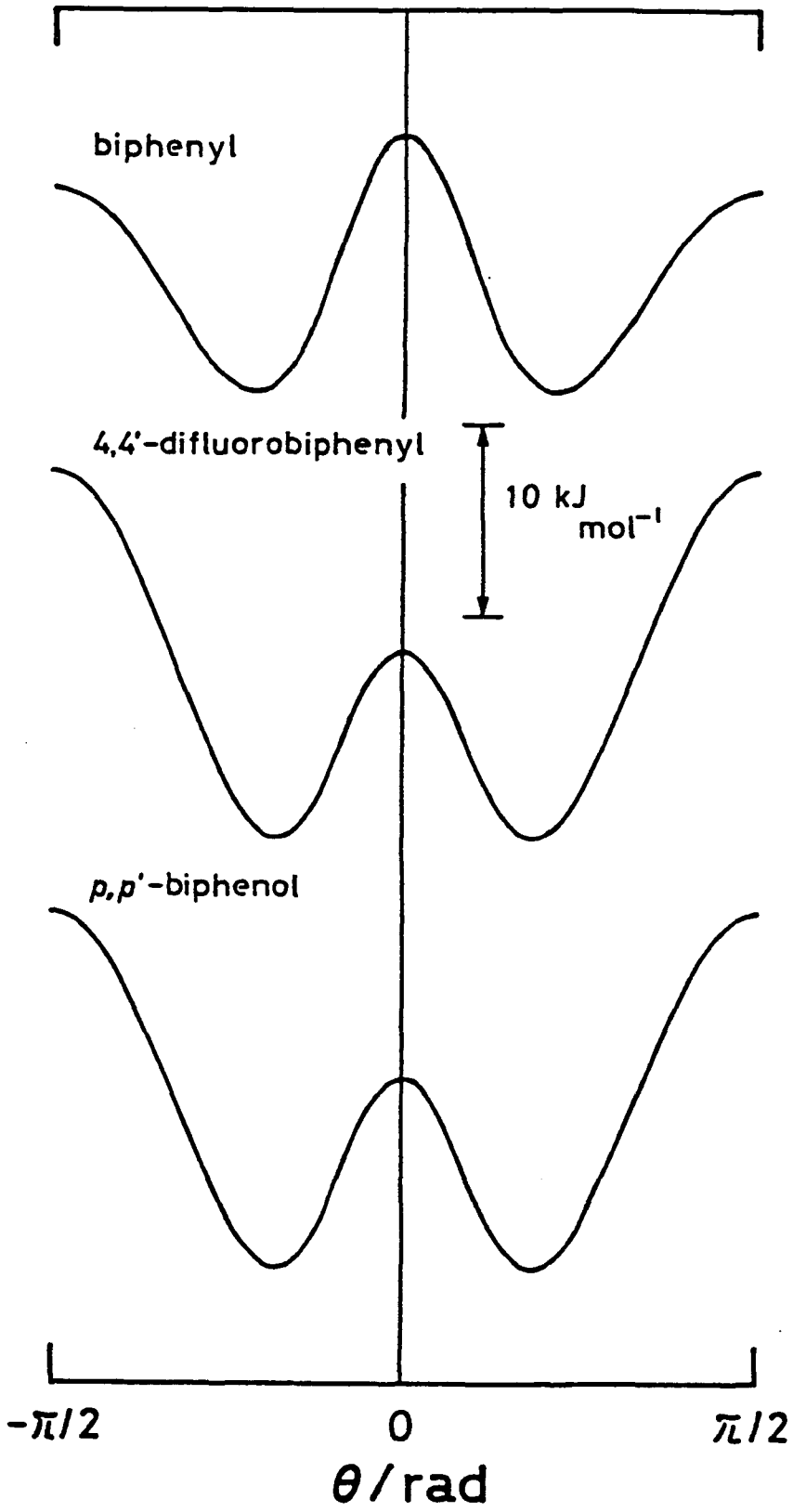

Figure II-3. Calculated intramolecular potential curves of biphenyl, 4,4'-difluorobiphenyl and p,p'-biphenol.

substitutents, potential curves for 4,4'-difluorobiphenyl and p,p'-biphenol are similar to each other; the barrier height at $\theta = 0^{\circ}$ is somewhat lower by about 3 $kJ \cdot mol^{-1}$ than biphenyl, and the barrier at $\theta = 90^{\circ}$ is enhanced by about 8 $kJ \cdot mol^{-1}$. Therefore, the difference in the properties between 4,4'-difluorobiphenyl and p,p'-biphenol crystals should come from the difference in the intermolecular interaction.

Calculation was not carried out for p-phenylphenol because the effects of the OH substitution could be deduced from the calculated potential curve for p,p'-biphenol: The OH substitution lowers the barrier at $\theta = 0^{\circ}$ by a few $kJ \cdot mol^{-1}$ and it softens the twisting force constant of the isolated molecule.

No such calculation was made either for perfluorobiphenyl and for perchlorobiphenyl. The substitutions not only at para and meta positions but also at ortho positions make the intramolecular potential very steep and the barrier hindering the rotation very high because the interatomic distance between ortho atoms is much shorter compared with the van der Waals radii at all twisting angles (Figure II-4). The motion of phenyl rings, therefore, must be strictly confined within the vicinity of the potential minimum below room temperature. These make it irksome to examine the intramolecular potential curves in the whole range of the twisting angle. The feature of the potential curve in the vicinity of the bottom will be deduced in

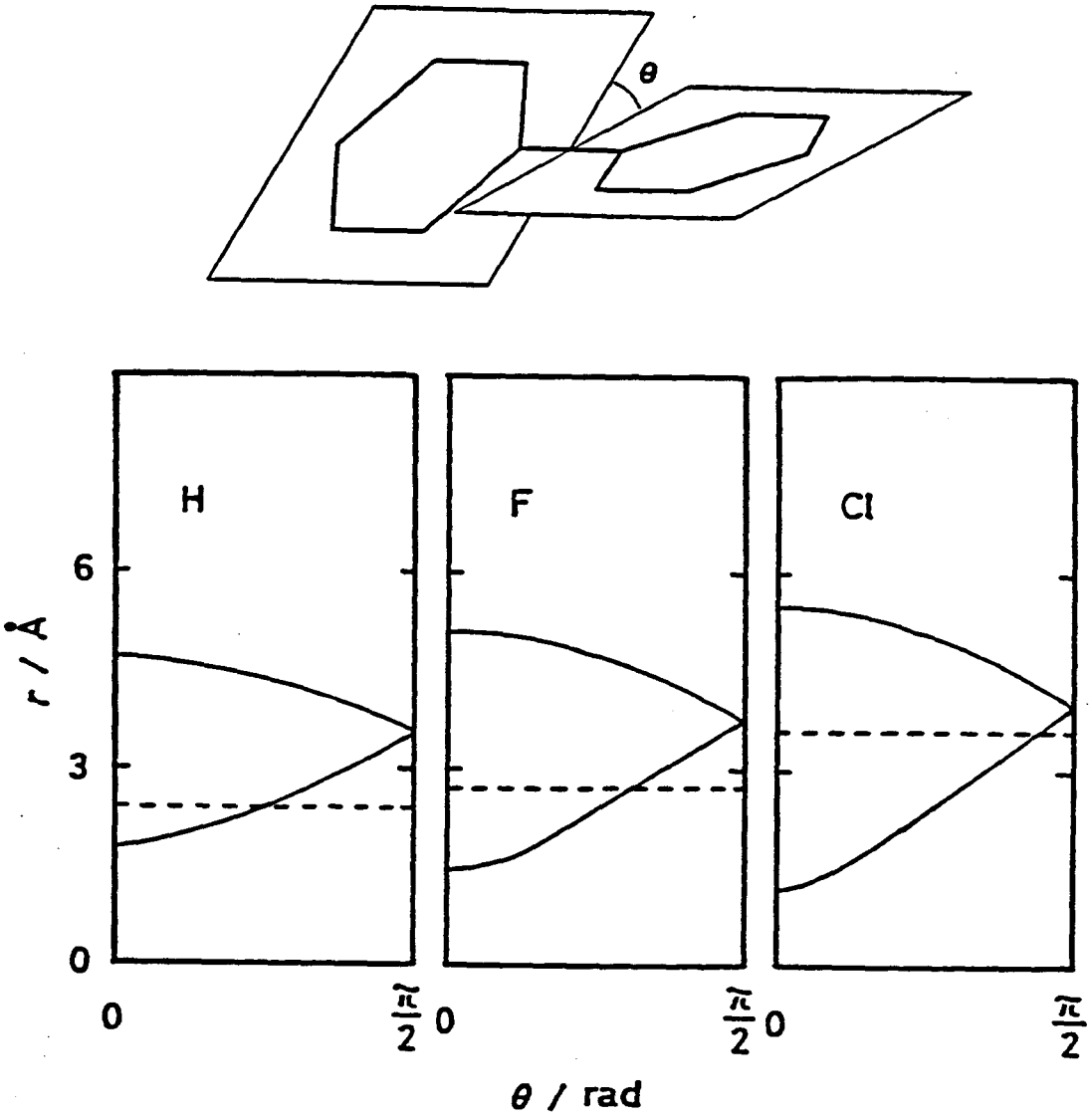

Figure II-4. Interatomic distance between ortho atoms as a function of the twist angle. Broken line shows van der Waals radii of ortho atoms.

Chapter VI from their heat capacities at low temperatures.

References to Chapter II

1. R. G. Parr and B. J. Crawford Jr., J. Chem. Phys., 16(1948), 526.
2. Y. Hirota, "Bunshikidouhou-nyumon", Baifukan, Tokyo, (1969).
3. G. M. Barrow, "Physical Chemistry" (4th ed.), McGraw-Hill Inc., New York, (1979).
4. D. E. Williams, J. Chem. Phys., 47(1967), 4680.
5. O. Bastiansen, Acta Chem. Scand., 3(1949), 408.
6. H. Suzuki, Bull. Chem. Soc. Jpn., 32(1959), 1340.
7. A. J. Grumadas and P. Poshkus, J. Chem. Soc. Faraday II, 75(1979), 1398.
8. A. J. Grumadas, D. P. Poshkus and A. V. Kiselev, J. Chem. Soc. Faraday II, 78(1982), 2013.
9. O. Bastiansen and L. Smedvik, Acta Chem. Scand., 8(1954), 1593.

Chapter III Phase transitions in p-polyphenylenes

III-1 Survey of previous studies

All the crystals of biphenyl, p-terphenyl and p-quaterphenyl at room temperature belong to the space group $P2_1/a$ (C_{2h}^5), in which two molecules are in the unit cell[1-12] (Figure III-1). The symmetry elements of this space group are identity $\{E|0\}$, inversion $\{I|0\}$, two-fold screw axis $\{C_2^b|\vec{a}/2+\vec{b}/2\}$ and glide plane $\{\sigma^{ac}|\vec{a}/2+\vec{b}/2\}$, and the point group is 2/m. Molecules occupy inversion sites, which fact implies a statistically planar molecular conformation, in contrast to the twisted conformation in the gaseous and the liquid states.[13-20]

Baudour et al.[11] refined the structure for p-terphenyl at room temperature under the assumption that the room temperature phase was a disordered one. They obtained a double peaked probability function for the central phenyl ring. This strongly suggests an order-disorder nature of the transition. For biphenyl and p-quaterphenyl, such kind of analysis has not been made so far.

The structures of low temperature phases of these compounds are not exactly the same but similar to each other; the molecules are twisted. In the case of biphenyl, the structure of the low temperature phase

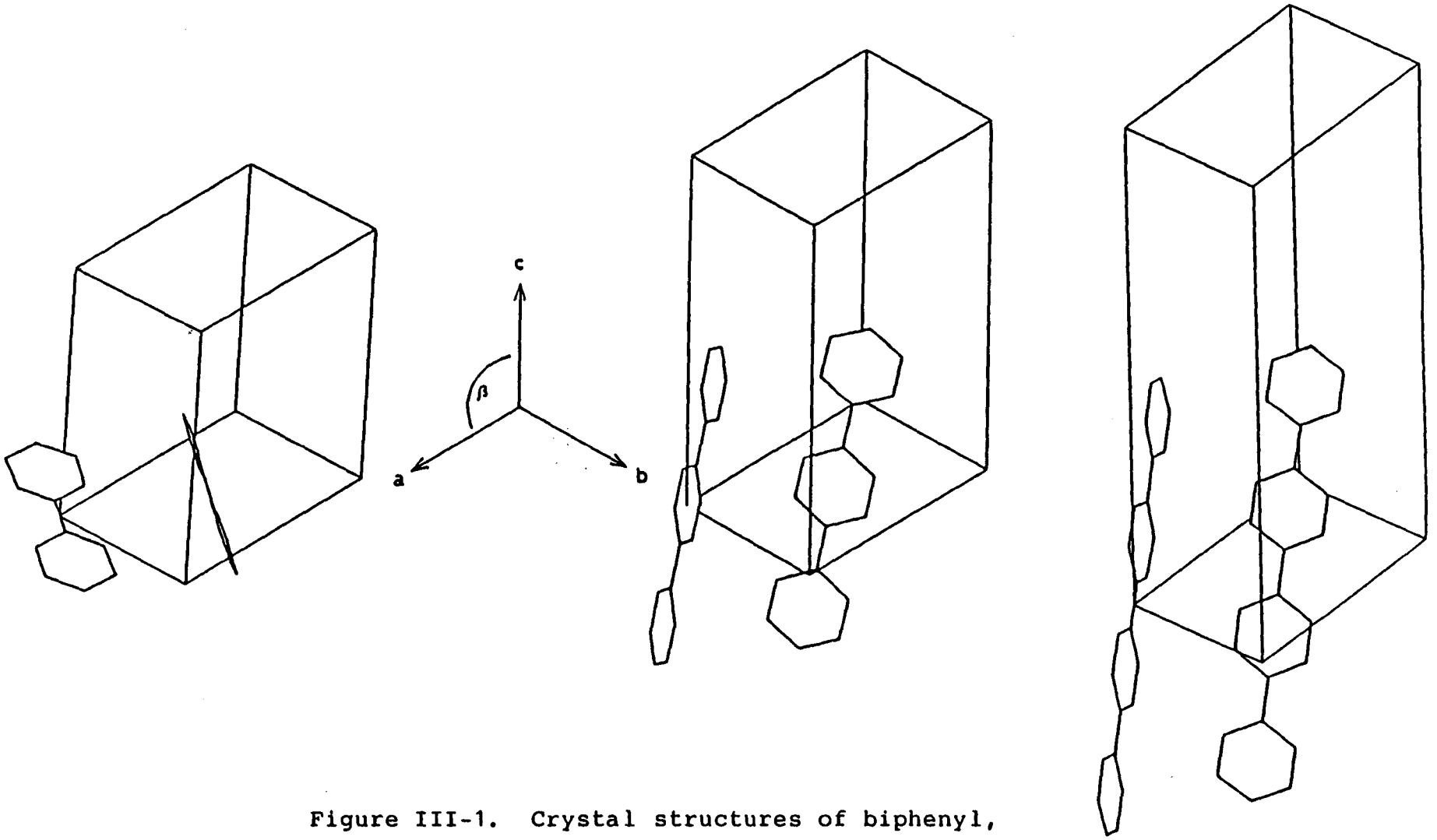

Figure III-1. Crystal structures of biphenyl, p-terphenyl and p-quaterphenyl at room temperature.

between about 17 and 40 K is incommensurate in the directions of both the a and b axes[21] and is classified to the five dimensional Bravais lattice of $P^{P2/m}_{cmm}$.[22] The mean, approximate structure was obtained neglecting satellite reflections and was classified to Pa.[23] An incommensurate-commensurate transition (so-called lock-in transition) in the direction of the a axis occurs at about 17 K.[21] However, the crystal is still incommensurate along the b axis below the lock-in transition for the a axis. The structure of this phase was determined to be of the super-space group $P^{P2_1/a}_{11}$[24,25] by using the neutron diffraction technique.[26] The essential aspect of the incommensurate modulation within a sinusoidal approximation was a torsion around the long molecular axis with an amplitude of 5.5° for each phenyl ring, the maximum deformation angle being 11°.

On the other hand, the structures of the low temperature phase of both p-terphenyl and p-quaterphenyl belong to the space group $P\bar{1}$ and the adjacent phenyl rings in the molecule are twisted alternately[27,28] (Figure III-2). In this structure, the symmetry elements except identity and inversion are lost due to twisting of molecules, it is considered as the super structure with the cell constants 2a, 2b and c in terms of those of the room temperature phase. However, reflecting the molecular symmetry, the

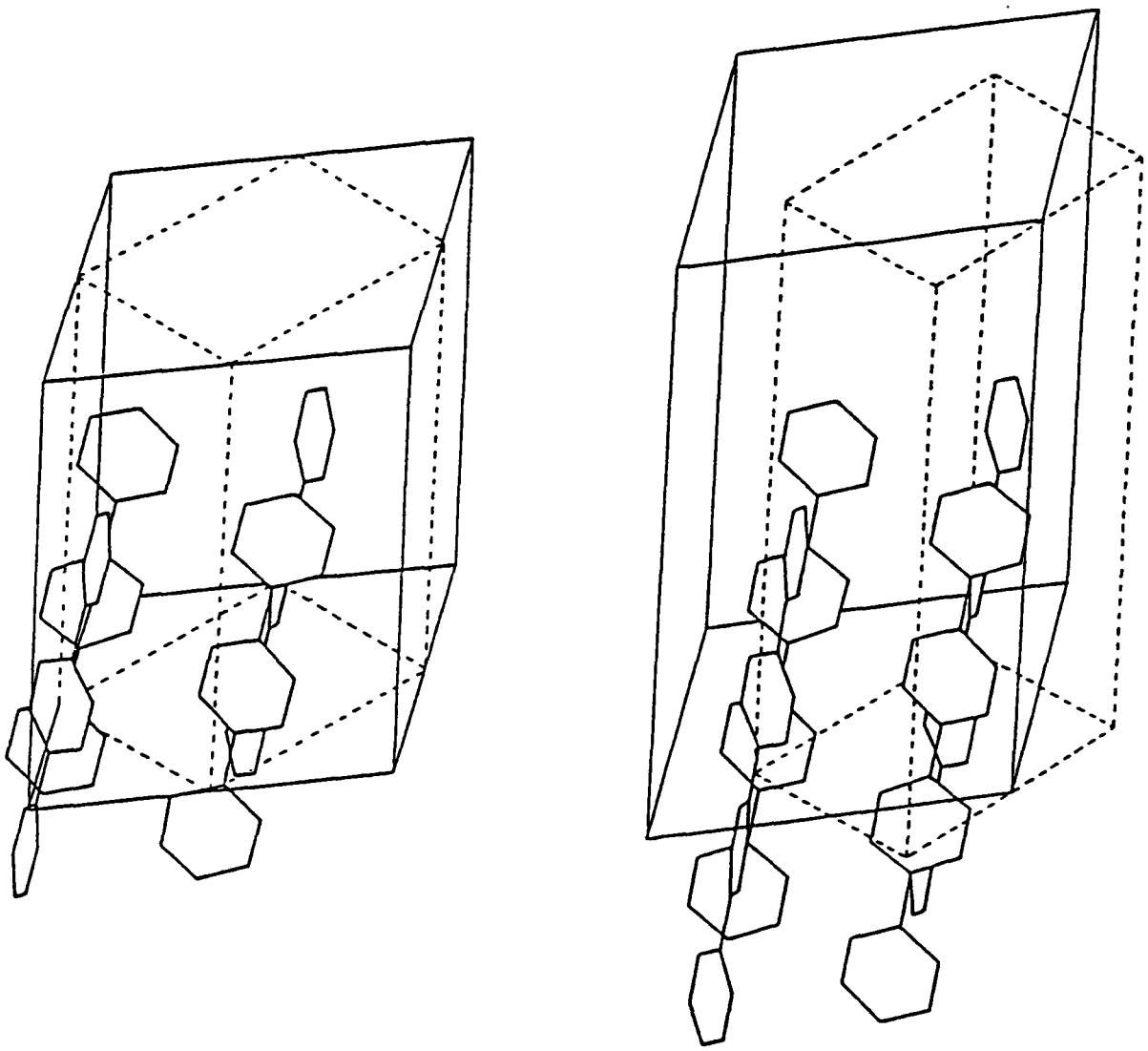

Figure III-2. Crystal structures of the low temperature phases of p-terphenyl and p-quaterphenyl. Broken lines represents the unit cell of the room temperature phase.

molecules of p-terphenyl are at the inversion site but this is not the case in p-quaterphenyl.

Concerning the phase transitions in biphenyl, it is important to note that the soft modes have been found in optical[29-31] and neutron[32] experiments, which fact is compatible with displacive nature of the transition. The softening occurs at the general point (x^*, y^*, 0) near the B(0, 1/2, 0) point in the reciprocal space and the new phase is of two dimensionally incommensurate structure.

Dworkin and Cailleau[33] reported the results of heat capacity measurements of biphenyl from 10 K to 50 K, in which they could not detect any anomaly in the heat capacity curve. On the other hand, Cullick and Gerkin[34] found the temperature halt in the cooling and the heating curves at 42 K, which strongly suggested that the transition is of the first-order. However, other authors[29-32,35-40] have reported by using other experimental techniques that the transition at about 40 K is of higher order.

The lock-in transition at about 17 K has been revealed to be of the first-order transition by optical[36] and neutron[21] techniques. More conclusive evidence of first-order nature of the transition is the co-existence of two phases observed in neutron experiments.[21] Theoretical considerations[41-43] within the Landau's phenomenology support the first-order nature of the transition. However, no abrupt

change was observed in the Brillouin scattering experiments,[39] and in the electronic spectra of the molecule.[38] The lock-in transition in the direction of the b axis has not been observed so far down to 1.4 K.[44]

Plakida et al.[45] proposed an internal-soft-mode mechanism for the twist transition at about 40 K based on the self-consistent phonon calculations, in which renormalized phonon frequencies were calculated in the lowest order self-consistent approximation. The phonon frequency of the twisting-acoustic coupled mode near the B point showed $(T-T_c)^{1/2}$ behavior, which is compatible with the experimental observation.[32] The approach made by Busing[46] is essentially static; lattice energies were calculated using the temperature-dependent atom-atom potentials. The instability of the planar molecular conformation was found at about 94 K, which is much higher than the actual transition temperature. The group theoretical considerations made by Ishibashi,[41] and Toledano and Toledano[43] showed that the phase transition at about 40 K (normal-incommensurate) is of higher-order, and that the lock-in transition is of the first-order.

Dynamics in the incommensurate phases of biphenyl were investigated by using some experimental techniques. The dispersion of the phason and the amplitudon branches were determined by neutron[32,47]

and Brillouin[39] scattering experiments. The damping of the phason branch near the zone center was relatively small compared with other incommensurate substances. NMR results by Liu and Conradi[48] showed the existence of the slow process ($\tau \simeq 10^3$ s at 4.2 K) in the incommensurate phase. They proposed the term, "incommensurate glass", in biphenyl in the lowest temperature region from their experimental result.

It is worthwhile to note that the pressure dependence of the transition temperature is negative.[40] This clearly shows that the transition is connected with a subtle balance between intra- and intermolecular interaction. While the intermolecular interaction, which prefers a planar conformation, is enhanced by the compression, the intramolecular interaction is not. This causes the fact that the transition temperature decreases as pressure increases.

In contrast to the case of biphenyl, no soft mode has been observed in p-terphenyl[49-51] and p-quaterphenyl.[51] Cailleau and Dworkin[52] and Chang[53] measured heat capacities of p-terphenyl and found the λ-shaped anomaly at about 194 K with the entropy of transition $\Delta_{trs}S = 1.80\ J \cdot K^{-1} \cdot mol^{-1}$.[53] Many experimental results by using optical,[40,49-51] EPR[54] and the other techniques[55-60] showed this transition being continuous. Critical exponents of p-terphenyl for some physical quantities have been reported as follows; $\alpha = 0.049$,[52] $\beta = 0.15$,[61] and

ν = 0.12.[62] These values correspond to the two dimensional Ising model. The two dimensionality of the interaction was supported by neutron[63,64] and NMR[65] experiments. Dynamical aspects of the transition were investigated by using neutron,[32,63,64,66] NMR,[65,67-70] and other[71] techniques and the critical phenomenon, the critical slowing down of the order parameter fluctuation, was found,[32,65-69] which implies order-disorder nature of the transition. The pressure dependence[40] of the transition temperature is negative as in biphenyl. The theoretical work on the phase transition was reported by Ramdas and Thomas.[72] They interpreted the transition by calculating static lattice energies and predicted the existence of the other unknown phase.

Only a few reports have been published on the phase transition of p-quaterphenyl. Bolton and Prasad[51] reported from their Raman study that there was a transition at about 230 K and that it was continuous. Toudic et al.[69] found the behavior of critical slowing down by NMR, which is very similar to p-terphenyl.[65,67-69]

III-2 Heat capacities of p-polyphenylenes

III-2-1 Biphenyl and biphenyl-d_{10}

Experimental

Commercially available biphenyl (Nakarai Chemicals, Ltd.) and biphenyl-d_{10} (Merck Sharp & Dohme Canada Ltd., nominal isotope purity of 99 per cent) were purified by fractional sublimation in vacuum at room temperature. In order to avoid the possible formation of metastable phases and/or the less-crystallinity, the sublimed specimens were melted under the helium atmosphere (10^5 Pa) and cooled gradually down to room temperature for recrystallization. Chemical purity of both the specimens were better than 99.9 moles per cent as confirmed by gas-chromatography, and the isotope purity of the bipheny-d_{10} specimen was 99 per cent as determined by the high resolution NMR spectra of the CCl_4 solutions.

The powdered specimens were loaded into the calorimeter vessel and sealed off after addition of a small amount of helium gas for heat exchange (3 kPa and 7 kPa at room temperature, respectively). The contribution of helium gas to the total heat capacity was negligibly small. The weights of samples of biphenyl and biphenyl-d_{10} used for calorimetry were 17.950 g (0.11640 mol) and 14.9825 g (0.091206 mol), respectively, after buoyancy correction. The

contribution of the samples to the total heat capacity including that of the calorimeter vessel was larger than 70 per cent below 20 K. It decreased to 46 per cent in biphenyl (41 per cent in biphenyl-d_{10}) at 100 K as the temperature increased, however, it increased again to 59 per cent (57 per cent) at 300 K.

The apparatus for calorimetry was the same as described elsewhere.[73] The operation was automated by the micro computer (model PC-9801, NEC Corp.); the program coded in BASIC language is given in Appendix. A platinum resistance thermometer (model 8164, Leeds & Northrup Co.) and a germanium resistance thermometer (model CR-1000, CryoCal Inc.) were used. Their temperature scales are based on IPTS-68, helium gas thermometry, and the 1958 ^{4}He scale.[74,75]

The measurements using the ordinary calorimeter vessel missed the lock-in transition in biphenyl at 16.8 K because of lack of sensitivity of a platinum resistance thermometer (0.01 Ω/K at 17 K), small amount of the powdered sample in the vessel and less precise adiabatic control. To search for lock-in transitions of biphenyl, therefore, a new calorimeter vessel was constructed. The following aspects were considered; (1) the sensitivity of the thermometer, (2) amount of the sample and its packing in the vessel, (3) the utility of the thermometer through the entire temperature region (3 - 20 K), (4) the attainment of

the true adiabatic condition, and (5) the unknown behavior of the helium gas for heat exchange in the vessel below 4 K.

The sectional plan of the new calorimeter vessel is shown in Figure III-3. In order to load a sufficient amount of the sample and to avoid the introduction of helium gas for heat exchange into the vessel, the purified biphenyl specimen was loaded and melted under the helium atmosphere (10^5 Pa) in the vessel. The vessel was then evacuated and sealed off without any addition of helium gas. The sample thus loaded weighed 24.957 g (0.16184 mol) in vacuum.

A germanium resistance thermometer (model N2D, SI Inc.) with commercial calibration was used. The calibration were based on the 1962 ^{3}He vapor pressure scale below 3.2 K and on the 1965 Provisional Helium Acoustic Scale between 2 and 20 K. The accuracy of the calibration was stated to be better than 0.005 K below 5 K and better than 0.01 K between 5 and 20 K. The 35 calibration points were fitted to the equation,

$$\ln(R/\Omega) = \sum_{i=1}^{9} A_i \{\ln(T/K)\}^{i-2}$$

using the SALS system.[76] The residuals of the fit are shown in Figure III-4. Since the main purpose of the measurements using this vessel is not a determination of absolute values of heat capacities but a search for lock-in transitions, it is not serious that the residuals show rather large deviations from the

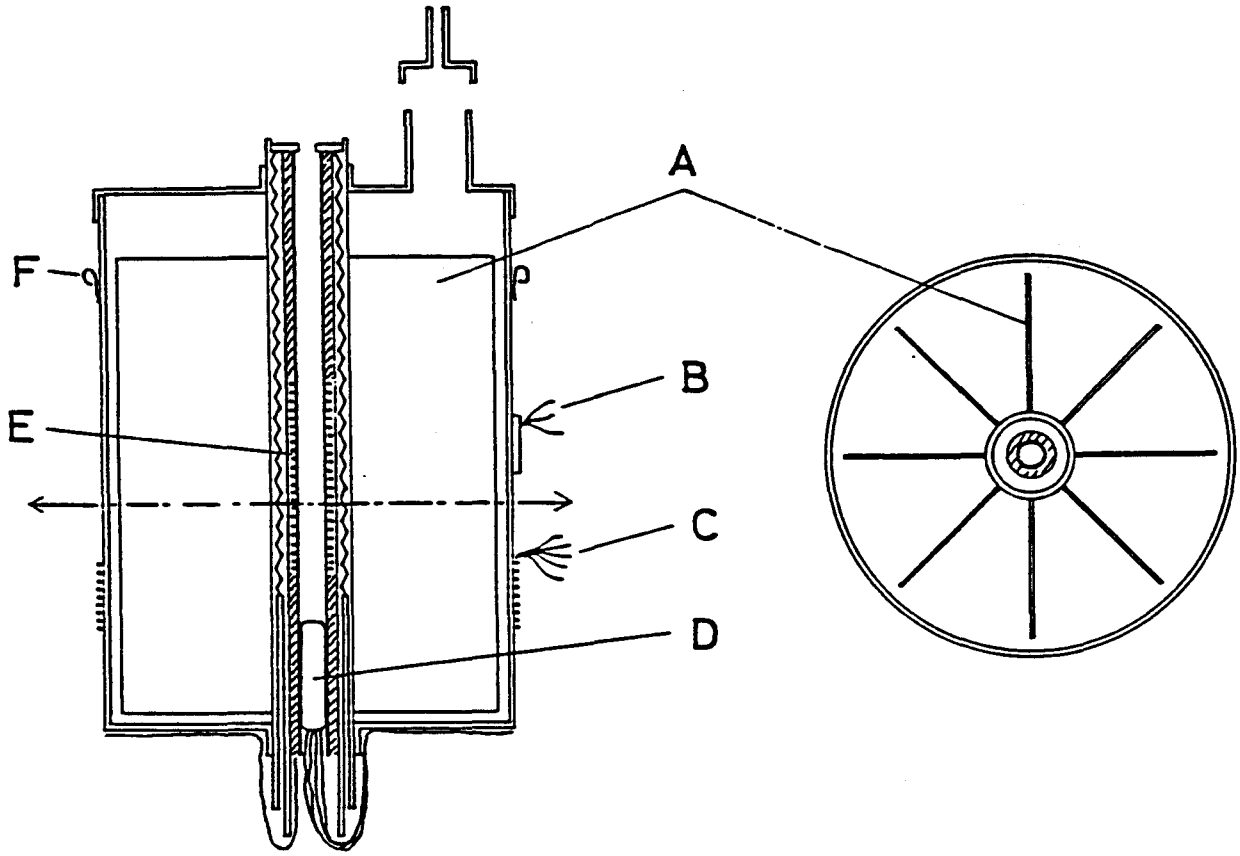

Figure III-3. Sectional plan of the newly constructed calorimeter vessel. A, eight vanes to assist in thermal uniformity; B, Au+0.07%Fe vs chromel thermocouples for adiabatic control (diameter 0.1 mm); C, lead wires (diameter 0.1 mm); D, germanium thermometer (model N2D, SI Inc.); E, heater (KARMA); F, hooks for hanging.

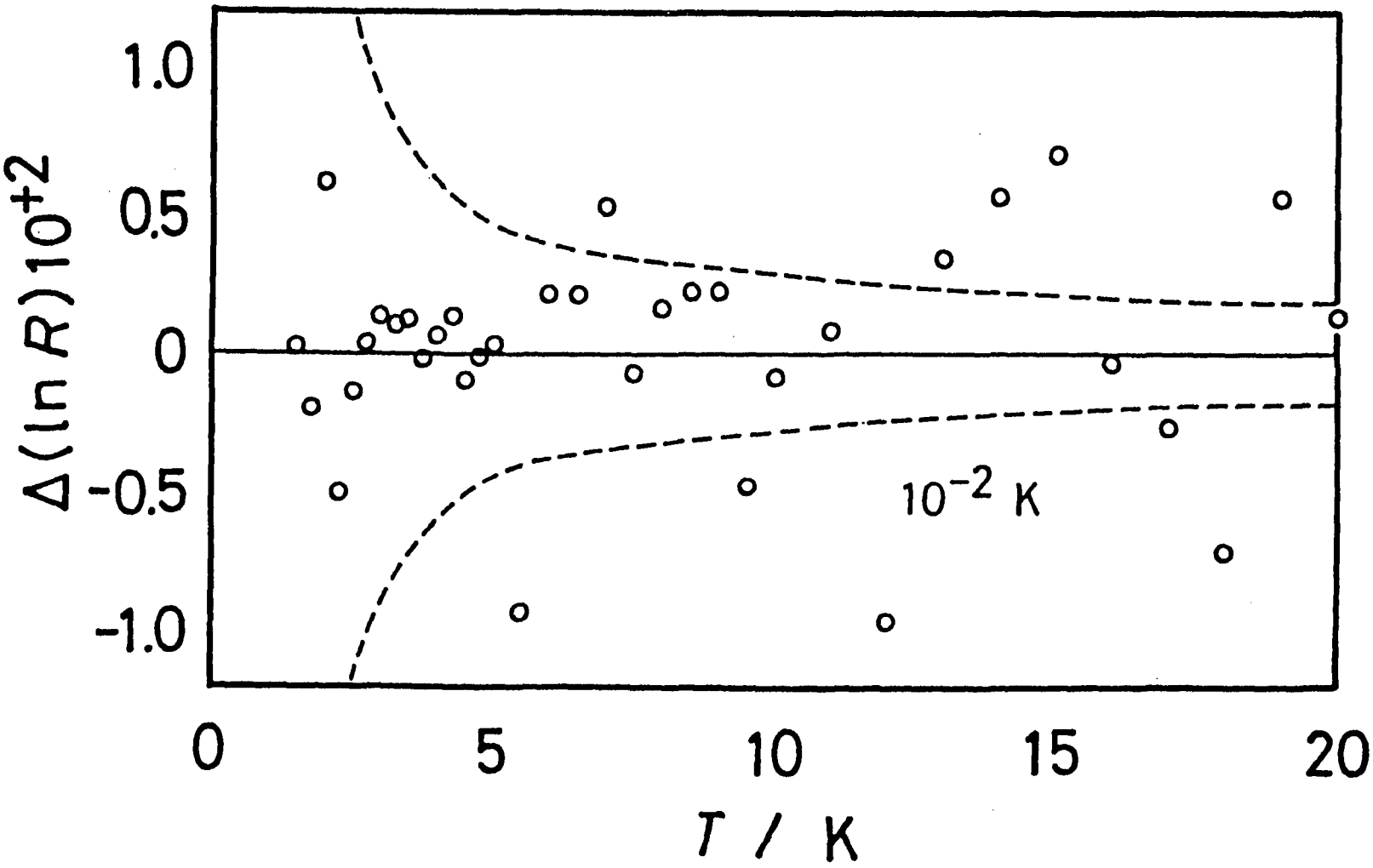

Figure III-4. Residuals of the least squares fit of the germanium thermometer.

equation.

The Au+0.07%Fe vs chromel thermocouple (0.1 mm in diameter) was used for a detection of the temperature difference between the vessel and the adiabatic shield wall in order to improve an adiabatic condition. The sensitivity of this thermocouple in the temperature region between 3 and 20 K is as large as ten times of that of chromel vs constantan thermocouple which has been attached to the ordinary vessel.

The new vessel thus constructed has a weight of 39.72 g excluding the sample and has a capacity of 25.06 cm^3. Apparatus except the vessel and operation of experiments were the same as described above. The sample contributed by more than 85 per cent to the total heat capacity through the entire temperature region and sufficiently accurate data were obtained.

Results and Discussion

The molar heat capacities measured with the ordinary vessel are shown in Figure III-5 and tabulated in Tables III-1 and III-2 in chronological order. The heat capacities of biphenyl obtained with the new vessel are not shown there because they are compatible with data obtained using the ordinary vessel except for the lock-in transition region. The temperature increment of each measurement can be deduced from the adjacent mean temperatures, which is small enough to

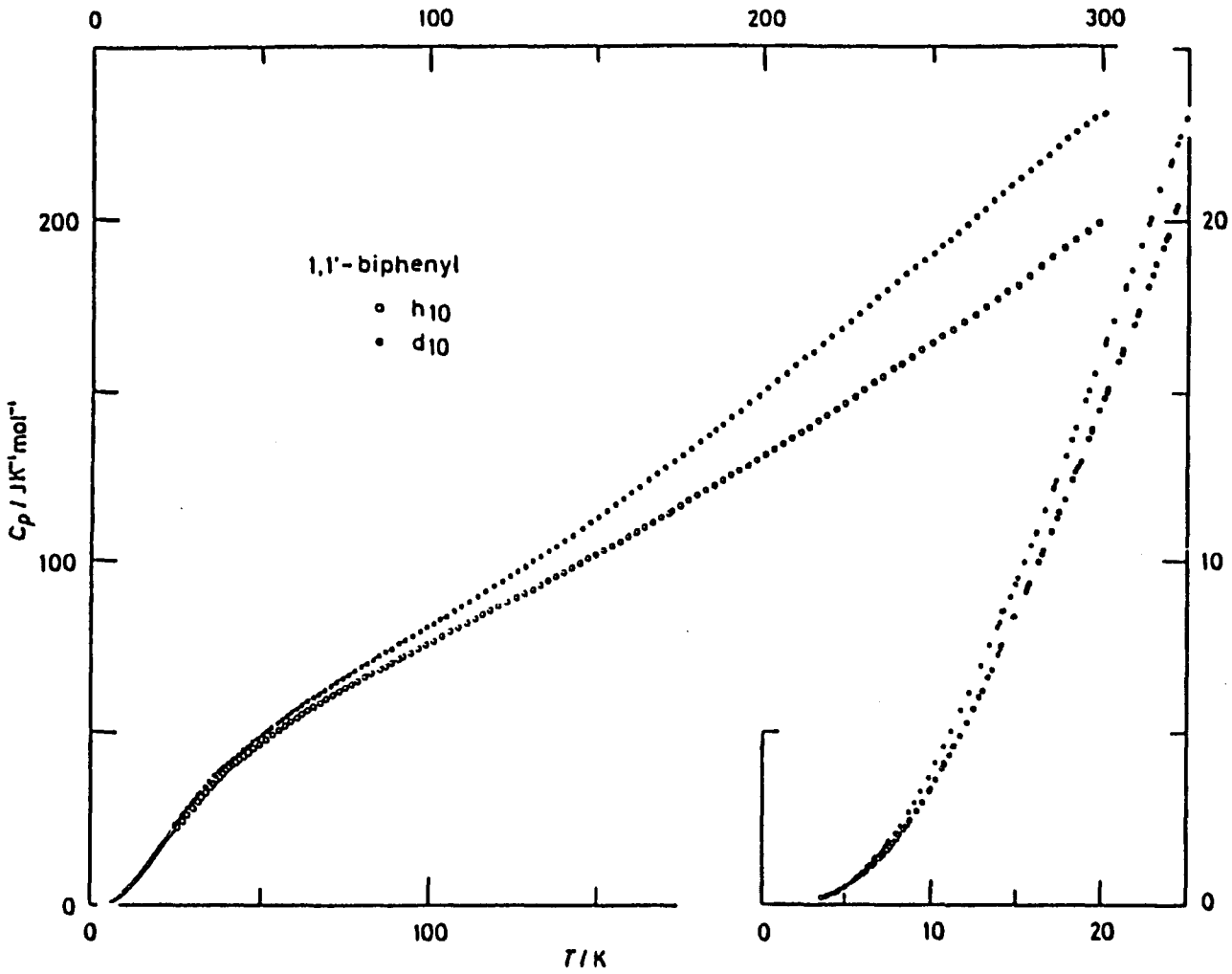

Figure III-5. Measured molar heat capacities of biphenyl (open circle) and biphenyl-d_{10} (filled circle).

Table III-1. Measured molar heat capacities of biphenyl.

T/K	C_p/J·K^{-1}·mol^{-1}	T/K	C_p/J·K^{-1}·mol^{-1}	T/K	C_p/J·K^{-1}·mol^{-1}	T/K	C_p/J·K^{-1}·mol^{-1}
Series 1		42.337	40.691	62.242	54.872	116.069	83.81
22.893	18.498	43.774	41.726	63.980	55.960	118.417	85.02
24.316	20.354	45.209	42.796	65.786	57.054	120.787	86.27
25.736	22.177	46.657	43.873	67.659	58.173	123.163	87.46
27.178	24.002	48.132	45.001	69.539	59.296	125.545	88.57
28.647	25.811	49.761	46.248	71.436	60.404	Series 9	
30.247	27.775	51.634	47.623	73.337	61.494	125.967	88.83
31.954	29.863	53.566	49.046	75.222	62.533	128.403	90.10
33.668	31.832	55.431	50.339	77.095	63.584	130.793	91.31
35.376	33.756	57.249	51.595	79.014	64.643	133.193	92.61
37.060	35.623	59.027	52.793	81.032	65.744	135.581	93.89
38.805	37.448	60.796	53.955	Series 6		137.956	95.12
40.600	39.223	Series 3		81.058	65.822	140.338	96.38
42.342	40.689	53.638	49.090	83.133	66.814	142.722	97.65
44.038	41.926	55.451	50.339	85.160	67.875	145.104	98.95
45.727	43.163	57.233	51.572	87.174	68.926	Series 10	
47.417	44.462	58.994	52.774	89.175	70.030	145.258	98.98
49.116	45.762	Series 4		91.166	71.037	147.664	100.27
Series 2		32.858	30.907	Series 7		150.066	101.53
22.785	18.352	34.022	32.239	90.405	70.652	152.484	102.87
24.241	20.261	35.130	33.482	92.570	71.807	154.930	104.28
25.688	22.112	36.186	34.659	94.766	72.905	157.365	105.64
27.155	23.970	37.201	35.775	96.977	74.063	159.778	106.99
28.656	25.823	38.188	36.823	99.242	75.199	162.177	108.36
30.218	27.742	39.152	37.800	101.587	76.333	Series 11	
31.859	29.728	40.094	38.742	103.975	77.585	164.585	109.71
33.493	31.639	41.031	39.619	106.377	79.00	167.013	111.11
35.048	33.404	41.958	40.392	108.758	80.24	169.462	112.48
36.532	35.041	42.883	41.110	Series 8		171.923	113.92
37.987	36.602	43.819	41.768	109.158	80.23	Series 12	
39.447	38.091	Series 5		111.493	81.49	172.821	114.52
40.897	39.493	60.493	53.726	113.761	82.67	175.305	116.04

Table III-1. (continued).

T/K	C_p/J·K^{-1}·mol^{-1}	T/K	C_p/J·K^{-1}·mol^{-1}	T/K	C_p/J·K^{-1}·mol^{-1}	T/K	C_p/J·K^{-1}·mol^{-1}
177.802	117.47	259.302	170.31	20.975	15.890	9.952	3.318
180.351	119.03	262.477	172.48	21.823	16.994	10.817	4.063
182.902	120.59	265.702	174.70	22.662	18.114	11.679	4.866
185.448	122.04	268.951	177.13	23.496	19.233	12.517	5.664
187.977	123.48	272.209	179.02	Series 18		13.353	6.568
190.505	125.01	275.491	181.90	4.051	0.300	Series 21	
193.048	126.59	278.789	184.12	4.487	0.403	9.882	3.267
195.582	128.11	282.116	186.40	4.969	0.530	10.642	3.917
198.157	129.76	285.481	188.86	5.491	0.703	11.384	4.585
Series 13		288.879	191.59	6.045	0.907	12.110	5.269
200.711	131.29	292.304	193.93	6.592	1.148	12.836	6.012
203.324	132.93	295.734	196.43	7.122	1.388	13.576	6.779
205.969	134.57	299.152	198.94	Series 19		Series 22	
208.606	136.40	Series 15		3.855	0.243	14.132	7.486
211.190	137.97	14.181	7.506	4.224	0.332	14.838	8.318
213.768	139.64	14.921	8.365	4.605	0.422	15.648	9.264
216.395	141.29	15.769	9.351	5.004	0.538	16.532	10.340
219.046	143.00	Series 16		5.447	0.678	17.451	11.490
221.726	144.89	18.738	12.984	5.935	0.857	18.406	12.691
224.437	146.63	19.828	14.495	6.461	1.078	19.370	13.942
227.180	148.49	20.927	15.903	7.003	1.334	20.302	15.111
229.946	150.29	22.009	17.314	Series 20		21.189	16.245
232.738	152.46	23.106	18.750	4.443	0.382	22.041	17.365
235.561	154.13	Series 17		4.884	0.503	22.865	18.432
238.415	156.46	14.089	7.394	5.331	0.640	23.667	19.481
Series 14		14.847	8.290	5.788	0.801	Series 23	
241.166	157.68	15.635	9.197	6.263	0.984	3.594	0.222
244.021	159.79	16.467	10.202	6.737	1.199	3.907	0.288
246.985	161.76	17.331	11.308	7.243	1.453	4.164	0.327
250.014	163.80	18.232	12.452	7.805	1.775	4.520	0.401
253.076	165.93	19.183	13.661	8.434	2.174	4.909	0.503
256.170	168.01	20.109	14.847	9.146	2.676	5.312	0.631

Table III-1. (continued).

T/K	C_p/J·K^{-1}·mol^{-1}	T/K	C_p/J·K^{-1}·mol^{-1}	T/K	C_p/J·K^{-1}·mol^{-1}	T/K	C_p/J·K^{-1}·mol^{-1}
5.719	0.774	5.940	0.851	11.114	4.319	18.551	12.850
6.131	0.938	6.311	1.005	12.057	5.234	19.372	13.893
6.556	1.154	6.709	1.183	13.030	6.186	20.239	15.012
7.005	1.323	7.137	1.396	13.963	7.228	21.130	16.142
7.477	1.570	7.610	1.658	Series 25		22.019	17.289
8.013	1.899	8.154	1.992	15.546	9.121	22.906	18.441
8.621	2.295	8.781	2.414	16.272	9.995	23.783	19.592
Series 24		9.479	2.935	17.008	10.912		
5.591	0.723	10.256	3.582	17.765	11.850		

Table III-2. Measured molar heat capacities of biphenyl-d_{10}.

T/K	C_p/J·K^{-1}·mol^{-1}	T/K	C_p/J·K^{-1}·mol^{-1}	T/K	C_p/J·K^{-1}·mol^{-1}	T/K	C_p/J·K^{-1}·mol^{-1}
Series 1		40.426	40.834	38.494	39.301	76.372	66.332
14.941	9.338	41.923	42.078	39.917	40.418	78.199	67.437
16.085	10.829	43.522	43.443	41.343	41.609	80.042	68.519
17.257	12.386	45.131	44.683	42.791	42.816	Series 12	
18.406	13.966	46.755	46.143	44.341	44.107	81.881	69.585
19.512	15.541	Series 4		45.893	45.365	83.696	70.671
20.594	17.066	51.881	50.168	47.696	46.855	85.545	71.809
21.667	18.525	53.845	51.676	49.490	48.339	87.430	72.921
22.751	20.009	Series 5		51.029	49.508	89.316	74.023
23.957	21.672	14.030	8.176	52.579	50.682	91.283	75.576
25.248	23.413	15.059	9.498	54.145	51.874	93.330	76.398
26.505	25.110	16.099	10.815	55.731	52.994	Series 13	
Series 2		17.135	12.212	Series 8		95.531	77.631
14.300	8.517	18.151	13.618	42.004	42.123	97.715	79.008
15.427	9.965	19.163	15.055	43.448	43.359	99.693	80.172
16.614	11.510	20.201	16.533	44.883	44.524	101.641	81.277
17.805	13.134	21.280	18.000	Series 9		103.560	82.446
18.978	14.766	Series 6		49.147	48.027	Series 14	
Series 3		24.853	22.884	50.593	49.169	105.551	83.31
20.115	16.388	26.135	24.580	52.051	50.266	107.649	84.85
21.346	18.081	27.440	26.341	53.522	51.394	109.839	86.13
22.651	19.859	28.735	27.998	54.988	52.473	112.150	87.52
23.905	21.583	30.008	29.638	Series 10		114.479	88.96
25.115	23.255	Series 7		57.837	54.468	116.843	90.40
26.297	24.818	24.306	22.156	59.272	55.537	119.242	91.84
27.458	26.366	25.557	23.853	60.773	56.506	Series 15	
28.609	28.837	26.778	25.484	62.347	57.523	119.385	91.84
29.757	29.309	27.979	27.032	64.109	58.715	121.776	93.31
30.907	30.770	29.169	28.557	65.772	59.766	124.127	94.87
32.159	32.349	30.355	30.089	Series 11		126.433	96.37
33.511	33.996	31.641	31.705	67.388	60.783	128.730	97.78
34.873	35.596	33.027	33.428	69.151	61.922	131.043	99.31
36.252	37.204	34.435	35.102	70.929	63.054	133.373	100.79
37.656	38.589	35.820	36.747	72.722	64.146	135.784	102.49
39.047	39.713	37.157	38.180	74.536	65.233		

Table III-2. (continued).

T/K	C_p/J·K^{-1}·mol^{-1}	T/K	C_p/J·K^{-1}·mol^{-1}	T/K	C_p/J·K^{-1}·mol^{-1}	T/K	C_p/J·K^{-1}·mol^{-1}
Series 16		Series 19		287.072	220.42	7.487	1.844
138.255	103.90	215.032	161.03	289.823	222.71	8.182	2.320
140.721	105.65	217.802	163.40	292.552	224.83	8.973	2.930
143.182	107.31	220.539	165.70	295.261	226.67	9.801	3.659
145.699	109.13	223.245	167.81	297.977	228.75	10.708	4.542
148.272	110.80	225.916	169.96	300.694	230.12	11.749	5.620
150.817	112.55	228.628	172.12	Series 24		12.923	6.917
153.333	114.33	231.386	174.52	3.957	0.325	Series 28	
155.845	116.15	Series 20		4.404	0.440	8.645	2.666
158.354	117.95	234.113	176.86	4.897	0.573	9.341	3.266
160.851	119.79	236.838	178.98	5.325	0.729	10.221	4.074
Series 17		239.563	181.41	5.742	0.888	11.161	5.000
163.372	121.44	242.289	183.71	6.161	1.112	12.228	6.127
165.924	123.38	245.018	185.88	6.593	1.321	13.420	7.502
168.470	125.25	247.753	187.77	7.069	1.563	Series 29	
171.020	127.05	250.492	189.94	Series 25		14.633	8.949
173.573	129.13	Series 21		3.878	0.281	15.822	10.478
176.127	130.83	250.333	189.96	4.216	0.365	17.081	12.132
178.680	132.93	252.701	192.09	4.546	0.461	18.403	13.960
181.235	134.98	255.136	193.72	4.876	0.551	19.712	15.727
183.789	137.01	257.647	195.88	5.211	0.689	20.977	17.666
Series 18		260.234	198.24	5.548	0.831	22.167	19.251
187.954	139.97	262.876	200.36	5.900	0.982	23.303	20.845
190.615	142.25	Series 22		6.278	1.151	24.455	22.378
193.312	144.28	265.537	202.39	6.698	1.353	Series 30	
196.036	146.52	268.192	204.50	7.186	1.641	45.568	45.068
198.714	148.64	270.847	206.81	Series 26		46.944	46.194
201.429	150.87	273.540	208.95	6.739	1.420	48.351	47.355
204.182	153.03	Series 23		7.249	1.675	49.791	48.520
206.898	155.19	276.230	211.29	7.859	2.060	51.271	49.648
209.607	157.37	278.924	213.55	Series 27		52.727	50.808
212.302	159.50	281.623	215.71	6.401	1.200	54.208	51.882
		284.329	218.02	6.902	1.461		

ignore the curvature correction in comparison with the experimental precision. After each energy input was over, thermal equilibrium within the calorimeter vessel was attained in 1 min below 10 K, in 5 min at 50 K, and 15 min above 100 K in the measurements on both biphenyl and biphenyl-d_{10}. Situation was the same also in the measurements on biphenyl using the newly constructed vessel. Concerning thermal equilibration, no anomalous behavior was observed in the transition regions contrary to the observation of Dworkin and Cailleau,[33] and also in the lowest temperature region.[48]

The comparison with the data on biphenyl reported by Huffman et al.[77] is shown in Figure III-6. Although our results are systematically larger by 0.4 per cent than theirs, two sets of data are in satisfactory agreement within experimental accuracy.

Some thermodynamic functions calculated from the present data are given in Tables III-3 and III-4, in which the small contribution below 4 K was estimated by smooth extrapolation from the high temperature side. The third law entropy of the biphenyl ideal gas in the standard state is calculated using the vapor pressure[78] and sublimation[79] data as summarized in Table III-5.

The anomalies due to the twist transition in both samples are clearly seen by plotting the Debye characteristic temperatures corresponding to the measured heat capacities as given in Figure III-7,

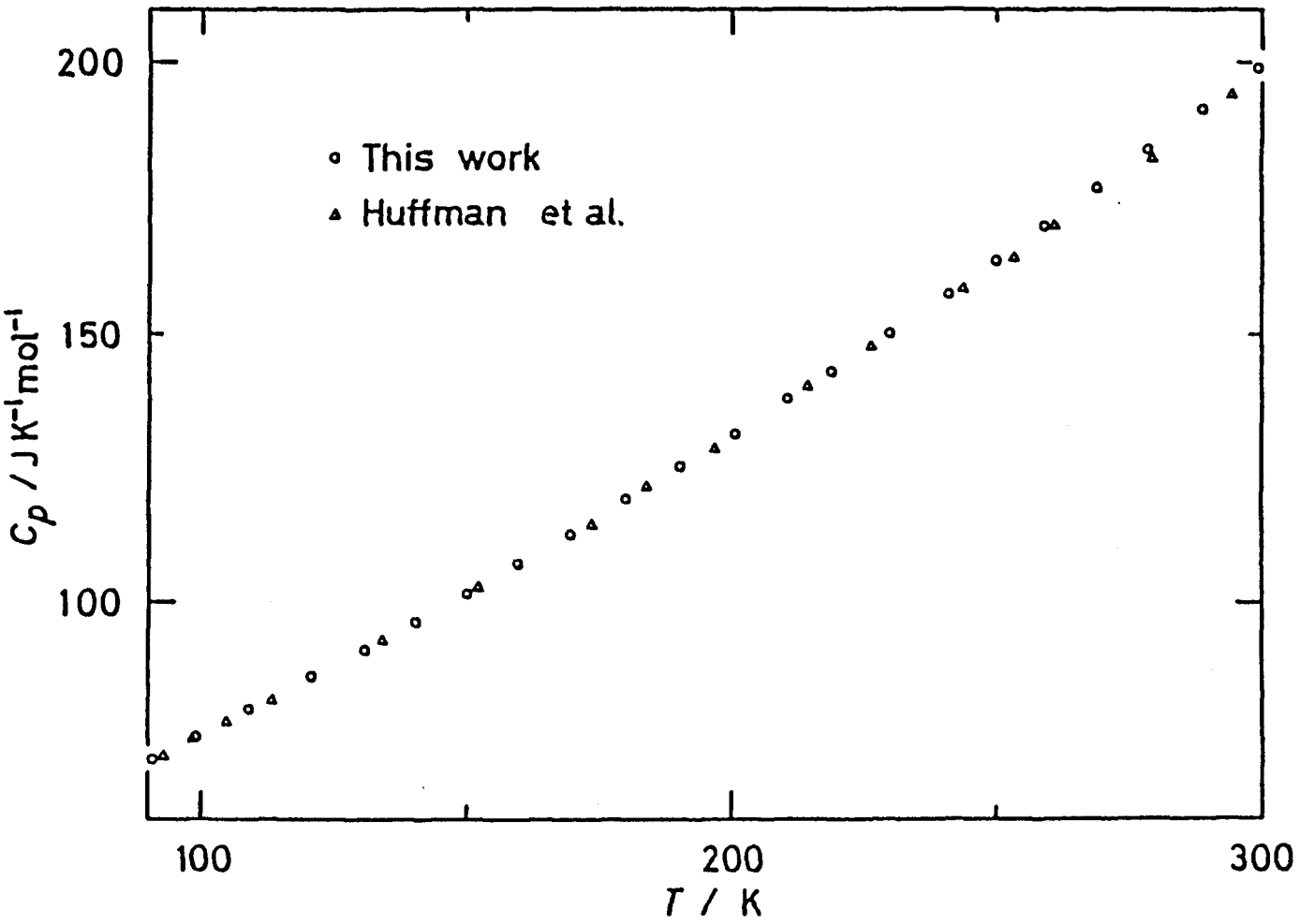

Figure III-6. Comparison between the present data (circle) and the data reported by Huffman et al.[75] (triangle) on biphenyl.

Table III-3. Molar thermodynamic functions of biphenyl.

T / K	C_p / J·K^{-1}·mol^{-1}	$\{H(T)-H(0)\}/T$ / J·K^{-1}·mol^{-1}	$S(T)-S(0)$ / J·K^{-1}·mol^{-1}	$-\{G(T)-H(0)\}/T$ / J·K^{-1}·mol^{-1}
5	0.504	0.133	0.173	0.040
10	3.26	0.90	1.21	0.32
20	14.68	4.75	6.71	1.96
30	27.46	10.21	15.11	4.89
40	38.63	15.97	24.59	8.62
50	46.42	21.30	34.07	12.77
60	53.43	26.08	43.17	17.08
70	59.57	30.44	51.87	21.44
80	65.19	34.44	60.20	25.76
90	70.44	38.14	68.18	30.04
100	75.57	41.63	75.87	34.24
110	80.72	44.95	83.31	38.36
120	85.83	48.14	90.56	42.41
130	90.89	51.24	97.63	46.39
140	96.23	54.26	104.56	50.30
150	101.53	57.23	111.38	54.14
160	107.11	60.18	118.11	57.93
170	112.85	63.11	124.77	61.67
180	118.82	66.03	131.39	65.36
190	124.75	68.97	137.97	69.00
200	130.90	71.91	144.53	72.62
210	137.21	74.87	151.07	76.20
220	143.68	77.85	157.60	79.75
230	150.49	80.86	164.13	83.28
240	157.19	83.90	170.68	86.78
250	163.77	86.96	177.23	90.27
260	170.73	90.05	183.79	93.74
270	177.90	93.17	190.37	97.20
280	185.10	96.33	196.97	100.64
290	192.30	99.51	203.59	104.08
300	199.50	102.72	210.23	107.50
298.15	198.17	102.13	209.00	106.87

Table III-4. Molar thermodynamic functions of biphenyl-d_{10}.

T / K	C_p / J·K^{-1}·mol^{-1}	$\{H(T)-H(0)\}/T$ / J·K^{-1}·mol^{-1}	$S(T)-S(0)$ / J·K^{-1}·mol^{-1}	$-\{G(T)-H(0)\}/T$ / J·K^{-1}·mol^{-1}
5	0.610	0.156	0.202	0.046
10	3.76	1.07	1.44	0.38
20	16.22	5.34	7.60	2.26
30	29.62	11.23	16.75	5.52
40	40.49	17.31	26.90	9.59
50	48.70	22.78	36.83	14.05
60	55.96	27.72	46.37	18.65
70	62.43	32.21	55.48	23.26
80	68.51	36.38	64.22	27.84
90	74.42	40.28	72.63	32.35
100	80.35	43.99	80.78	36.79
110	86.23	47.57	88.72	41.15
120	92.24	51.04	96.48	45.44
130	98.62	54.45	104.12	49.66
140	105.22	57.84	111.66	53.82
150	112.04	61.23	119.15	57.93
160	119.09	64.63	126.61	61.99
170	126.43	68.04	134.05	66.01
180	134.03	71.49	141.49	69.99
190	141.73	74.98	148.94	73.95
200	149.71	78.52	156.41	77.89
210	157.64	82.10	163.91	81.81
220	165.23	85.71	171.42	85.71
230	173.34	89.34	178.94	89.60
240	181.74	93.01	186.49	93.48
250	189.87	96.73	194.08	97.35
260	197.96	100.47	201.68	101.21
270	206.07	104.23	209.30	105.08
280	214.47	108.01	216.95	108.94
290	222.76	111.83	224.62	112.79
300	230.08	115.65	232.30	116.65
298.15	228.86	114.95	230.88	115.93

Table III-5. Third law entropy of biphenyl.

	S / J·K^{-1}·mol^{-1}
0 to 4 K (smooth extrapolation)	0.089
4 to 298.15 K (graphical)	208.9
sublimation[a]	274.2
entropy of real gas at 298.15 K	483.2
compression[b] and correction to ideal gas[c]	-93.7
$S°$(biphenyl, 298.15 K, g, P = 100000 Pa)	389.5

[a] $\Delta_{vap}H$ = 81760 J·mol^{-1} at 298.15 K.[77)]

[b] P = 1.30 Pa at 298.15 K.[76)]

[c] Using Berthelot's equation of state.

where it is arbitrarily assumed that there are 9 degrees of freedom per molecule. By assuming normal portion as shown by the solid lines in Figure III-7, excess heat capacities are separated as shown in Figures III-8 and III-9. The anomaly of biphenyl is very broad extending from 30 K to 47 K with a maximum at 40.4 K; the shape of the anomaly of biphenyl-d_{10} is very similar to that of biphenyl and it is from 28 K to 44 K with a maximum at 36.8 K. The entropies of transition of biphenyl and biphenyl-d_{10} are determined as 0.129 $J \cdot K^{-1} \cdot mol^{-1}$ and 0.128 $J \cdot K^{-1} \cdot mol^{-1}$, respectively. The shape of the anomalies and the smallness of the entropies of transition are consistent with higher-order, displacive nature of the twist transition in both compounds.

In addition to the anomaly at 36.8 K, a very small anomaly due to the lock-in transition is seen at about 20 K in the heat capacity curve of biphenyl-d_{10}. On the other hand, the corresponding anomaly can not be recognized in the curve of biphenyl; the distortion around 11 K is probably due to some failure in germanium temperature scale. The results of one typical series of measurements on biphenyl using the newly constructed vessel are shown in Figure III-10. In this series the temperature increment of each measurement was about 0.2 K. A broad anomaly due to the lock-in transition is clearly seen. The anomaly

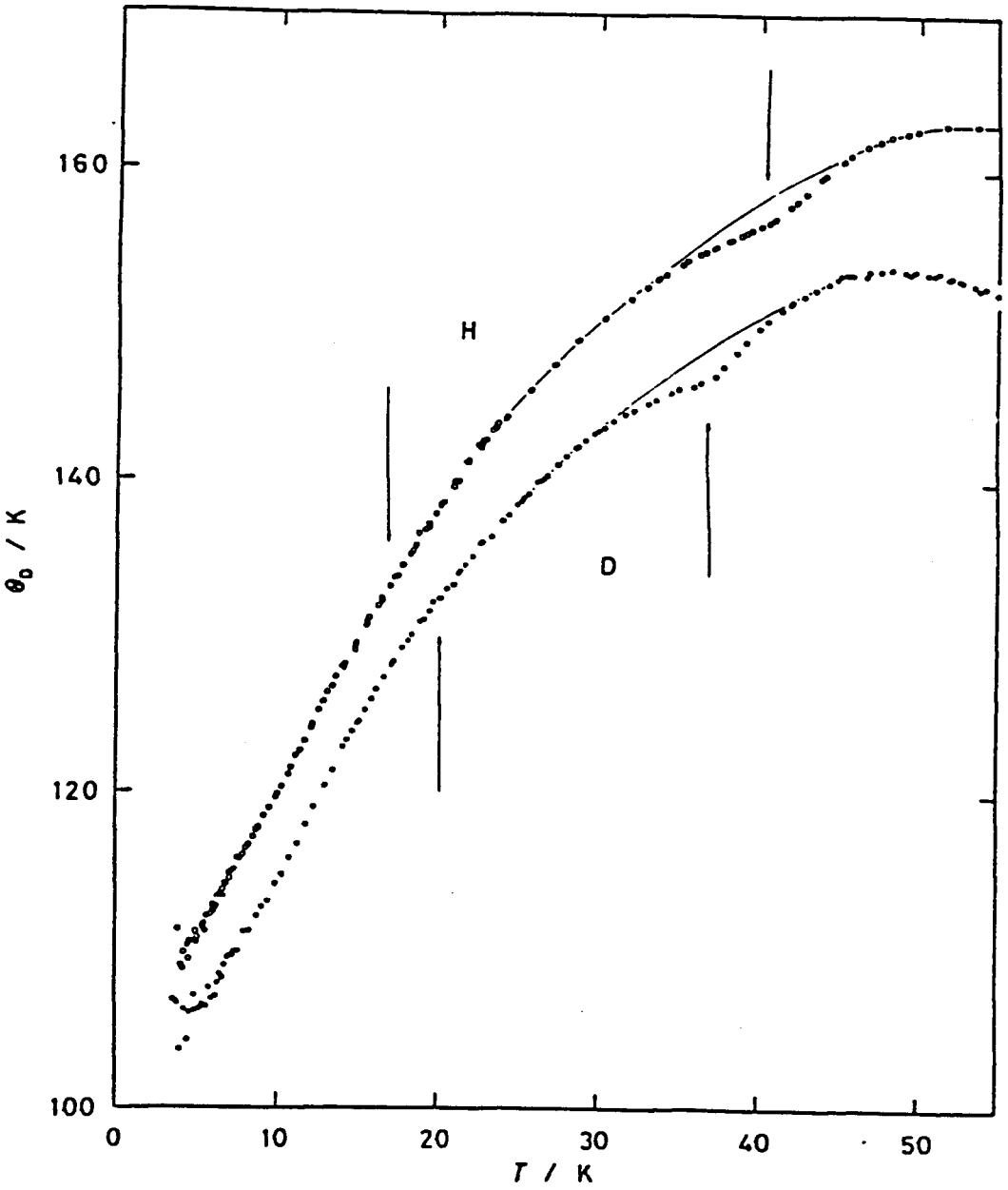

Figure III-7. Debye characteristic temperatures corresponding to measured heat capacities of biphenyl (open circle) and biphenyl-d_{10} (filled circle), assuming 9 degrees of freedom per molecule.

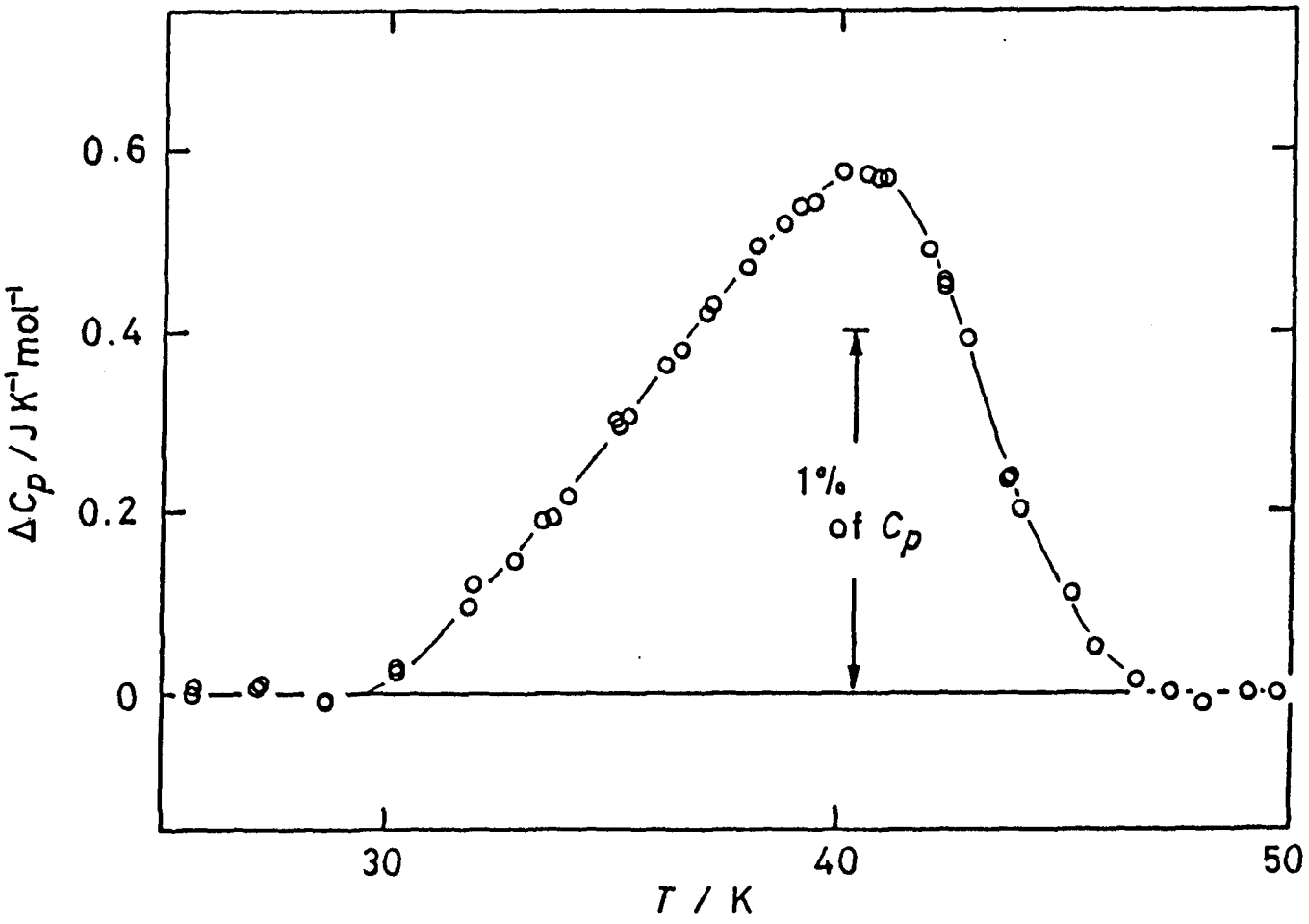

Figure III-8. Excess molar heat capacities due to the twist transition of biphenyl.

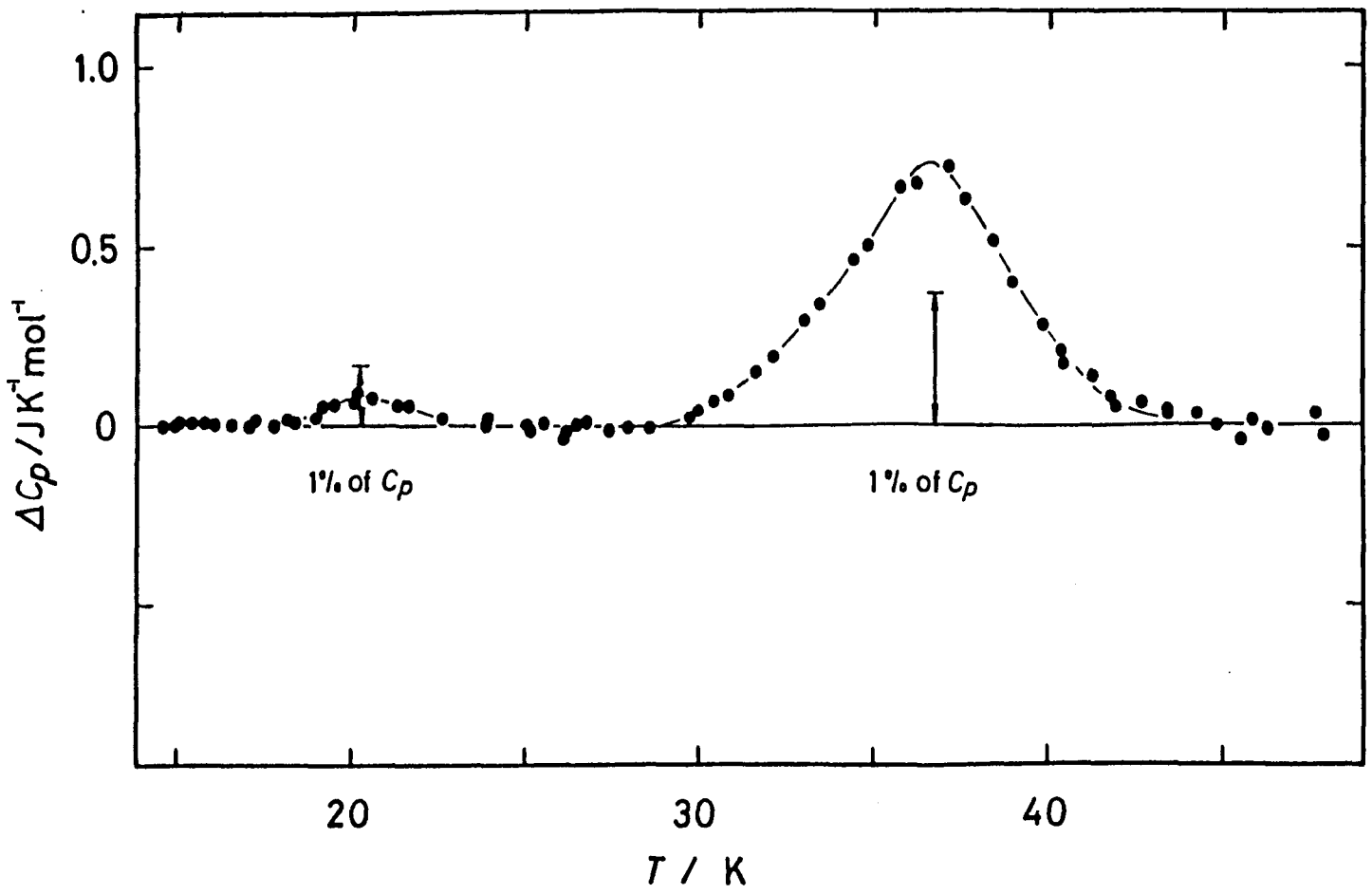

Figure III-9. Excess molar heat capacities of biphenyl-d_{10}.

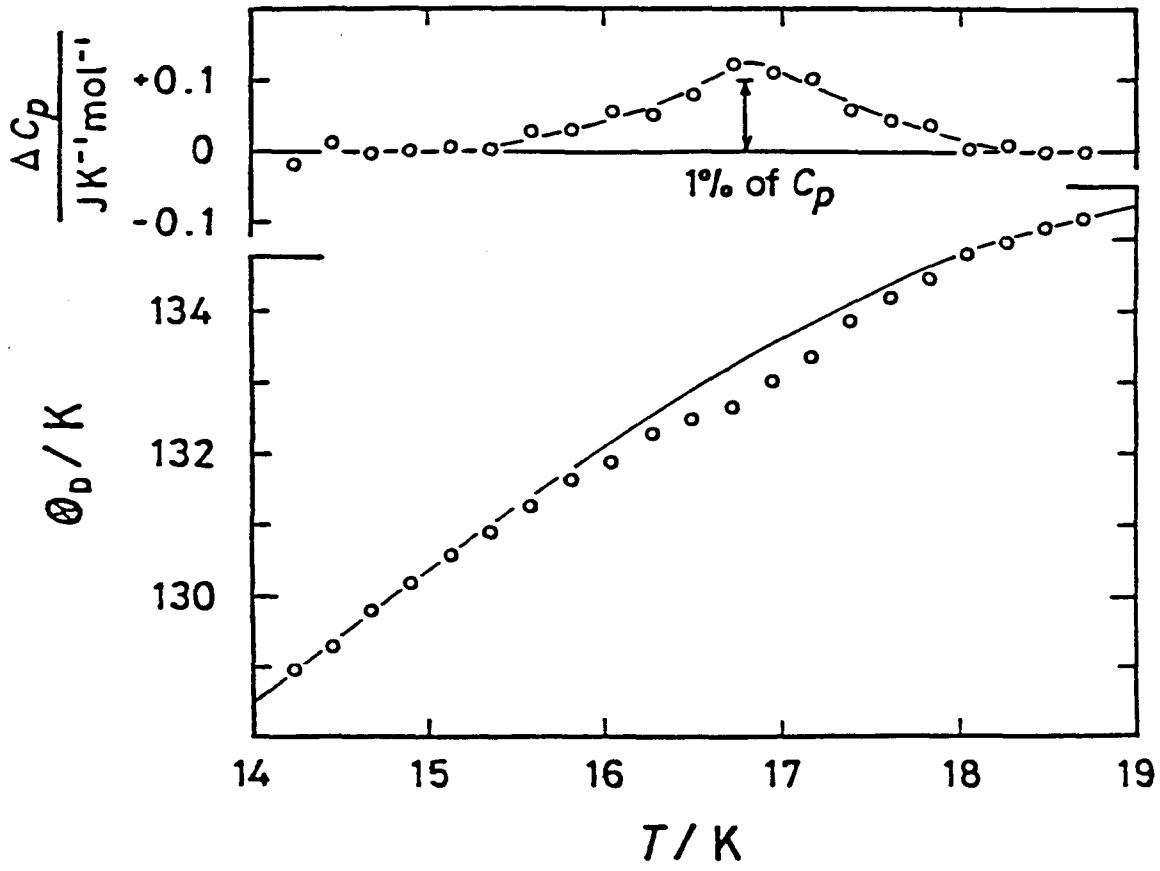

Figure III-10. Excess molar heat capacities due to the lock-in transition of biphenyl (upper) and the Debye characteristic temperatures corresponding to the heat capacities of a typical run of measurements assuming 9 degrees of freedom per molecule (lower).

due to the lock-in transition is extremely small (0.009 $J \cdot K^{-1} \cdot mol^{-1}$ in terms of the entropy of transition, for both compounds), broad and showing a large tail on the high temperature side. Thus, the lock-in transition of biphenyl and biphenyl-d_{10} seems to be of a higher-order transition. However, as described in the last section, some evidences that the lock-in transition was of the first-order have been reported,[21,36] and the Landau's phenomenology[41-43] also predicts that it is so. Similar situation happened in the case of K_2SeO_4. Nomoto et al.[80] interpreted that as follows: The lock-in transition of K_2SeO_4 is of the first-order in nature; however, the latent heat of the transition is very small and could not be detected experimentally. Such an interpretation should be adapted also in the cases of biphenyl and biphenyl-d_{10}.

The large tail on the high temperature side at the lock-in transition has been observed in other substances,[80-82] and it may be accompanied with discommensuration mechanism proposed by McMillan.[83]

Properties of phase transitions are summarized in Table III-12. The entropies of transition in the two compounds are equal to each other, impling the two compounds undergo transitions of the same mechanism. The major difference between the two compounds is that the region of the two dimensionally incommensurate phase is narrower in biphenyl-d_{10}.

No anomaly corresponding to the lock-in transition

in the direction of the b axis was found in both the samples. Two cases are possible; existence of the lock-in transition in the b direction below the lowest temperature reached in the present experiments, and "stability" of incommensurate phase till the absolute zero. If the later was true, the question is open whether the incommensurate phase existing at 0 K is stable in the thermodynamic sense, or a glassy state of new type.

III-2-2 p-Terphenyl and p-terphenyl-d_{14}

Experimental

p-Terphenyl was purchased from Nakarai Chemicals, Ltd., and p-terphenyl-d_{14} from Merck Sharp & Dohme Canada, Ltd. (isotope purity, 98 per cent). They were purified by the method of fractional sublimation in vacuum at about 400 K.

In the case of p-terphenyl, both specimens non-melted and melted under the helium atmosphere (10^5 Pa) were used for the calorimetry for the sake of comparison. In the case of p-terphenyl-d_{14}, the measurements were made only on the specimen melted under the helium atmosphere (10^5 Pa).

The purity of the specimens used for the calorimetry were better than 99.9 moles per cent as

confirmed by gas-chromatography. The isotope purity of p-terphenyl-d_{14} was determined to be 98 per cent by using the high resolution proton NMR technique. Each of the powdered specimens was loaded into the calorimeter vessel, which was sealed after addition of a small amount of helium gas (7 kPa, 7 kPa and 6 kPa for melted, non-melted p-terphenyl and p-terphenyl-d_{14}, respectively) for heat exchange. The contribution of helium to the total heat capacity was negligibly small. The amount of the melted and the non-melted p-terphenyl samples and the p-terphenyl-d_{14} sample were 21.0704 g (0.091488 mol), 15.2290 g (0.066124 mol) and 8.7131 g (0.035652 mol), respectively. The contribution of the sample to the total heat capacity including that of the calorimeter vessel was, in p-terphenyl, 64 per cent at 10 K, which decreased to 40 per cent at 100 K and then increased to 54 per cent at 300 K as temperature rose; in p-terphenyl-d_{14} 51 per cent at 10 K, 27 per cent at 100 K, and 42 per cent at 300 K.

The working thermometers, and the apparatus and the operation of the adiabatic calorimeter were the same as used in the measurements on biphenyl and biphenyl-d_{10}.

Results and Discussion

The measurements of the heat capacities were made between 3 and 300 K; the primary data are tabulated in

Tables III-6 and III-7 in chronological order, and shown in Figure III-11, where the data of the non-melted p-terphenyl sample are not included. The temperature increment of each measurement may be deduced from the adjacent mean temperatures, which is small enough to neglect the curvature corrections in comparison with the experimental precision. After each energy input was over, thermal equilibrium within the calorimeter vessel was attained within 2 min below 20 K, in 10 min at 80 K; the time needed for equilibration then increased to 20 min at about the transition temperature as temperature rose, and it abruptly reduced to 10 min above the transition, in all the three samples.

Some thermodynamic functions calculated from the present results are given for rounded temperatures in Tables III-8 and III-9, in which small contributions below 4 K were estimated by smooth extrapolation from the high temperature side.

The λ-shaped anomaly due to the twist transition is clearly seen in p-terphenyl from 145 K to 225 K with a maximum at 193.5 K, and the very similar one in p-terphenyl-d_{14} from 130 K to 210 K with a maximum at 180.3 K. In spite of sharp rise in heat capacity, a latent heat was not observed in both cases, which is in agreement with the results reported by Chang[53] and Cailleau and Dworkin.[52] By assuming the normal

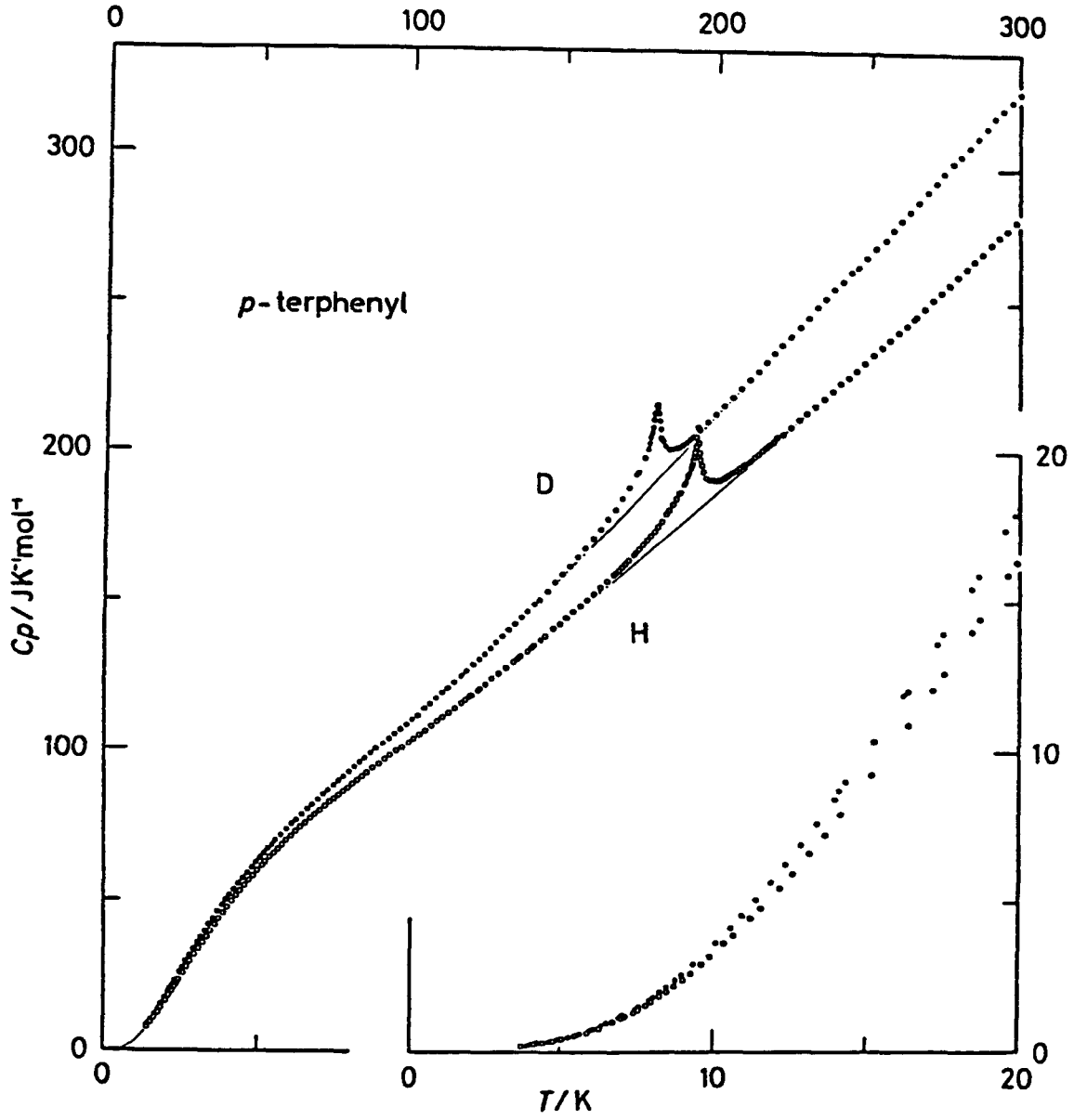

Figure III-11. Measured molar heat capacities of p-terphenyl (open circle) and p-terphenyl-d_{14} (filled circle).

Table III-6. Measured molar heat capacities of *p*-terphenyl.

T / K	C_p / J·K^{-1}·mol^{-1}	T / K	C_p / J·K^{-1}·mol^{-1}	T / K	C_p / J·K^{-1}·mol^{-1}	T / K	C_p / J·K^{-1}·mol^{-1}
non-melted sample		Series 4		235.026	218.32	97.461	101.15
Series 1		159.931	152.59	237.725	220.77	99.337	102.73
118.932	117.87	162.093	154.73	240.404	223.51	101.230	104.07
120.636	119.82	164.230	156.87	Series 6		103.079	105.45
122.532	120.82	166.387	159.03	243.063	225.35	Series 9	
124.595	122.44	168.563	161.29	245.714	227.74	104.949	106.85
126.794	124.29	170.717	163.60	248.401	230.28	106.850	108.42
129.081	126.00	172.854	165.87	251.110	233.11	108.727	109.90
Series 2		174.974	168.29	253.820	235.56	110.581	111.27
129.181	125.88	177.114	170.75	256.511	238.22	112.459	112.70
131.472	127.80	179.273	173.41	259.160	240.71	114.364	114.18
133.763	129.71	181.410	176.38	261.845	242.95	116.248	115.66
136.027	131.62	183.520	179.37	264.277	245.37	118.112	117.18
138.259	133.43	185.649	182.59	Series 7		119.971	118.65
140.461	135.17	187.795	186.42	265.118	246.09	Series 10	
142.655	136.94	189.955	191.09	267.871	248.87	116.646	115.94
144.841	138.86	192.121	198.23	270.598	251.68	119.536	118.27
146.986	140.98	194.313	200.52	273.358	254.20	121.996	120.12
149.059	142.65	196.515	192.22	276.152	256.83	Series 11	
151.056	144.76	198.679	190.77	278.924	259.69	167.071	159.49
152.989	145.90	200.840	191.22	281.670	262.39	168.073	160.68
Series 3		202.991	192.04	284.395	264.95	169.090	161.76
132.987	128.86	205.132	193.46	287.157	267.44	170.141	162.87
135.299	130.88	207.263	194.91	289.959	270.62	171.228	163.91
137.593	132.92	209.394	196.46	292.736	273.02	172.355	165.23
139.847	134.66	Series 5		295.492	275.42	173.522	166.52
142.087	136.67	210.577	197.08	298.228	278.16	174.730	167.98
144.356	138.52	213.355	199.13	Series 8		175.957	169.33
146.611	140.57	216.112	201.75	84.253	90.983	177.177	170.79
148.884	142.43	218.845	204.04	86.121	92.552	178.394	172.23
151.173	144.51	221.560	206.31	87.982	94.001	179.607	173.66
153.429	146.53	224.244	208.60	89.838	95.456	180.807	175.25
155.620	148.53	226.936	211.01	91.722	96.907	182.015	176.98
157.745	150.60	229.619	213.39	93.632	98.347	183.231	178.75
		232.307	216.14	95.562	99.842	184.437	180.65

Table III-6. (continued).

T / K	C_p / J·K^{-1}·mol^{-1}	T / K	C_p / J·K^{-1}·mol^{-1}	T / K	C_p / J·K^{-1}·mol^{-1}	T / K	C_p / J·K^{-1}·mol^{-1}
185.646	182.52	209.909	196.80	3.873	0.239	Series 19	
186.861	184.59	211.129	197.80	3.991	0.268	6.720	0.989
188.067	186.85	212.344	198.78	Series 16		7.111	1.174
189.277	189.40	213.555	199.73	4.627	0.321	7.528	1.391
Series 12		214.776	200.78	5.073	0.425	7.983	1.669
190.003	190.22	216.005	201.78	5.491	0.536	8.478	2.003
190.250	191.46	217.224	202.87	5.882	0.635	9.019	2.419
190.520	191.88	218.437	203.77	6.285	0.759	9.631	2.941
190.806	192.90	219.651	205.10	Series 17		10.358	3.622
191.106	193.95	Series 14		3.843	0.207	11.218	4.456
191.415	194.89	51.458	61.431	4.079	0.222	12.184	5.471
191.726	196.09	53.397	63.571	4.436	0.287	13.175	6.623
192.042	197.26	54.967	65.232	4.838	0.369	Series 20	
192.358	198.77	56.523	66.812	5.235	0.467	17.163	12.094
192.677	200.09	58.044	68.382	5.610	0.576	18.440	14.041
192.996	202.20	59.573	69.909	Series 18		19.654	15.946
193.313	205.17	61.113	71.344	4.077	0.221	20.789	17.740
193.628	208.36	62.648	72.843	4.422	0.278	21.939	19.591
193.943	203.25	64.185	74.331	4.790	0.363	23.105	21.503
194.259	199.35	65.742	75.647	5.164	0.449	24.292	23.462
194.575	197.55	67.319	77.107	5.549	0.549	Series 21	
194.892	195.77	68.905	78.503	5.928	0.673	14.022	7.737
Series 13		70.475	79.884	6.293	0.809	15.155	9.246
195.549	193.55	72.029	81.161	6.650	0.946	16.338	10.899
196.588	191.55	73.594	82.532	7.014	1.109	17.524	12.633
197.719	190.65	75.145	83.762	7.397	1.301	18.724	14.478
198.921	190.32	76.688	85.031	7.811	1.548	19.920	16.375
200.148	190.59	78.224	86.303	8.258	1.840	21.113	18.250
201.373	190.94	79.754	87.473	8.741	2.181	22.311	20.199
202.595	191.68	81.303	88.765	9.279	2.619	23.517	22.186
203.813	192.58	82.847	89.977	9.897	3.168	24.732	24.183
205.026	193.29	84.388	91.148	10.646	3.870	Series 22	
206.237	194.11	Series 15		11.555	4.794	21.983	19.641
207.456	194.99	3.732	0.184	12.590	5.928	23.168	21.574
208.685	195.91			13.663	7.239	24.373	23.544

Table III-6. (continued).

T/K	C_p/J·K^{-1}·mol^{-1}	T/K	C_p/J·K^{-1}·mol^{-1}	T/K	C_p/J·K^{-1}·mol^{-1}	T/K	C_p/J·K^{-1}·mol^{-1}
25.599	25.537	55.328	65.649	Series 27		Series 30	
Series 23		Series 25		195.123	195.31	189.949	191.44
26.845	27.628	56.689	67.044	196.436	192.09	191.053	195.01
28.106	29.627	58.033	68.438	Series 28		192.087	199.51
29.383	31.666	Series 26		188.569	187.35	192.621	201.61
30.671	33.715	189.034	188.97	189.662	189.94	192.721	202.54
31.965	35.765	190.434	192.46	198.214	190.15	192.829	203.63
33.266	37.775	191.770	196.96	199.291	190.12	192.940	204.74
34.590	39.748	192.414	200.65	melted sample		193.052	205.69
35.929	41.715	192.478	200.89	Series 29		193.164	206.94
37.298	43.709	192.562	201.15	187.284	185.49	193.275	208.30
38.699	45.627	192.671	201.04	188.348	187.52	193.387	209.50
40.101	47.563	192.805	201.83	189.461	190.24	193.501	209.35
41.509	49.465	192.962	203.13	190.605	193.43	193.614	209.55
42.928	51.319	193.144	204.02	191.471	196.46	193.726	208.13
44.344	53.107	193.342	206.54	192.043	199.33	193.839	206.00
45.747	54.813	193.521	209.80	192.598	202.73	193.950	204.54
47.109	56.480	193.672	210.71	193.136	207.25	194.063	202.34
48.460	58.096	193.810	207.64	193.669	208.85	194.174	201.13
49.838	59.713	193.935	205.46	194.206	201.47	194.285	199.73
51.207	61.229	194.051	203.97	194.752	196.11	194.396	198.26
Series 24		194.163	202.47	195.306	193.07	194.506	197.15
52.567	62.714	194.279	201.77	195.859	191.58	195.088	194.20
53.948	64.261	194.405	200.39	196.693	190.35		

Table III-7. Measured molar heat capacities of *p*-terphenyl-d_{14}.

T/K	C_p/J·K^{-1}·mol^{-1}	T/K	C_p/J·K^{-1}·mol^{-1}	T/K	C_p/J·K^{-1}·mol^{-1}	T/K	C_p/J·K^{-1}·mol^{-1}
Series 1		223.936	238.89	100.633	110.38	71.408	85.110
142.267	150.48	226.839	242.18	102.585	111.84	73.158	86.590
144.794	153.56	229.707	245.29	104.553	114.02	74.912	88.235
147.334	156.47	232.554	249.10	106.523	115.67	76.648	89.721
149.665	158.99	235.392	251.79	108.483	117.52	78.371	91.207
152.056	161.76	238.209	255.00	110.431	119.24	80.105	92.711
154.573	164.81	241.003	257.48	112.369	121.05	81.853	94.290
157.063	167.87	243.829	260.69	114.299	122.72	83.618	95.826
159.418	170.97	Series 3		116.236	124.58	85.388	97.317
161.791	174.03	245.835	262.31	Series 6		87.152	98.842
164.181	177.40	248.683	265.60	116.432	125.01	88.910	100.47
166.546	180.78	251.509	268.74	118.359	126.66	90.677	101.93
168.889	184.39	254.342	271.74	120.292	128.72	Series 8	
171.228	188.13	257.182	274.92	122.251	130.46	182.115	203.82
173.583	192.67	260.001	278.28	124.224	132.27	183.211	201.27
175.931	197.74	262.830	281.33	126.209	134.21	184.327	200.84
178.266	205.75	265.691	284.55	128.206	136.13	185.440	200.68
180.605	213.00	268.533	287.87	130.215	138.23	186.551	201.29
182.942	203.25	271.358	291.07	132.287	140.32	187.659	201.91
185.250	201.87	274.188	294.01	134.353	142.47	188.782	202.69
187.531	202.89	276.997	297.81	136.368	144.67	189.925	203.43
Series 2		Series 4		138.399	146.73	191.065	204.32
187.146	201.92	279.816	299.94	140.446	148.97	Series 9	
189.571	203.70	282.655	302.99	142.509	151.18	173.981	193.16
192.027	205.25	285.502	306.32	144.589	153.51	176.192	198.38
194.514	207.51	288.352	309.64	Series 7		177.476	201.00
197.057	210.10	291.174	313.32	55.803	69.701	177.849	202.93
199.680	212.87	294.009	315.59	57.703	71.753	178.215	205.09
202.363	215.69	296.862	318.24	59.411	73.517	178.579	206.24
205.077	218.47	299.698	321.16	61.058	75.264	178.942	208.32
207.832	221.30	Series 5		62.739	76.782	179.304	210.69
210.595	224.50	91.195	102.03	64.447	78.554	179.663	213.16
213.330	227.39	93.075	103.75	66.162	80.104	180.022	215.83
216.071	230.42	94.948	105.45	67.914	81.788	180.379	215.97
218.647	233.40	96.816	107.06	69.660	83.441	180.737	215.33
221.162	236.11	98.711	108.73			181.096	210.46

Table III-7. (continued).

T / K	C_p / J·K^{-1}·mol^{-1}	T / K	C_p / J·K^{-1}·mol^{-1}	T / K	C_p / J·K^{-1}·mol^{-1}	T / K	C_p / J·K^{-1}·mol^{-1}
181.457	207.66	7.168	1.268	21.130	21.121	50.675	64.101
181.819	204.79	7.549	1.502	Series 18		52.022	65.602
182.183	203.68	Series 13		14.082	8.687	53.393	67.179
182.548	203.27	6.149	0.830	15.169	10.325	54.795	68.648
182.914	202.14	6.573	0.990	16.215	11.889	Series 20	
184.172	201.70	7.004	1.244	17.287	13.602	177.334	200.67
Series 10		7.442	1.421	18.402	15.467	178.121	201.93
3.955	0.205	7.893	1.736	19.544	17.417	178.246	202.69
4.233	0.267	Series 14		20.739	19.469	178.368	201.06
4.599	0.316	7.378	1.377	22.015	21.650	178.496	202.09
4.962	0.401	7.799	1.663	23.289	23.931	178.627	202.17
5.325	0.518	8.248	1.999	24.493	26.040	178.760	204.15
5.702	0.639	8.757	2.402	Series 19		178.896	204.23
6.096	0.783	9.360	2.931	21.611	20.968	179.032	204.44
6.501	0.954	10.069	3.632	22.837	23.127	179.166	205.76
6.899	1.152	10.924	4.532	24.063	25.303	179.301	207.58
Series 11		11.869	5.644	25.287	27.439	179.434	209.39
3.921	0.186	12.858	6.878	26.497	29.520	179.567	210.85
4.245	0.250	13.939	8.403	27.712	31.555	179.700	210.80
4.604	0.319	Series 15		28.927	33.609	179.833	211.06
4.965	0.431	8.032	1.844	30.140	35.636	179.967	211.99
5.283	0.490	8.463	2.179	31.362	37.661	180.099	211.82
5.624	0.601	8.964	2.588	32.617	39.710	180.231	212.56
5.988	0.729	Series 16		33.940	41.746	180.364	213.68
Series 12		10.569	4.126	35.319	43.847	180.497	211.43
3.789	0.145	11.381	5.073	36.883	46.212	180.630	211.20
3.981	0.191	12.342	6.238	38.322	48.250	180.763	209.40
4.219	0.240	13.372	7.594	39.553	49.948	180.896	208.35
4.519	0.296	Series 17		40.866	51.805	181.030	206.38
4.839	0.359	14.286	9.005	42.205	53.627	181.164	205.34
5.192	0.463	15.205	10.365	43.587	55.481	181.299	204.20
5.558	0.565	16.317	12.033	45.003	57.230	181.433	202.35
5.936	0.714	17.483	13.932	46.463	59.014		
6.342	0.869	18.657	15.896	47.950	60.875		
6.753	1.068	19.863	17.955	49.351	62.591		

Table III-8. Molar thermodynamic functions of *p*-terphenyl.

T / K	C_p / J·K^{-1}·mol^{-1}	$\{H(T)-H(0)\}/T$ / J·K^{-1}·mol^{-1}	$S(T)-S(0)$ / J·K^{-1}·mol^{-1}	$-\{G(T)-H(0)\}/T$ / J·K^{-1}·mol^{-1}
5	0.392	0.101	0.131	0.030
10	3.27	0.82	1.08	0.27
20	16.49	5.07	7.01	1.95
30	32.67	11.57	16.75	5.19
40	47.44	18.75	28.23	9.49
50	59.86	25.76	40.19	14.44
60	70.28	32.33	52.05	19.73
70	79.46	38.43	63.59	25.17
80	87.72	44.08	74.74	30.67
90	95.57	49.37	85.53	36.17
100	103.19	54.37	96.00	41.64
110	110.81	59.15	106.19	47.05
120	118.63	63.78	116.16	52.39
130	126.68	68.31	125.98	57.68
140	134.84	72.77	135.66	62.90
150	143.45	77.19	145.26	68.08
160	152.70	81.62	154.81	73.20
170	162.77	86.09	164.36	78.28
180	174.45	90.66	173.98	83.33
190	191.06	95.47	183.81	88.35
200	190.33	100.43	193.81	93.39
210	196.86	104.86	203.24	98.40
220	204.98	109.22	212.58	103.37
230	213.81	113.57	221.88	108.32
240	222.75	117.93	231.17	113.25
250	231.85	122.31	240.45	118.16
260	241.23	126.70	249.72	123.03
270	250.91	131.12	259.01	127.90
280	260.71	135.58	268.31	132.74
290	270.30	140.06	277.63	137.58
300	279.90	144.56	286.95	142.40
298.15	278.12	143.72	285.23	141.52

Table III-9. Molar thermodynamic functions of *p*-terphenyl-d_{14}.

T / K	C_p / J·K^{-1}·mol^{-1}	$\{H(T)-H(0)\}/T$ / J·K^{-1}·mol^{-1}	$S(T)-S(0)$ / J·K^{-1}·mol^{-1}	$-\{G(T)-H(0)\}/T$ / J·K^{-1}·mol^{-1}
5	0.421	0.109	0.142	0.033
10	3.56	0.89	1.17	0.28
20	18.19	5.59	7.71	2.12
30	35.41	12.68	18.37	5.68
40	50.64	20.32	30.69	10.38
50	63.30	27.68	43.39	15.71
60	74.10	34.53	55.91	21.37
70	83.77	40.89	68.07	27.18
80	92.67	46.81	79.84	33.03
90	101.22	52.39	91.25	38.87
100	109.83	57.69	102.36	44.66
110	118.88	62.85	113.25	50.40
120	128.26	67.90	123.99	56.09
130	137.97	72.92	134.64	61.72
140	148.43	77.94	145.24	67.31
150	159.32	82.99	155.85	72.86
160	171.76	88.14	166.52	78.38
170	185.90	93.46	177.34	83.88
180	215.90	99.21	188.59	89.38
190	203.50	104.70	199.60	94.90
200	213.19	109.87	210.27	100.40
210	223.79	115.04	220.93	105.89
220	234.82	120.24	231.59	111.36
230	245.72	125.46	242.27	116.82
240	256.22	130.69	252.95	122.27
250	266.93	135.92	263.63	127.71
260	278.16	141.17	274.31	133.14
270	289.48	146.46	285.03	138.57
280	300.54	151.76	295.75	143.99
290	311.27	157.08	306.49	149.41
300	321.55	162.39	317.22	154.82
298.15	319.66	161.41	315.23	153.82

portion as shown by the solid lines in Figure III-11, the excess heat capacities are separated as shown in Figure III-12. Although the transition temperature shifts to the lower temperature on deuteration as in the twist transition of biphenyl, the shape of the anomalies of the two compounds are very similar and the entropies of transition (1.63 $J \cdot K^{-1} \cdot mol^{-1}$) are equal to each other, which fact suggests the same mechanism of the transition in the two compounds.

The critical exponent for heat capacity is determined by plotting the excess heat capacities of p-terphenyl measured in the series 26 as shown in Figure III-13, in which the temperature interval between the adjacent points was about 0.1 K. The same value of 0.13 is obtained below and above the transition. The positive value should result in the infinite heat capacity at the transition temperature, but the evidence of that was not found in our experiments. Chang[53] reported an apparent rounding of the anomaly near the transition temperature using the higher temperature resolution (0.025 K).

The comparison of the results of the melted and the non-melted samples is shown in Figure III-14. There is no apparent difference between the two samples; it rules out the possibilities of the formation of metastable phases and poor crystallinity that affects the phase transition.

No anomaly was observed at about 8 K in contrast

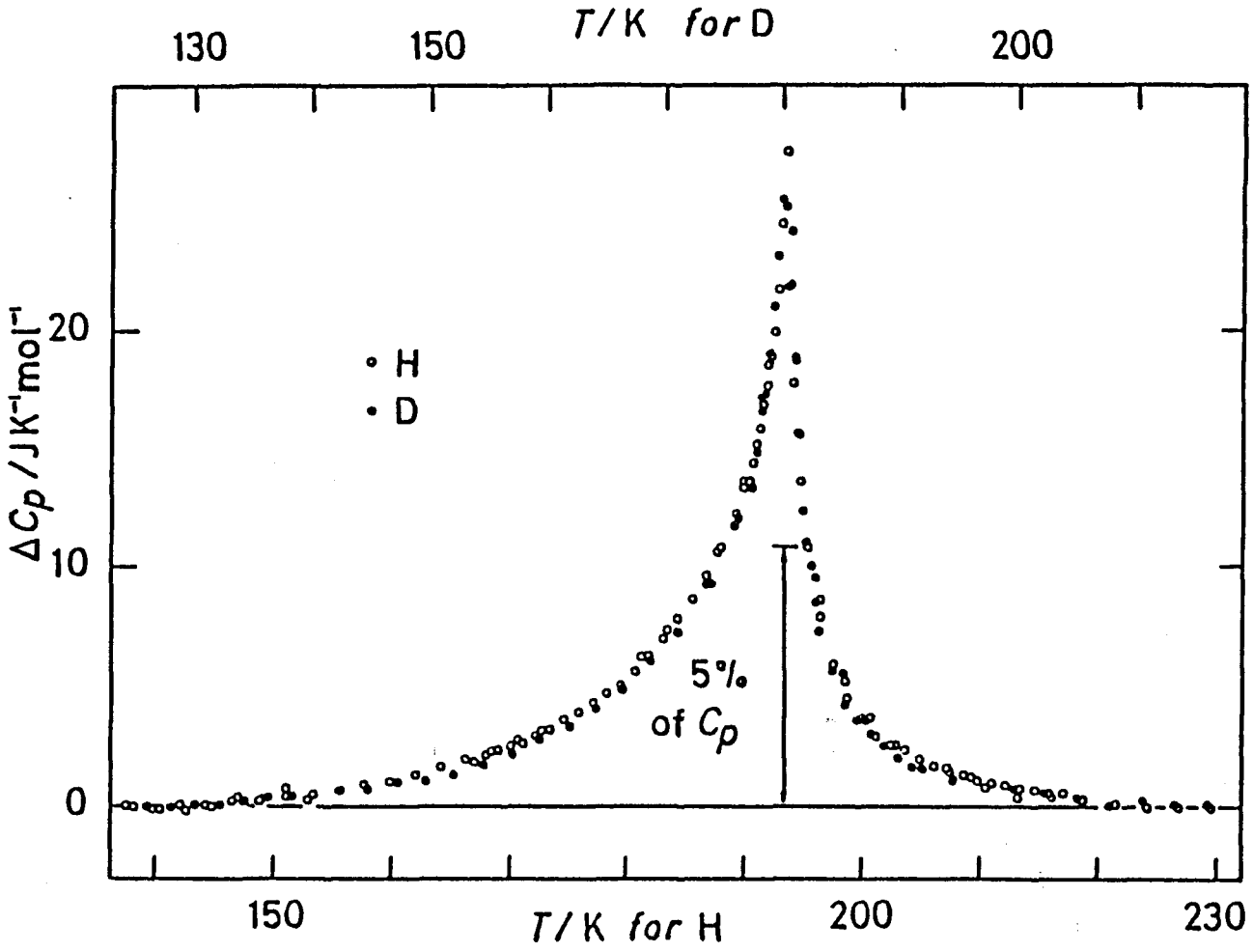

Figure III-12. Excess molar heat capacities of p-terphenyl (open circle) and p-terphenyl-d_{14} (filled circle).

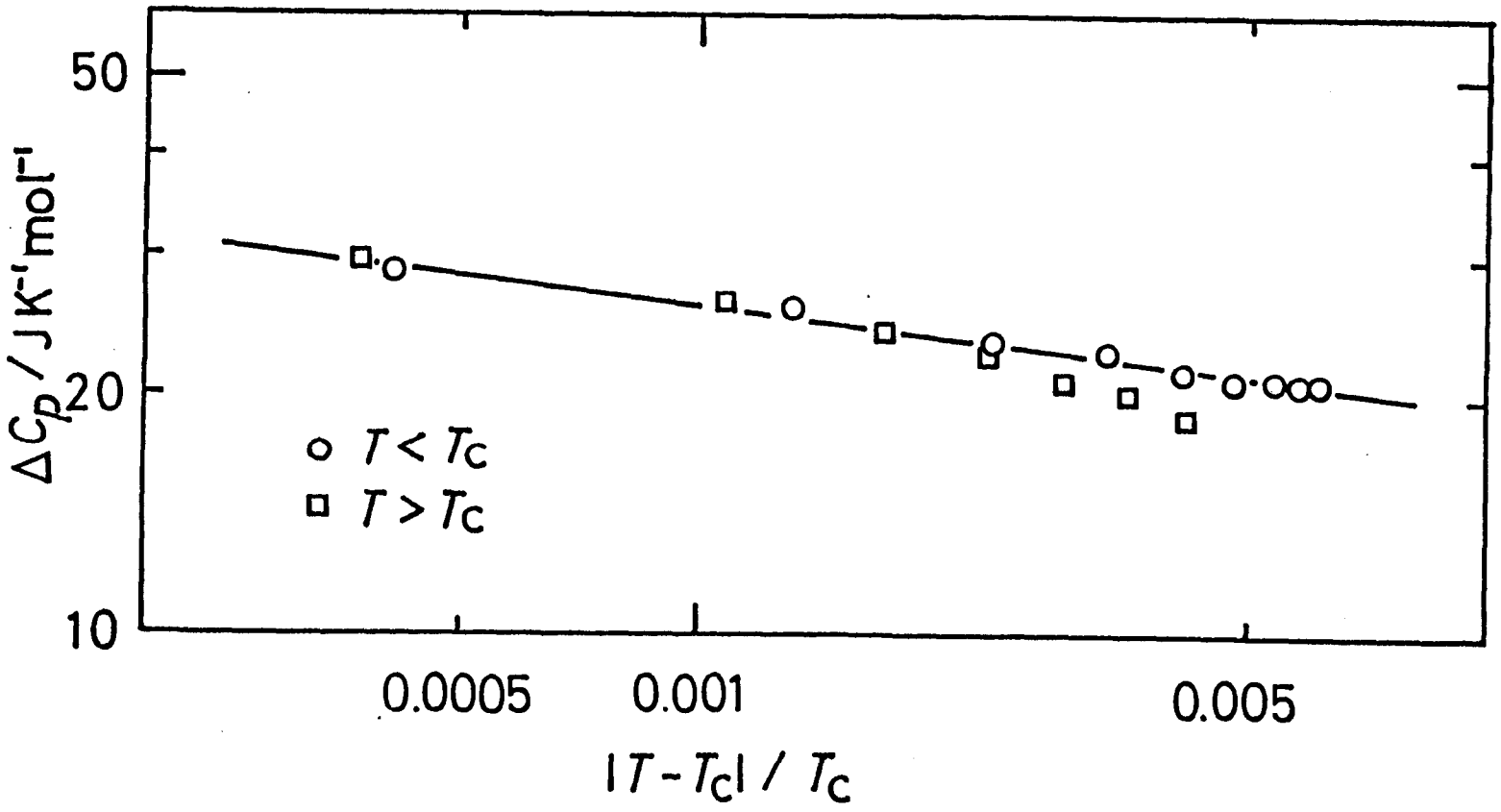

Figure III-13. Determination of the critical exponent at the twist transition of p-terphenyl.

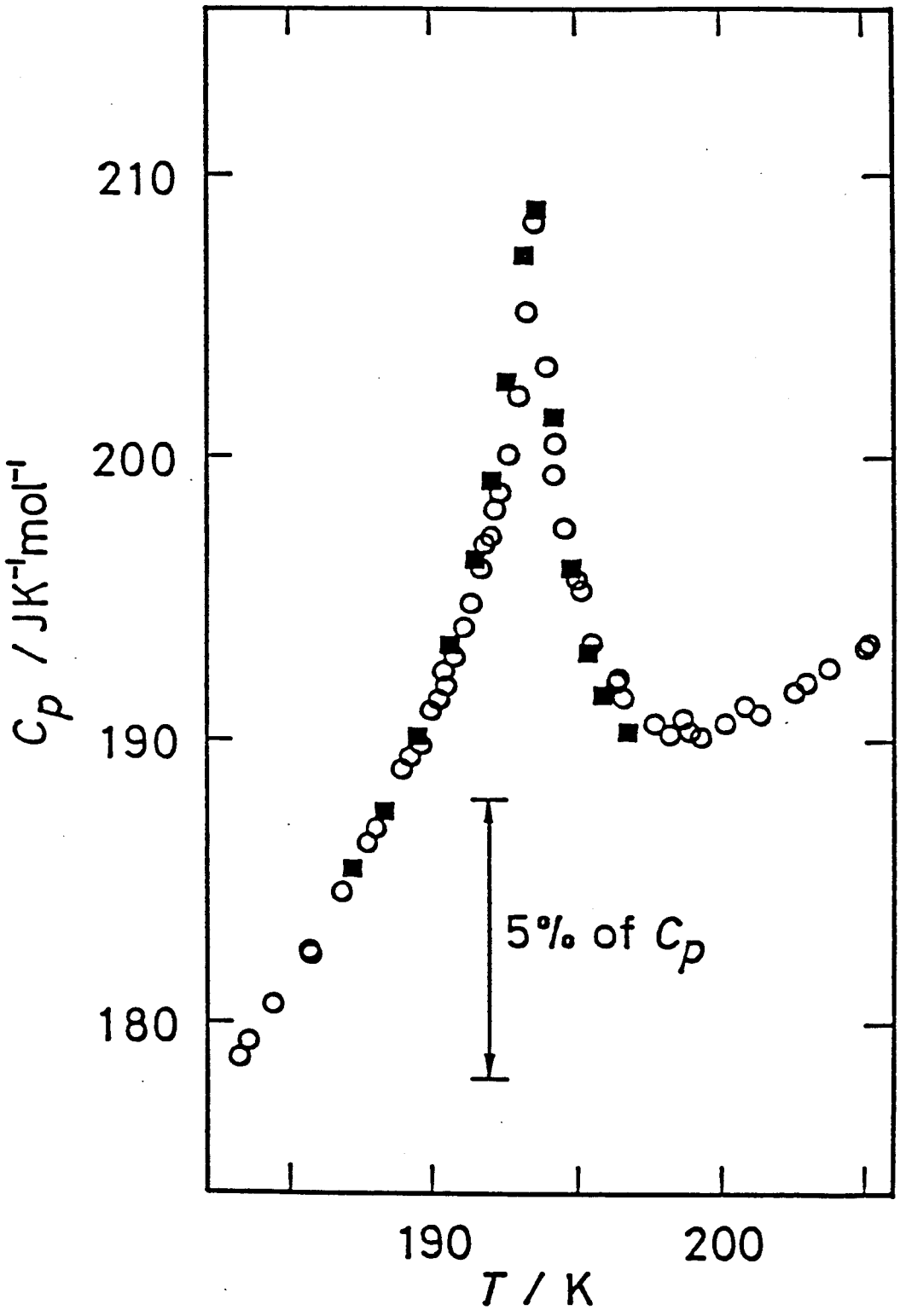

Figure III-14. Comparison of the anomaly due to the twist transition of p-terphenyl between the melted (square) and the non-melted (circle) samples.

to the report by Chen et al.[54]

Properties of the phase transitions are summarized in Table III-12. The heat capacity values reported for p-terphenyl by Chang[53] are in good agreement with ours. The differences in the enthalpy and the entropy of transition reflect the difference in the estimation of the normal portion. The value of the entropy of transition (1.63 $J \cdot K^{-1} \cdot mol^{-1}$) is extremely larger than that of biphenyl although it is smaller than Rln2 ($\simeq$ 5.76 $J \cdot K^{-1} \cdot mol^{-1}$). The transition temperature is also much higher than biphenyl. These are consistent with order-disorder nature of the transition[11,51] of p-terphenyl.

III-2-3 p-Quaterphenyl

Experimental

Commercially available p-quaterphenyl (nominal purity 99.9 moles per cent, Tokyo Kasei Kogyo Co., Ltd.) was purified further by fractional sublimation at about 470 K.

The powdered specimen, which weighed 9.9818 g (0.032577 mol) in vacuum, was loaded into the calorimeter vessel. The calorimeter was evacuated and sealed after the addition of a small amount of helium gas for heat exchange (8 kPa at room temperature); the

contribution of the helium to the total heat capacity was negligibly small. The sample contributed about 50 per cent to the total heat capacity including that of the calorimeter vessel below 20 K. As the temperature increased, the contribution of the sample decreased to 29 per cent at 100 K. Above 100 K, however, it increased again up to 43 per cent at room temperature.

The working thermometers, and the apparatus and the operation of the adiabatic calorimeter were the same as used in the measurements on biphenyl and biphenyl-d_{10}.

Results and Discussion

The measured molar heat capacities are shown in Figure III-15 and tabulated in Table III-10 in chronological order. The temperature increment due to each energy input may be deduced from the adjacent mean temperatures; it was small enough to permit the curvature correction to be ignored in comparison with the experimental precision. After each energy input, thermal equilibrium within the vessel was attained in about 2 min below 15 K, 10 min at about 50 K, 20 min at about 150 K, and 10 min above 200 K. Concerning thermal equilibration, no anomalous behavior was observed in the transition region.

Some thermodynamic functions at rounded temperatures were calculated from the primary results and given in Table III-11, in which the small

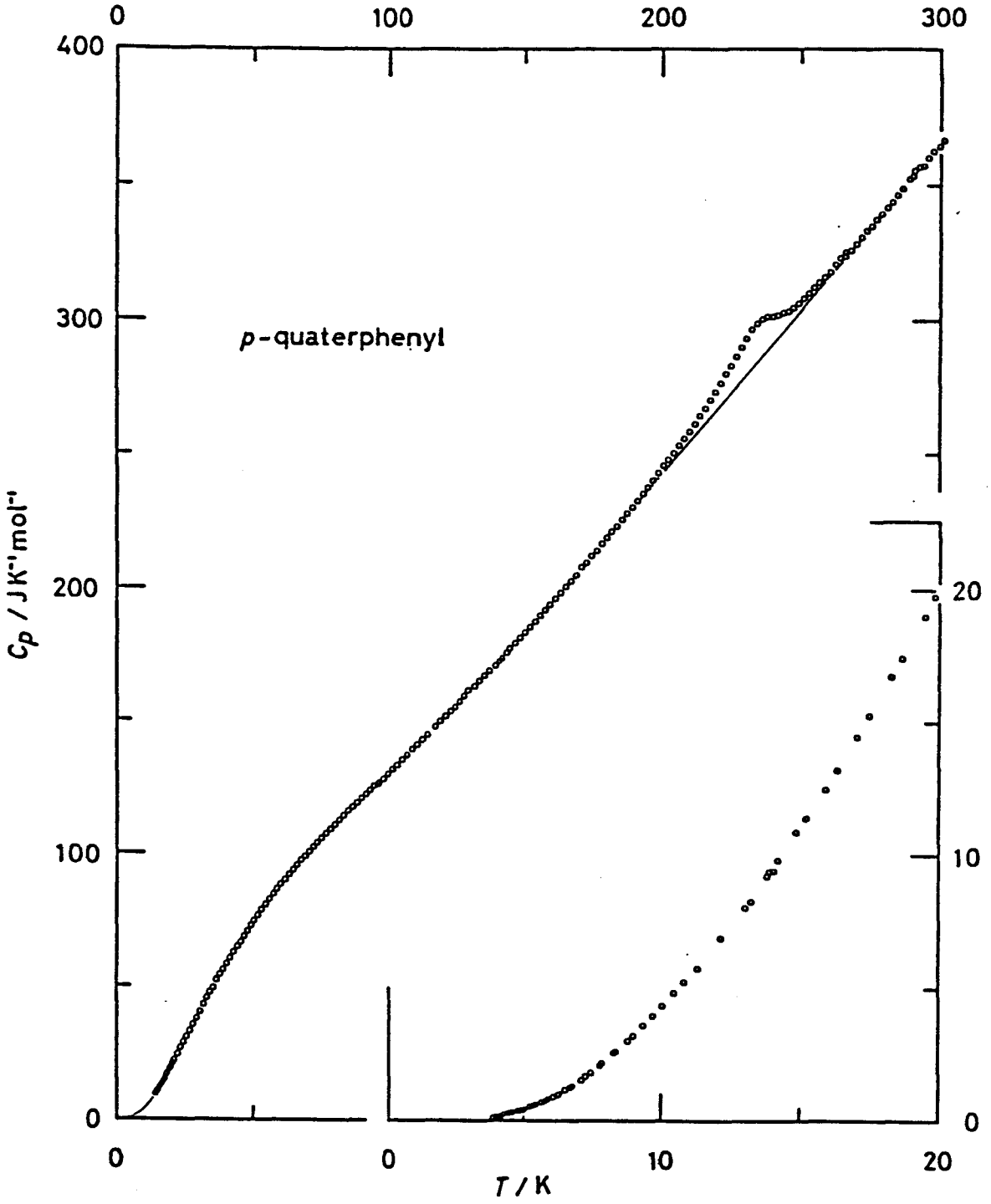

Figure III-15. Measured molar heat capacities of p-quaterphenyl.

Table III-10. Measured molar heat capacities of *p*-quaterphenyl.

T / K	C_p / J·K^{-1}·mol^{-1}	T / K	C_p / J·K^{-1}·mol^{-1}	T / K	C_p / J·K^{-1}·mol^{-1}	T / K	C_p / J·K^{-1}·mol^{-1}
Series 1		7.767	2.099	34.290	47.842	81.930	112.57
4.223	0.251	8.342	2.613	35.505	49.473	83.538	114.21
4.580	0.337	8.981	3.192	36.676	52.280	85.145	115.79
4.976	0.474	9.698	3.958	37.818	54.304	86.755	117.35
5.421	0.623	10.484	4.804	38.974	56.273	88.365	118.93
5.865	0.811	11.310	5.724	40.227	58.523	89.978	120.59
6.295	1.036	12.131	6.861	41.524	60.687	91.592	122.27
6.696	1.276	12.953	7.935	42.787	62.827	Series 8	
7.073	1.533	13.796	9.204	44.041	64.848	93.186	123.48
7.450	1.828	Series 4		45.290	66.786	94.749	125.28
7.851	2.175	14.858	10.872	46.553	68.748	96.387	126.79
8.288	2.556	15.902	12.476	47.833	70.748	Series 9	
8.776	3.011	17.071	14.474	49.116	72.754	96.237	126.25
9.342	3.586	18.315	16.740	50.443	74.689	97.912	128.08
10.030	4.331	19.530	18.993	51.826	76.646	99.641	129.89
10.829	5.233	20.694	21.232	53.210	78.655	101.401	131.53
Series 2		Series 5		54.627	80.651	103.195	133.28
3.884	0.161	14.186	9.795	56.077	82.519	105.008	135.23
4.099	0.239	15.211	11.381	57.520	84.492	106.827	137.21
4.419	0.306	16.334	13.210	58.960	86.394	108.654	139.17
4.804	0.407	17.511	15.267	60.398	88.285	110.488	140.98
5.227	0.553	18.694	17.435	61.858	89.973	112.316	142.92
5.663	0.726	19.909	19.741	63.344	91.873	114.123	144.72
6.093	0.921	21.126	22.046	64.834	93.651	Series 10	
6.506	1.154	22.311	24.356	66.331	95.400	117.152	147.71
Series 3		23.483	26.745	67.812	97.160	118.954	149.85
3.951	0.190	Series 6		69.251	98.852	120.769	151.67
4.210	0.222	24.567	28.868	Series 7		122.582	153.55
4.498	0.327	25.623	30.962	70.712	100.40	124.393	155.02
4.887	0.429	26.749	33.223	72.247	102.25	126.203	157.17
5.331	0.589	27.931	35.493	73.812	103.94	128.010	159.07
5.811	0.793	29.169	37.930	75.413	105.60	129.817	161.23
6.288	1.030	30.450	40.475	77.055	107.33	131.697	162.96
6.754	1.323	31.746	43.027	78.689	109.14	133.617	164.97
7.237	1.669	33.033	45.540	80.313	110.86	135.503	167.06

Table III-10. (continued).

T / K	C_p / J·K^{-1}·mol^{-1}	T / K	C_p / J·K^{-1}·mol^{-1}	T / K	C_p / J·K^{-1}·mol^{-1}	T / K	C_p / J·K^{-1}·mol^{-1}
137.389	169.07	181.861	220.81	226.478	286.32	271.460	330.66
139.257	171.01	Series 14		228.312	289.75	273.328	333.05
141.109	173.06	181.749	220.43	230.192	292.85	275.205	334.85
Series 11		183.617	223.11	232.061	296.46	277.090	337.28
144.793	177.15	185.487	225.41	233.936	298.66	278.982	339.52
146.636	179.29	187.360	227.94	235.817	300.29	280.866	341.65
148.481	181.15	189.236	230.14	237.691	301.26	282.727	343.65
150.328	183.21	191.102	232.64	239.560	301.32	284.596	346.40
152.176	185.27	192.956	235.24	241.426	301.92	286.473	348.66
154.028	187.49	194.816	237.60	243.287	302.68	288.341	351.01
155.867	189.63	196.679	240.21	245.159	303.24	290.218	353.26
157.708	191.69	198.545	242.78	247.040	304.55	292.102	355.66
159.551	193.86	200.416	245.61	248.914	306.35	293.979	357.36
161.390	196.04	202.276	247.91	250.781	308.09	295.849	359.83
163.253	198.28	204.142	250.42	252.656	309.83	297.713	362.25
165.133	200.63	206.012	253.21	254.539	312.03	299.585	364.10
Series 12		207.871	255.65	256.414	313.92	301.467	366.27
166.994	202.52	209.736	258.43	258.296	315.89	Series 16	
168.848	204.95	211.606	261.29	260.188	317.62	288.784	352.21
170.706	207.06	213.480	264.36	262.071	320.59	290.641	355.40
172.566	209.44	215.359	267.06	263.946	322.96	292.506	356.64
174.428	212.04	217.227	270.14	265.813	325.11	Series 17	
176.292	214.00	219.083	273.18	Series 15		141.906	173.52
Series 13		220.943	276.47	265.822	323.85	143.722	175.59
178.139	216.53	222.807	279.84	267.699	325.85		
179.998	218.76	224.661	282.63	269.584	328.27		

Table III-11. Molar thermodynamic functions of *p*-quaterphenyl.

T / K	C_p / J·K^{-1}·mol^{-1}	$\{H(T)-H(0)\}/T$ / J·K^{-1}·mol^{-1}	$S(T)-S(0)$ / J·K^{-1}·mol^{-1}	$-\{G(T)-H(0)\}/T$ / J·K^{-1}·mol^{-1}
5	0.469	0.114	0.146	0.032
10	4.28	1.09	1.41	0.33
20	19.94	6.23	8.67	2.44
30	39.63	14.07	20.46	6.39
40	58.08	22.82	34.45	11.63
50	74.02	31.50	49.17	17.66
60	87.70	39.75	63.90	24.14
70	99.67	47.47	78.33	30.86
80	110.52	54.69	92.36	37.67
90	120.63	61.46	105.97	44.51
100	130.19	67.85	119.17	51.32
110	140.49	73.98	132.06	58.08
120	150.82	79.96	144.73	64.77
130	161.14	85.80	157.20	71.40
140	171.80	91.56	169.54	77.97
150	182.84	97.28	181.76	84.48
160	194.41	102.98	193.93	90.94
170	206.24	108.71	206.07	97.36
180	218.48	114.46	218.20	103.74
190	231.27	120.27	230.35	110.08
200	244.74	126.16	242.56	116.40
210	258.86	132.14	254.83	122.70
220	274.72	138.25	267.23	128.99
230	292.98	144.57	279.84	135.27
240	301.70	151.00	292.55	141.56
250	307.23	157.10	304.95	147.85
260	317.50	163.07	317.20	154.13
270	328.80	169.00	329.39	160.39
280	340.74	174.92	341.56	166.64
290	352.80	180.84	353.73	172.89
300	364.74	186.78	365.89	179.12
298.15	362.52	185.68	363.64	177.96

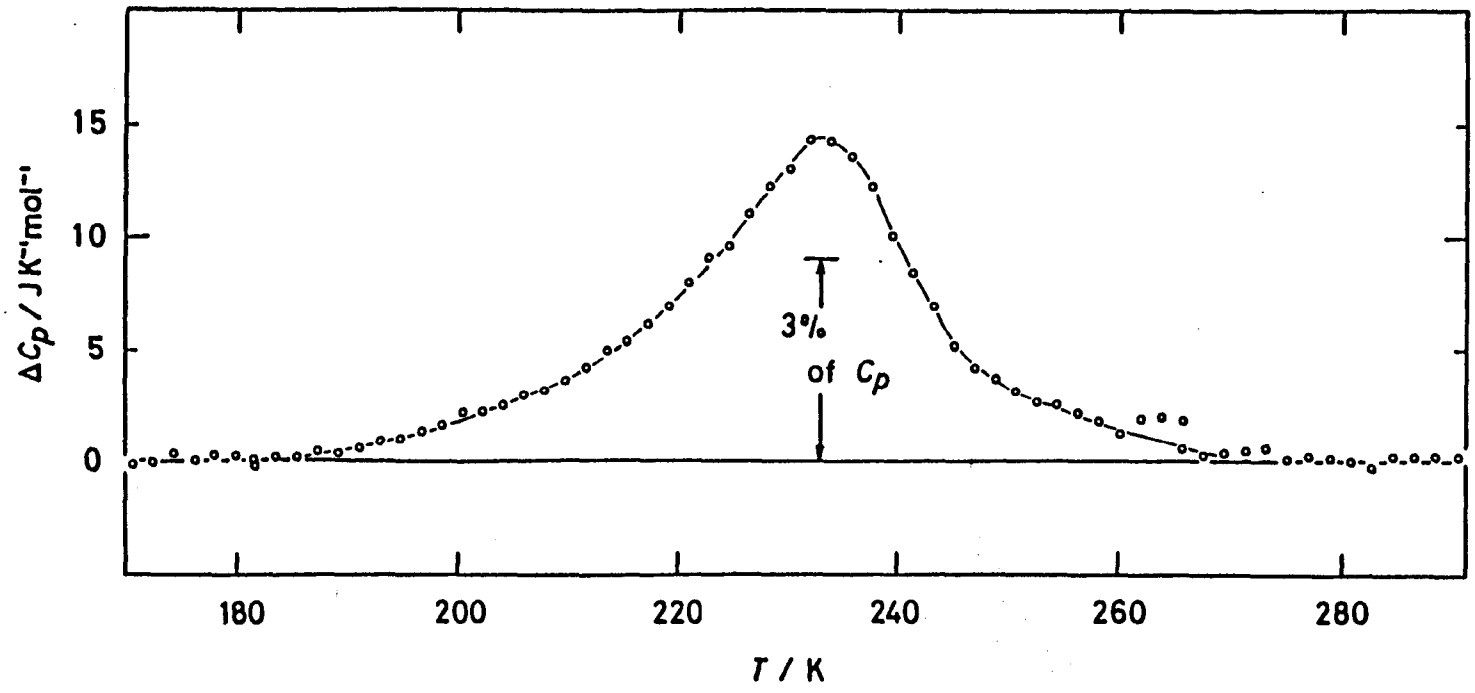

Figure III-16. Excess molar heat capacities of p-quaterphenyl.

Table III-12. Properties of phase transitions of *p*-polyphenylenes.

		biphenyl		*p*-terphenyl	*p*-quaterphenyl
H	T_{trs} / K	16.8 ± 0.1	40.4 ± 0.2	193.5 ± 0.1	233.0 ± 0.5
	region / K	15.3 - 18.3	30 - 47	145 - 225	180 - 270
	$\Delta_{trs}H$ / J·mol^{-1}	0.15 ± 0.02	5.02 ± 0.08	304 ± 20	414 ± 20
	$\Delta_{trs}S$ / J·K^{-1}·mol^{-1}	0.009 ± 0.001	0.129 ± 0.003	1.63 ± 0.10	1.82 ± 0.10
D	T_{trs} / K	20.2 ± 0.1	36.8 ± 0.2	180.3 ± 0.1	
	region / K	18.5 - 22.5	28 - 44	130 - 210	
	$\Delta_{trs}H$ / J mol^{-1}	0.18 ± 0.004	4.61 ± 0.08	288 ± 20	
	$\Delta_{trs}S$ / J K^{-1} mol^{-1}	0.009 ± 0.002	0.128 ± 0.003	1.63 ± 0.10	

contributions below 4 K were evaluated by smooth extrapolation to 0 K.

As seen in Figure III-15, the twist transition is observed as a broad anomaly with a heat capacity maximum at 233.0 K. The excess heat capacities due to the phase transition was obtained subtracting the normal portion of the heat capacity by drawing a smooth interpolating curve between the lower and the higher temperature sides as shown by the solid line in Figure III-15. The shape and the magnitude of the anomaly thus determined can be seen in Figure III-16, which extend over a very wide temperature range of about 90 K. The shape of the anomaly indicates that the transition is of higher-order.

Properties of the phase transition is given in Table III-12. The entropy of transition is the largest and the transition temperature is the highest in the first three members of p-polyphenylenes.

III-3 Qualitative interpretation of twist phase transitions of p-polyphenylenes

It is interesting to compare the three lowest members of the p-polyphenylenes with regard to behavior at the twist transition. In biphenyl, the transition temperature is the lowest of the three and the entropy

value of the transition and the shape of the heat capacity anomaly are consistent with displacive nature of the transition associated with soft modes.[29-32)]

p-Quaterphenyl also shows a broad anomaly which extends over a wide temperature range comparable to the case of biphenyl (about 40 per cent of the center temperature of the transition). However, the entropy of transition is larger by a factor of 14 than that of biphenyl although it is smaller than Rln2, which is expected if the mechanism of the transition is of a simple order-disorder type arising from the twisting of the molecule about the central C-C bond.

p-Terphenyl is different from the other two in regard to the shape of the heat capacity anomaly, i.e. it is more like an Ising spin transition. The entropy of transition is, on the other hand, close to that in p-quaterphenyl. A critical phenomenon is reported for this transition.[32,63-69)]

The reason why the transition temperatures are in the order of increasing molecular size may be understood if we take into account the increasing number of interacting atom pairs between adjacent molecules and within a molecule as the molecular size becomes larger.[84)] It is therefore the overall combination of those intermolecular and intramolecular interactions that determines the force constant for the twisting motion.

The twisting of phenyl rings in a molecule is a

result of a subtle balancing of various forces. Inside a molecule, the repulsion between hydrogen atoms at the ortho positions favors the twisted conformation but delocalization of π-electrons is against it. Therefore, there must be an optimum twisting angle. Usually such a double-minimum potential tends to cause an order-disorder type of transition if there is a mechanism by which the probability of a molecule to assume one of the two minima is strongly dependent on the orientation of the neighboring molecules, i.e. a kind of stochastic effect. However, if dynamical coupling between neighboring molecules is such that there is a dispersion in a branch of the vibrational spectrum dependent on temperature, a soft mode transition would occur. In the intermediate cases, the stochastic and dynamical effects may be present at various ratio.

It probably depends on the distribution of vibrational modes whether the stochastic or the dynamical effects prevails in a particular substance. For biphenyl the dynamical effect plays a more important role while p-terphenyl seems to lie at the other extreme case where the stochastic mechanism is dominant.

Such situation may have a certain relation to the intramolecular twisting modes. As discussed in Chapter II, there are two intramolecular twisting modes in

p-terphenyl and three in p-quaterphenyl if phenyl rings are treated as rigid and the molecular symmetry as D_{2h}. Biphenyl has only one twisting mode. It has been demonstrated that the twisting force-constant in biphenyl is small and that the coupling between the twisting degree of freedom and translational and rotational ones must be taken into account on considering the lattice vibration of biphenyl crystal.[45,85-88] It is also shown by a lattice-dynamics calculation that the small force constant can explain the low temperature heat capacities (see Chapter IV). If one compares the shape of the anomalous portion of the heat capacity in p-quaterphenyl with that in biphenyl, one can infer that there must be twisting mode or modes in the p-quaterphenyl molecule that have small force constants. That is the A_u mode, which has only one node as shown in Chapter II, oscillates in the same way as the biphenyl molecule and has a small force constant. In contrast to this, the two modes of p-terphenyl oscillate with larger force constant.

It is difficult to make quantitative calculations at this time because of lack of detailed information of the crystal structure, the intra- and intermolecular interactions, etc. However, it is possible qualitatively to understand the behavior of the three substances by using the composite model outlined here, and the isotope effect that the transition temperature

shift to the lower temperature on deuteration will also be rationalized within this model.

III-4 Ising type theory for p-terphenyl crystal

The examination of the crystal structures of p-polyphenylenes makes us to expect that the interaction within the ab plane is much stronger than in the direction of the c axis, because the nearest neighbor distance between the molecular center of mass in the ab plane is 0.49 nm in contrast to 1.35 nm in the c direction in the case of p-terphenyl. Indeed, the two dimensionality has been reported experimentally.[52,61-64]

The room temperature phase of p-terphenyl is, as described in Section III-1, the disordered one. Therefore, we do the examination based on the low temperature ordered structure.[27] The structure viewed along the c axis is schematically shown in Figure III-17, where Roman numerals distinguish translationally inequivalent molecules. The solid line represents the triclinic unit cell, and the broken line shows the cell having the lattice constants 2a and 2b in terms of those of the room temperature phase. The intermolecular distances between the centers of mass are $R_{I-II} = R_{II-III} = R_{III-IV} = R_{IV-I} = 0.487$ nm,

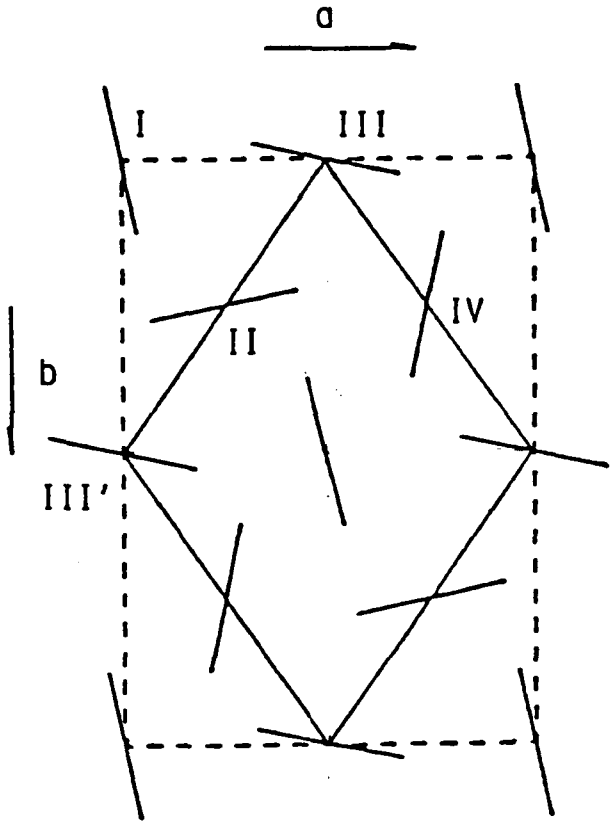

Figure III-17. Crystal structure of the low temperature phase of p-terphenyl viewed along the c axis (schematic). Broken line represents 4 unit cells of the room temperature phase.

$R_{I-III} = R_{II-IV} = 0.555$ nm in the ab plane, and $R_{I-I} = R_{II-II} = R_{III-III} = R_{IV-IV} = 1.353$ nm in the c direction. Roughly estimated molecular dimension is 1.350×0.423 nm^2.

It was assumed that the intermolecular interaction was expressed by the sum of interatomic potentials of Buckingham type, with parameters also used in Chapter II.

Since the "spin" in this case corresponds to the twisting of the central phenyl ring with respect to the plane determined by the two outer phenyl rings, the atomic positions of "wrong" molecules must be calculated first from those of "right" molecules reported experimentally.[27] The atomic positions of "wrong" molecules were calculated under the conditions; no translation of the molecular center of mass and no rotation of the principal axes of the moment of inertia tensor. Summation was made over all the atom pairs within the molecule pair under consideration.

The calculated intermolecular and inter-"spin" interactions are summarized in Table III-13, where the inter-"spin" interaction energy is defined as,

$$J = \frac{1}{2}(E_{r-r} + E_{w-w}) - \frac{1}{2}(E_{r-w} + E_{w-r}).$$

It is clear that the interaction within the ab plane are much stronger than those perpendicular to the plane, and that the values for the inter-"spin" interaction energies for the I-III and II-IV pairs are

Table III-13. Calculated inter-"spin" interaction energies within the ab plane (upper) and along the c axis (lower). r, "right" molecule; w, "wrong" molecule.

$J = \frac{1}{2}(E_{r-r} + E_{w-w}) - \frac{1}{2}(E_{r-w} + E_{w-r})$.

	E_{r-r} / kJ·mol^{-1}	E_{r-w} / kJ·mol^{-1}	E_{w-r} / kJ·mol^{-1}	E_{w-w} / kJ·mol^{-1}	J / kJ·mol^{-1}
I - II	-39.54	-39.46	-39.72	-39.75	-0.06
II -III	-39.98	-39.91	-37.64	-39.21	-1.17
III- IV	-38.75	-36.86	-36.59	-37.97	-1.64
IV - I	-39.80	-38.60	-39.00	-38.89	-0.55
I -III	-28.59	-22.72	-13.90	-28.55	-10.26
II - IV	-28.28	-20.65	-25.43	-28.32	-5.26
I - I	-7.25	-7.34	-7.34	-7.43	0.00
II - II	-7.28	-7.14	-7.14	-6.97	0.02
III-III	-7.40	-7.10	-7.10	-6.76	0.02
IV - IV	-7.16	-7.13	-7.13	-7.06	0.02

larger than those for the I-II, II-III, III-IV and IV-I pairs. The later indicates the importance of the colinearlity of the molecular figure axes in the decision of the intermolecular interaction, which suggests the penetrating sublattice model (shown in Figure III-18) for the twist phase transition of p-terphenyl.

The penetrating sublattice model is reduced to the rectangular model neglecting the inter-sublattice interaction because of its small values (Table III-13), where the anisotropy in the ab plane is also neglected for simplicity. The heat capacity of the two dimensional rectangular Ising model is given by[89]

$$C/Nk_B = \frac{2}{\pi}(L \coth 2L)^2\left\{2K_1 - 2E_1 - (1-\kappa_1'')\left(\frac{\pi}{2} + \kappa_1'' K_1\right)\right\},$$

$$L = J / 2k_B T ,$$

$$K_1 = 2\tanh 2L / \cosh 2L ,$$

$$\kappa_1'' = 2\tanh^2 2L - 1 ,$$

$$K_1 = \int_0^{\pi/2} \frac{d\varphi}{\sqrt{1-\kappa_1^2 \sin^2\varphi}} ,$$

$$E_1 = \int_0^{\pi/2} \sqrt{1-\kappa_1^2 \sin^2\varphi}\, d\varphi .$$

The theoretical heat capacity curve with T_c = 193.5 K is shown in Figure III-19. There exist large tails on both the lower and the higher temperature sides of the transition.

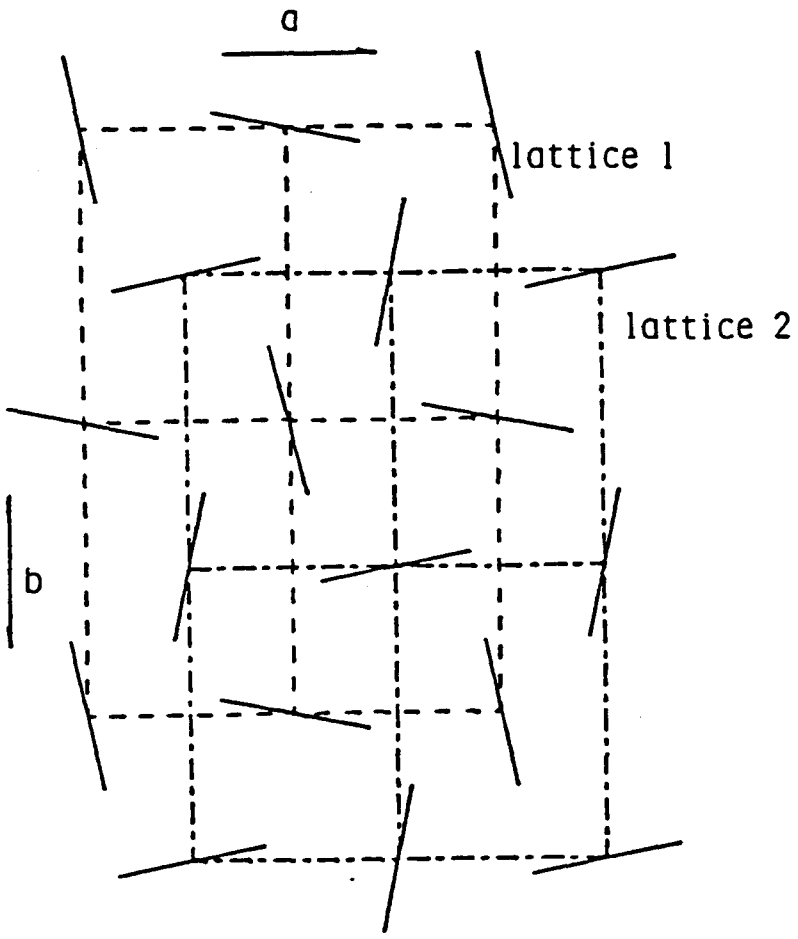

Figure III-18. Penetrating sub-lattice model for the twist phase transition of p-terphenyl.

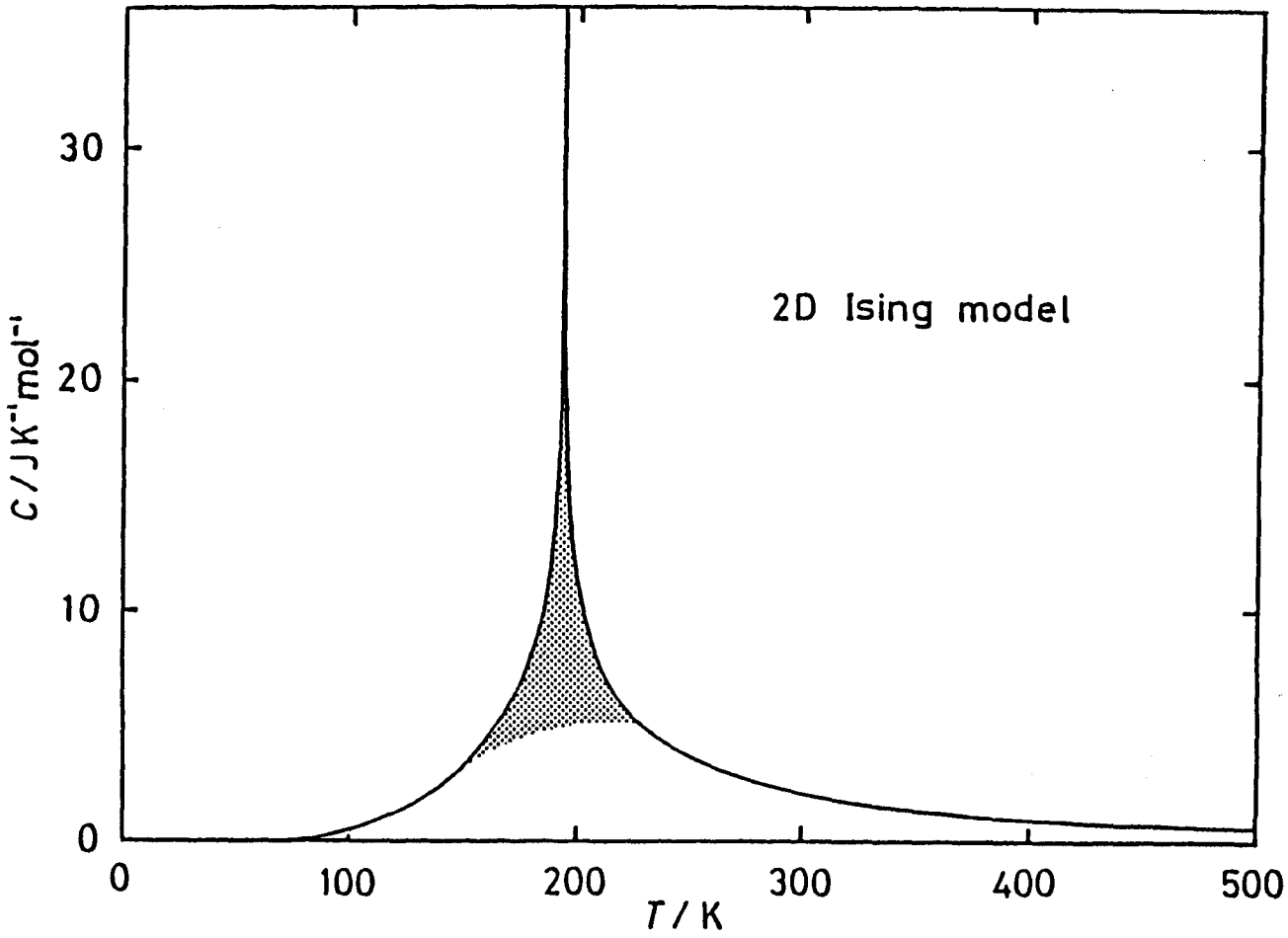

Figure III-19. Heat capacity of the two-dimensional square lattice of Ising model with the critical temperature of 193.5 K.

The experimental excess heat capacities due to the transition were obtained by subtracting the effective normal portion (Section III-2-2), which was determined by drawing the smooth interpolating curve. Therefore, the "excess" part of the theoretical heat capacity should be separated also in the same manner as the experimental for the sake of consistent comparison. This was done by drawing the smooth interpolating curve in the transition region experimentally determined (145 K to 225 K), and the "excess part" is shadowed in Figure III-19.

The comparison of the experimental and the theoretical excess heat capacities is shown in Figure III-20. The agreement of the curves is satisfactory.

It is well known that the heat capacity of the two dimensional Ising model diverges as $\ln|T-T_c|$ at T_c and gives the critical exponent $\alpha = 0$. On the other hand, the experimental value is not 0 but 0.13. However, the discrepancy is not crucial because the exact formula of the heat capacity given above gives the slope of about 0.1 at $|T-T_c|/T_c \simeq 0.001$, where the experiments were done.

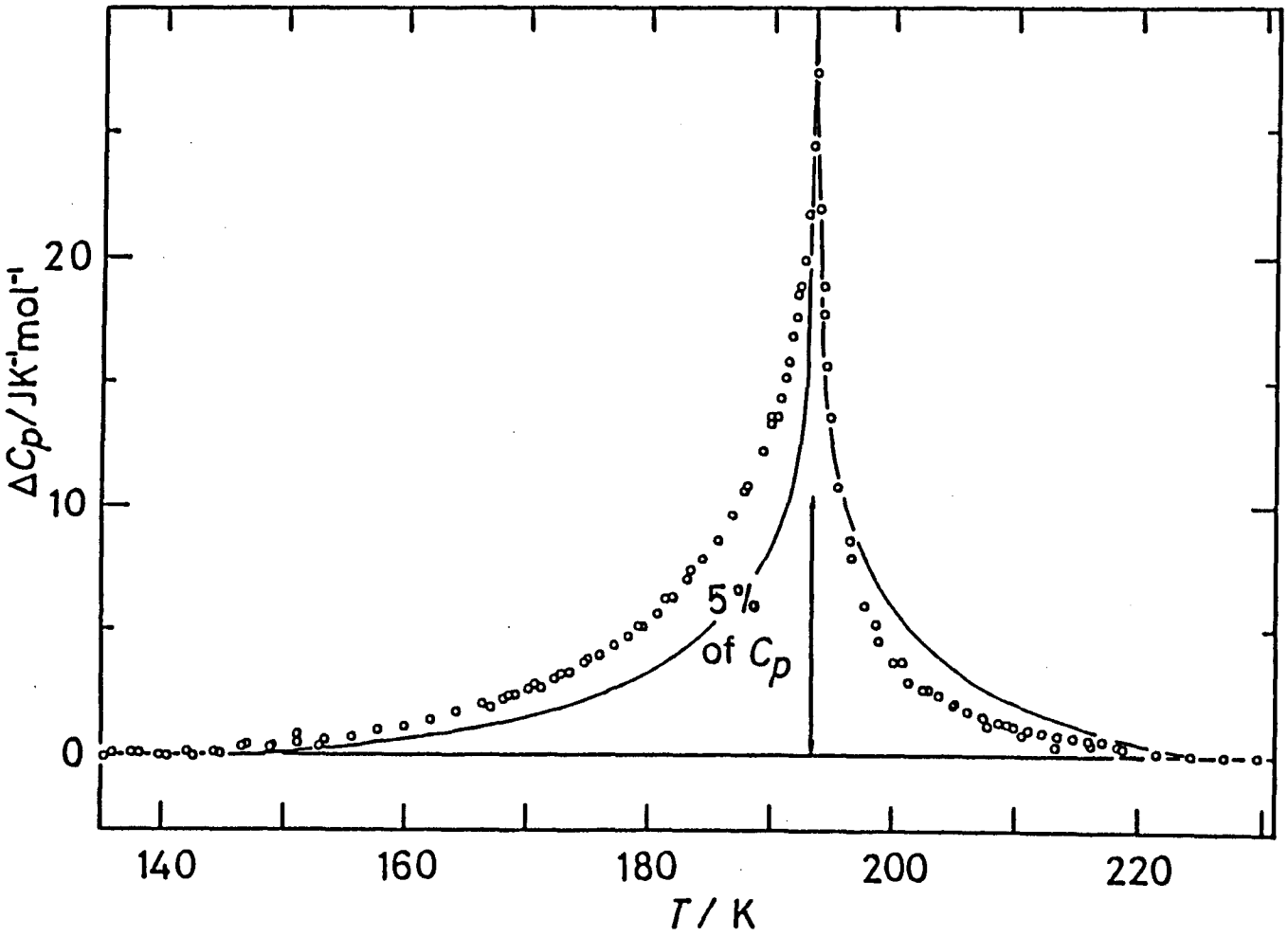

Figure III-20. Comparison between the measured (open circle) and the calculated (solid curve) excess heat capacities due to the twist transition of p-terphenyl.

References to Chapter III

1. G. L. Clark and L. W. Pickett, J. Am. Chem. Soc., 53(1931), 167.
2. J. Dhar, Indian J. Phys., 7(1932), 43.
3. J. Trotter, Acta Cryst., 14(1961), 1135.
4. G. B. Robertson, Nature, 191(1961), 593.
5. A. Hargreaves and S. H. Rizvi, Acta Cryst., 15(1962), 365.
6. V. M. Kozhin and K. V. Mirskaya, Sov. Phys. Cryst., 14(1970), 938.
7. G. P. Charboneau and Y. Delugeard, Acta Cryst., B32(1976), 1420.
8. G. P. Charboneau and Y. Delugeard, Acta Cryst., B33(1977), 1586.
9. H. M. Rietveld, E. N. Maslen and C. J. B. Clews, Acta Cryst., B26(1970), 693.
10. P. J. L. Baudour, Acta Cryst., B28(1972), 1649.
11. P. J. L. Baudour, H. Cailleau and W. B. Yelon, Acta Cryst., B33(1977), 1773.
12. Y. Delugeard, J. Desuche and J. L. Baudour, Acta Cryst., B32(1976), 702.
13. O. Bastiansen, Acta Chem. Scand., 3(1949), 408.
14. J. Dale, Acta Chem. Scand., 11(1957), 640; ibid 11(1957), 650.
15. H. Suzuki, Bull. Chem. Soc. Jpn., 32(1959), 1340.
16. V. J. Eaton and D. Steele, J. Chem. Soc. Faraday II, 69(1973), 1601.

17. A. J. Grumadas and P. Poshkus, J. Chem. Soc. Faraday II, 75(1979), 1398.
18. A. J. Grumadas, D. P. Poshkus and A. V. Kiselev, J. Chem. Soc. Fararday II, 78(1982), 2013.
19. H. Kuwata, J. Sci. Hiroshima Univ. Ser A-II, 32(1968), 87.
20. S. Hino, K. Seki and H. Inokuchi, Chem. Phys. Lett., 36(1975), 335.
21. H. Cailleau, F. Moussa and J. Mons, Solid State Commun., 31(1979), 521.
22. A. Janner, T. Janssen and P. M. de Wolfe, Acta Cryst., A39(1983), 671.
23. H. Cailleau, J. L. Baudour and C. M. E. Zeyen, Acta Cryst., B35(1979), 426.
24. V. Heine and S. L. Price, J. Phys. C, 18(1985), 5259.
25. V. Petricek and P. Coppens, Acta Cryst., A41(1985), 478.
26. J. L. Baudour and M. Sanquer, Acta Cryst., B39(1983), 671.
27. P. J. L. Baudour, Y. Delugeard and H. Cailleau, Acta Cryst., B32(1976), 150.
28. J. L. Baudour, Y. Delugeard and P. Rivet, Acta Cryst., B34(1978), 625.
29. P. S. Friedman, P. Kopelman and P. N. Prasad, Chem. Phys. Lett., 24(1974), 15.

30. A. Bree and M. Edelson, Chem. Phys. Lett., 46(1977), 500.
31. M. Wada, A. Sawada and Y. Ishibashi, J. Phys. Soc. Jpn., 50(1980), 737.
32. H. Cailleau, A. Girard, F. Moussa and C. M. E. Zeyen, Solid State Commun., 29(1979), 259.
33. A. Dworkin and H. Cailleau, J. Phys. (Paris) Lett., 41(1980), L-83.
34. A. S. Cullick and R. E. Gerkin, Chem. Phys., 23(1977), 217.
35. A. S. Cullick and R. E. Gerkin, Chem. Phys. Lett., 42(1976), 589.
36. A. Bree and M. Edelson, Chem. Phys. Lett., 55(1978), 319.
37. T. Atake and H. Chihara, Solid State Commun., 35(1980), 131.
38. N. I. Wakayama, Chem. Phys. Lett., 83(1981), 413.
39. C. Ecolivet, M. Sanquer, J. Pellegrin and J. DeWitte, J. Chem. Phys., 78(1983), 6317.
40. D. Kirin, S. L. Chaplot, G. A. Mackenzie and G. S. Pawley, Chem. Phys. Lett., 102(1983), 105.
41. Y. Ishibashi, J. Phys. Soc. Jpn., 50(1981), 1255.
42. P. Toledano and M. Guilluy, Ferroelectrics, 54(1984), 211.
43. J. C. Toledano and P. Toledano, Jpn. J. Appl. Phys., 24(1985), Suppl. 24-2, (in press).
44. H. Cailleau, F. Moussa, C. M. E. Zeyen and J. Bouillot, to be published.

45. N. M. Plakida, A. V. Belushkin, I. Natkaniec and T. Wasintyński, Phys. Status Solidi b, 118(1983), 129.
46. W. R. Busing, Acta Cryst., A39(1983), 340.
47. H. Cailleau, F. Moussa, C. M. E. Zeyen and J. Bouillot, Solid State Commun., 33(1980), 407.
48. S. B. Liu and M. S. Conradi, Phys. Rev. Lett., 54(1985), 1287.
49. B. Wyncke, F. Brehad and A. Hadni, J. Phys. (Paris), 38(1977), 1171.
50. A. Girard, H. Cailleau, Y. Marqueton and C. Ecolivet, Chem. Phys. Lett., 54(1978), 479.
51. B. A. Bolton and P. N. Prasad, Chem. Phys., 35(1981), 331.
52. H. Cailleau and A. Dworkin, Mol. Cryst. Liq. Cryst., 50(1979), 217.
53. S. S. Chang, J. Chem. Phys., 79(1983), 6229.
54. M. C. Chen, A. S. Cullick, R. E. Gerkin and A. P. Lundstedt, Chem. Phys., 46(1980), 423.
55. J. O. Williams, Chem. Phys. Lett., 42(1976), 171.
56. N. I. Wakayama, Chem. Phys. Lett., 70(1980), 397.
57. N. I. Wakayama, S. Matsuzaki and M. Mizuno, Chem. Phys. Lett., 74(1980), 37.
58. N. I. Wakayama, S. Matsuzaki and M. Mizuno, Chem. Phys. Lett., 75(1980), 587.
59. Z. Burnstein and D. F. Williams, J. Chem. Phys., 68(1978), 983.

60. J. Funfschilling, L. Altwegg, I. Z. Granacher, M. Chabr and D. F. Williams, J. Chem. Phys., 70(1970), 4622.

61. H. Cailleau, J. L. Baudour, A. Girard and W. B. Yelon, Solid State Commun., 20(1976), 577.

62. H. Cailleau, J. L. Baudour, W. B. Yelon, A. Girard, Y. Delugeard and J. Desuche, J. Phys. (Paris), 37(1976), c1-233.

63. R. E. Lechner, B. Toudic and H. Cailleau, J. Phys. C, 17(1984), 405.

64. B. Toudic and R. E. Lechner, J. Phys. C, 17(1984), 5503.

65. T. Gullion, M. S. Conradi and A, Rigamonti, Phys. Rev. B, 31(1985), 4388.

66. H. Cailleau, A. Heidemann and C. M. E. Zeyen, J. Phys. C, 12(1979), L411.

67. Z. Pajak, N. Pislewski and J. Wasicki, Proc. XIth Sem. NMR, (1978), 190.

68. K. Kohda, N. Nakamura and H. Chihara, J. Phys. Soc. Jpn., 51(1982), 3936.

69. B. Toudic, J. Gallier, P. Rivet and H. Cailleau, Solid State Commun., 47(1983), 291.

70. T. Gullion and M. S. Conradi, Phys. Rev. B, 30(1984), 1133.

71. C. Ecolivet, B. Toudic and M. Sanquer, J. Chem. Phys., 81(1984), 599.

72. S. Ramdas and J. M. Thomas, J. Chem. Soc. Faraday II, 72(1976), 1251.

73. T. Atake and H. Chihara, J. Chem. Thermodyn., 3(1971), 51.

74. T. Atake and H. Chihara, Bull. Chem. Soc. Jpn., 47(1974), 2126.

75. T. Atake and H. Chihara, (unpublished); see also ref. 80.

76. T. Nakagawa et al., "SALS", Program Library, Computer Center, The University of Tokyo.

77. H. G. Huffman, G. S. Parks and A. C. Daniels, J. Am. Chem. Soc., 52(1930), 1547.

78. R. S. Bradley and T. G. Cleasby, J. Chem. Soc., (1953), 1690.

79. E. Morawetz, J. Chem. Thermodyn., 4(1972), 455.

80. K. Nomoto, T. Atake, B. K. Chaudhuri and H. Chihara, J. Phys. Soc. Jpn., 52(1983), 3475.

81. T. Atake, K. Nomoto, B. K. Chaudhuri and H. Chihara, J. Chem. Thermodyn., 15(1983), 339.

82. T. Atake, K. Nomoto, B. K. Chaudhuri and H. Chihara, J. Chem. Thermodyn., 15(1983), 383.

83. W. L. McMillan, Phys. Rev. B, 14(1976), 1496.

84. J. C. Raich and E. R. Bermstein, Mol. Phys., 53(1984), 597.

85. E. Burgos, H. Bonadeo and E. D'Alessio, J. Chem. Phys., 65(1976), 2460.

86. I. Natkaniec, A. V. Belushkin and T. Wasiutyński, Phys. Status Solidi b, 105(1981), 43.

87. H. Takeuchi, S. Suzuki, A. J. Dianoux and G. Allen, Chem. Phys., 55(1981), 153.

88. H. Bonadeo and E. Burgos, Acta Cryst.,A38(1982), 29.

89. L. Onsager, Phys. Rev., 65(1944), 117.

Chapter IV Crossover of low temperature heat capacities of p-polyphenylenes

In the course of thermodynamic studies on phase transitions of p-polyphenylenes, the interesting phenomenon that the heat capacity curve of biphenyl crosses those of p-terphenyl and p-quaterphenyl at low temperature was found. The results of heat capacity measurements on biphenyl, on p-terphenyl, and on p-quaterphenyl are shown in Figure IV-1 in terms of the corresponding Debye characteristic temperatures assuming 6 degrees of freedom per molecule. Below about 20 K, the heat capacity of biphenyl decreases less steeply than that of p-terphenyl as the temperature decreases, and they cross each other at about 12 K. The crossover between biphenyl and p-quaterphenyl is also observed at about 6 K. The situation is the same for the deuterated analogues (biphenyl-d_{10} and p-terphenyl-d_{14}).

Since the three compounds have a similar crystal structure and their intermolecular interactions are also similar, one would expect that the relative values of their heat capacities are primarily determined by the relative molecular mass, i.e. the heavier molecule should show a larger heat capacity in the low temperature region, where only low-lying lattice modes are excited. Therefore, there must be some motional

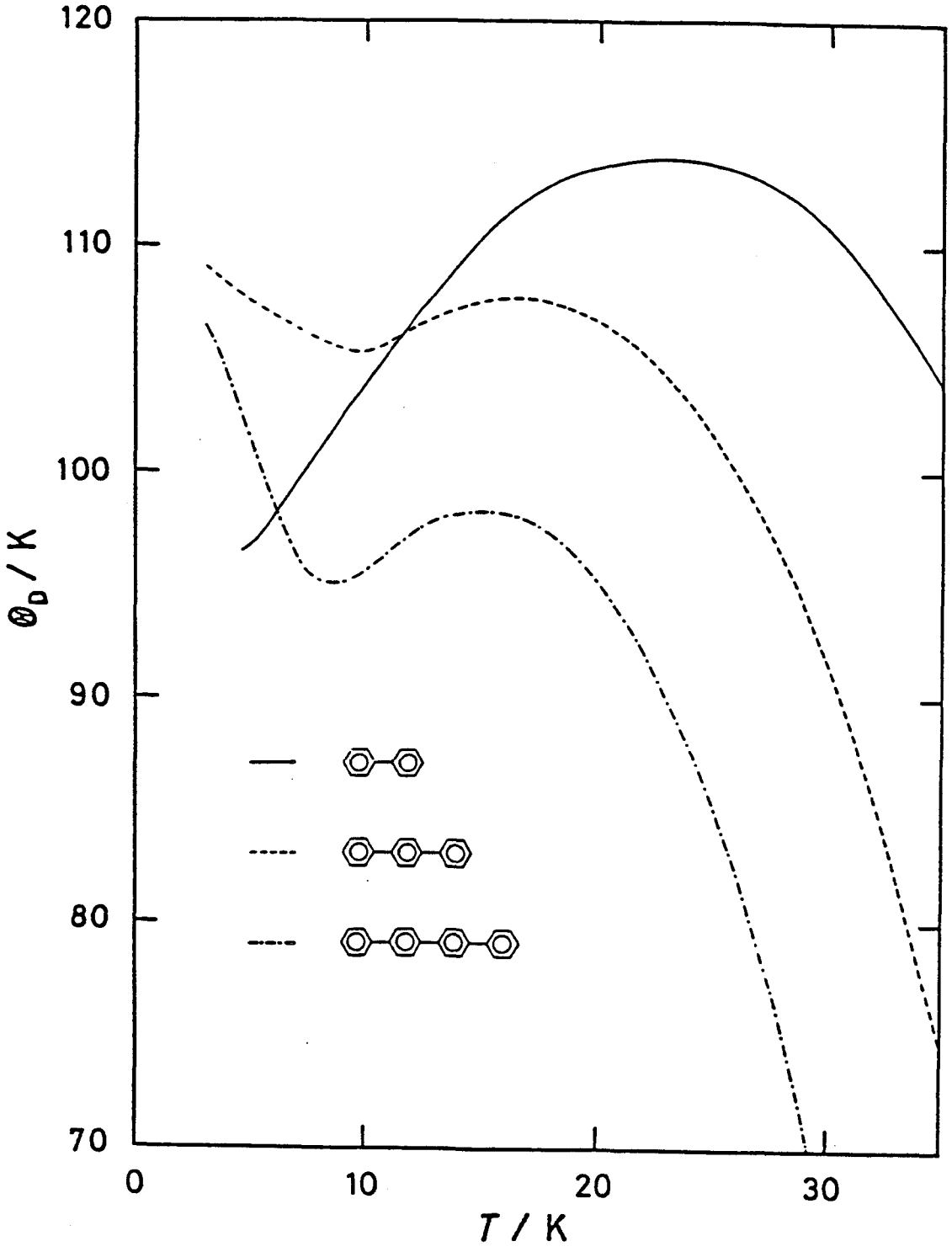

Figure IV-1. Debye characteristic temperatures corresponding to the measured heat capacities of biphenyl (solid curve), p-terphenyl (broken curve) and p-quaterphenyl (dot-dash curve), assuming 6 degrees of freedom per molecule.

mode or modes in biphenyl for which the force constant is much smaller than for the corresponding mode(s) in p-terphenyl and in p-quaterphenyl. It was suspected that the twisting mode about the central C-C bond in biphenyl would be the candidate of such a mode, because (1) the force constant for the twisting vibration in biphenyl would be, as discussed in Chapter II, smaller than those of p-terphenyl and p-quaterphenyl, (2) the coupling of the twisting motion with the lattice vibration has been pointed out in many experimental[1-3] and theoretical[1,2,4-6] studies of the lattice vibrations of biphenyl crystal, and (3) the twisted conformation in p-terphenyl and in p-quaterphenyl is established below their order-disorder transition[7-9] in contrast with biphenyl in which the incommensurate structure in the b direction continues to exist even below the lock-in transition at 16.8 K.[10,11]

It was then tried to rationalize the observed crossover by a simple model calculation of lattice vibration spectra for biphenyl and p-terphenyl crystals; the calculation was not made for p-quaterphenyl because the crossover between biphenyl and p-quaterphenyl must be explained in the same way. For biphenyl the average crystal structure at 22 K[12] (Figure IV-2) was adapted, ignoring the incommensurability[13] which will play an important role only in the very low temperature region where the

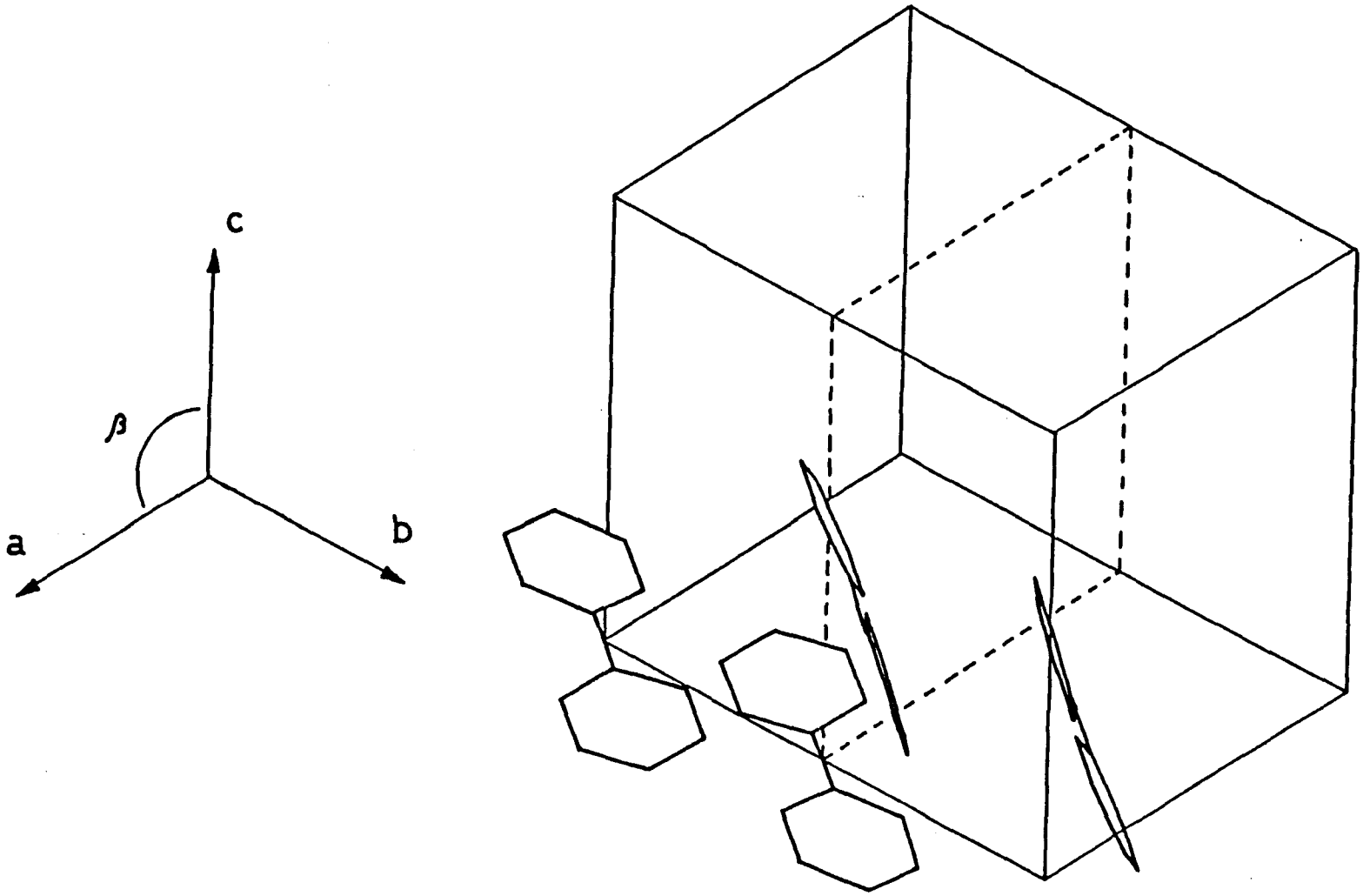

Figure IV-2. Average crystal structure of biphenyl at 22 K.[12]

contribution of phason becomes dominant.[14] The structure of p-terphenyl at 113 K[7] was corrected for thermal expansivity down to 22 K by the method of linear extrapolation using the room temperature data.[8]

The intermolecular interaction was expressed by the sum of atom-atom pair potentials of Buckingham type, in which the parameters were the same as in Chapters II and III.[15] The interactions were summed over molecules within the radius, 1 nm.

Phenyl rings are assumed to be rigid. Then, the Lagrangian L of the system is written in terms of translational (superscript; t), rotational (r), and twisting (τ) coordinates in the harmonic approximation as follows;[16]

$$L = T - V,$$

$$T = \frac{1}{2}\sum_{l}\sum_{\kappa}\sum_{\alpha} m\left[\dot{u}^{t}_{\alpha}(l\kappa)\right]^2 + \frac{1}{2}\sum_{l}\sum_{\kappa}\sum_{\alpha,\beta} I_{\alpha\beta}(\kappa)\dot{u}^{r}_{\alpha}(l\kappa)\dot{u}^{r}_{\beta}(l\kappa)$$

$$+ \frac{1}{2}\sum_{l}\sum_{\kappa} I_{\tau}\left[\dot{u}^{\tau}(l\kappa)\right]^2,$$

$$V = V_0 + \frac{1}{2}\sum_{l,l'}\sum_{\kappa,\kappa'}\sum_{\alpha,\beta}\Phi^{tt}_{\alpha\beta}(l\kappa;l'\kappa')u^{t}_{\alpha}(l\kappa)u^{t}_{\beta}(l'\kappa')$$

$$+ \frac{1}{2}\sum_{l,l'}\sum_{\kappa,\kappa'}\sum_{\alpha,\beta}\Phi^{tr}_{\alpha\beta}(l\kappa;l'\kappa')u^{t}_{\alpha}(l\kappa)u^{r}_{\beta}(l'\kappa')$$

$$+ \frac{1}{2}\sum_{l,l'}\sum_{\kappa,\kappa'}\sum_{\alpha,\beta}\Phi^{rt}_{\alpha\beta}(l\kappa;l'\kappa')u^{r}_{\alpha}(l\kappa)u^{t}_{\beta}(l'\kappa')$$

$$+ \frac{1}{2}\sum_{l,l'}\sum_{\kappa,\kappa'}\sum_{\alpha,\beta}\Phi^{rr}_{\alpha\beta}(l\kappa;l'\kappa')u^{r}_{\alpha}(l\kappa)u^{r}_{\beta}(l'\kappa')$$

$$+ \frac{1}{2}\sum_{l,l'}\sum_{\kappa,\kappa'}\sum_{\alpha} \Phi_{\alpha}^{tr}(l\kappa;l'\kappa')\,u_{\alpha}^{t}(l\kappa)\,u^{r}(l'\kappa')$$

$$+ \frac{1}{2}\sum_{l,l'}\sum_{\kappa,\kappa'}\sum_{\alpha} \Phi_{\alpha}^{rt}(l\kappa;l'\kappa')\,u^{r}(l\kappa)\,u_{\alpha}^{t}(l'\kappa')$$

$$+ \frac{1}{2}\sum_{l,l'}\sum_{\kappa,\kappa'}\sum_{\alpha} \Phi_{\alpha}^{r\tau}(l\kappa;l\kappa')\,u_{\alpha}^{r}(l\kappa)\,u^{\tau}(l'\kappa')$$

$$+ \frac{1}{2}\sum_{l,l'}\sum_{\kappa,\kappa'}\sum_{\alpha} \Phi_{\alpha}^{\tau r}(l\kappa;l'\kappa')\,u^{\tau}(l\kappa)\,u_{\alpha}^{r}(l'\kappa')$$

$$+ \frac{1}{2}\sum_{l,l'}\sum_{\kappa,\kappa'} \Phi^{\tau\tau}(l\kappa;l'\kappa')\,u^{\tau}(l\kappa)\,u^{\tau}(l'\kappa'),$$

$$\Phi_{\alpha\beta}^{ab}(l\kappa;l'\kappa') = \frac{\partial^2 V}{\partial u_{\alpha}^{a}(l\kappa)\,\partial u_{\beta}^{b}(l'\kappa')},$$

where u is a displacement from an equilibrium position, "·" denotes derivative with respect to time, and α and β mean x, y, or z. A cell in the crystal is labelled by l and a molecule in a cell is by κ. The equations of motion derived from the above Lagrangian were solved numerically for 512 points picked up uniformly in the first Brillouin zone.

The results of calculation are shown in Figures IV-3 and IV-4. On the assumption of the rigid body, where there are no terms involving the twisting coordinates in the Lagrangian, p-terphenyl shows larger heat capacities than biphenyl at all temperatures, as expected from the mass difference. It was then attempted to introduce a much greater flexibility in the biphenyl molecule, as compared with the p-terphenyl

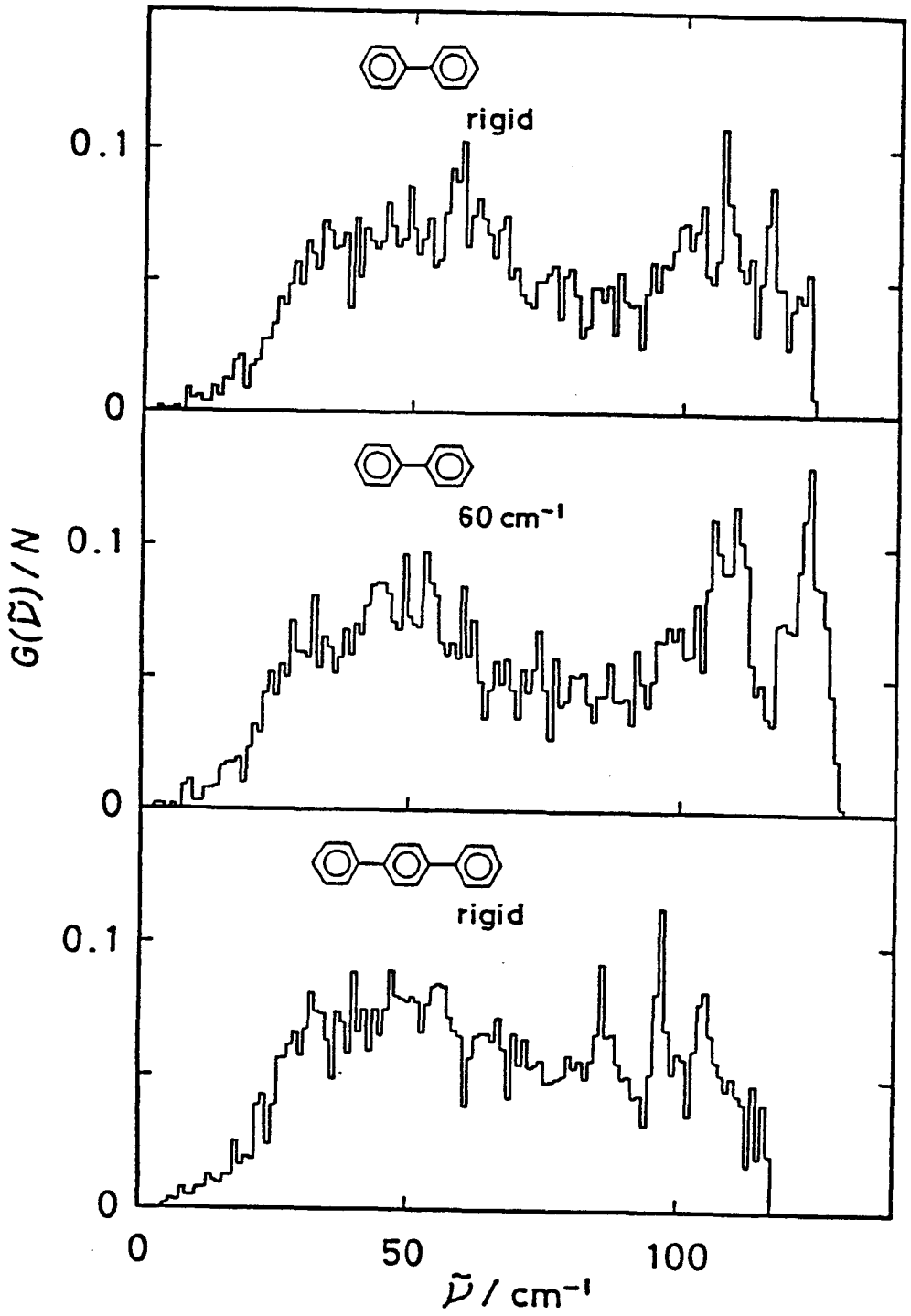

Figure IV-3. Calculated vibration spectra for rigid biphenyl, flexible biphenyl, and rigid p-terphenyl.

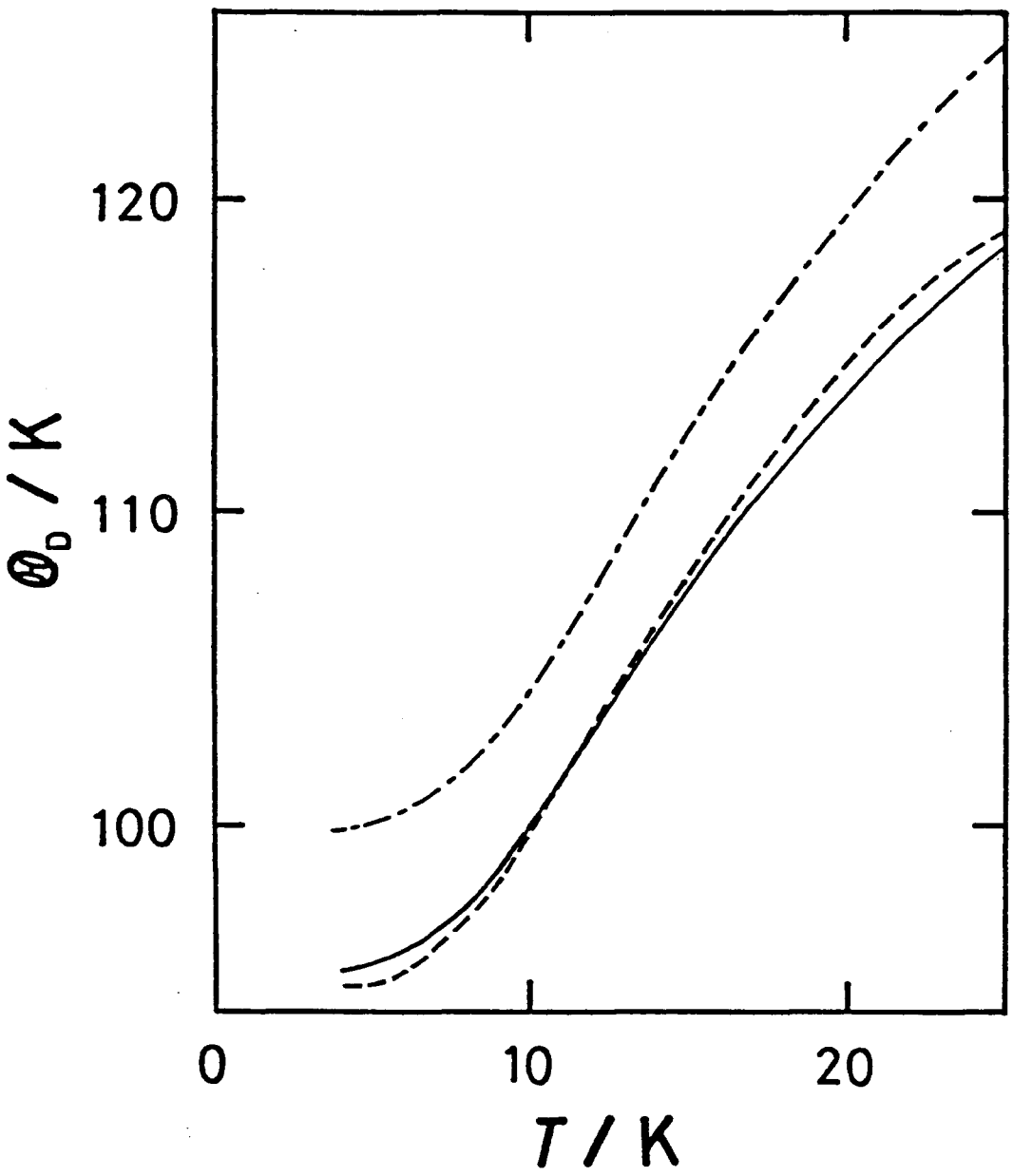

Figure IV-4. Calculated Debye characteristic temperatures for rigid p-terphenyl (solid curve), flexible biphenyl (broken curve), and rigid biphenyl (dot-dash curve), assuming 6 degrees of freedom per molecule.

molecule, with regard to the twisting of phenyl rings. For the overall twisting force constant in the biphenyl crystal which should include intermolecular part in principle, the same intramolecular contribution, which would lead to a frequency of 60 cm^{-1}, is used as in an isolated molecule. The corresponding force constants for p-terphenyl were assumed to be so large that the twisting modes begin to contribute to its heat capacities only at sufficiently higher temperatures. If it was done, biphenyl comes to show higher density of states in the low frequency region. On the other hand, p-terphenyl has higher density between 25 and 45 cm^{-1} due to its larger mass. Figure IV-4 shows the Debye temperature curves calculated from the spectra of Figure IV-3 and the greater torsional flexibility in biphenyl is reflected in the crossover in the heat capacities at about 12 K. Thus, it was concluded qualitatively that the crossover can be attributed to the twisting mode contribution of phenyl rings.

The interpretation given above has a certain consequence at still lower temperatures. Molecules having a small force constant for the twisting vibration as biphenyl molecule should show large heat capacities at low temperatures. These points were investigated by comparing the low temperature heat capacities with those of the similar molecule, 4,4'-difluorobiphenyl, on which the experimental details will be described in Section V-2-1. The

crystal structure of 4,4'-difluorobiphenyl at low temperatures is the same as that at room temperature, i.e. it is of the biphenyl type (see Sections V-2-1 and V-3), and the greater π-conjugation is considered to favor greater softening of the twisting vibration because it will help flatten the potential at $\theta = 0^{\circ}$, as discussed in Chapter II.

The behavior of the Debye temperature assuming 6 degrees of freedom per molecule in the low temperature region is shown in Figure IV-5. The heat capacity of biphenyl becomes larger than that of 4,4'-difluoro-biphenyl below about 11 K in spite of the smaller mass of the former molecule. Thus, it is clear that the heat capacities of biphenyl crystal are much larger at low temperatures than those of the homologous molecules and derivatives. Therefore, the properties of biphenyl is very unique: The competing effect of the intra- and intermolecular interactions is very subtle and it play a critical role in the incommensurate structure of the crystal in such a way that the twisting motion is strongly coupled to the lattice vibration.

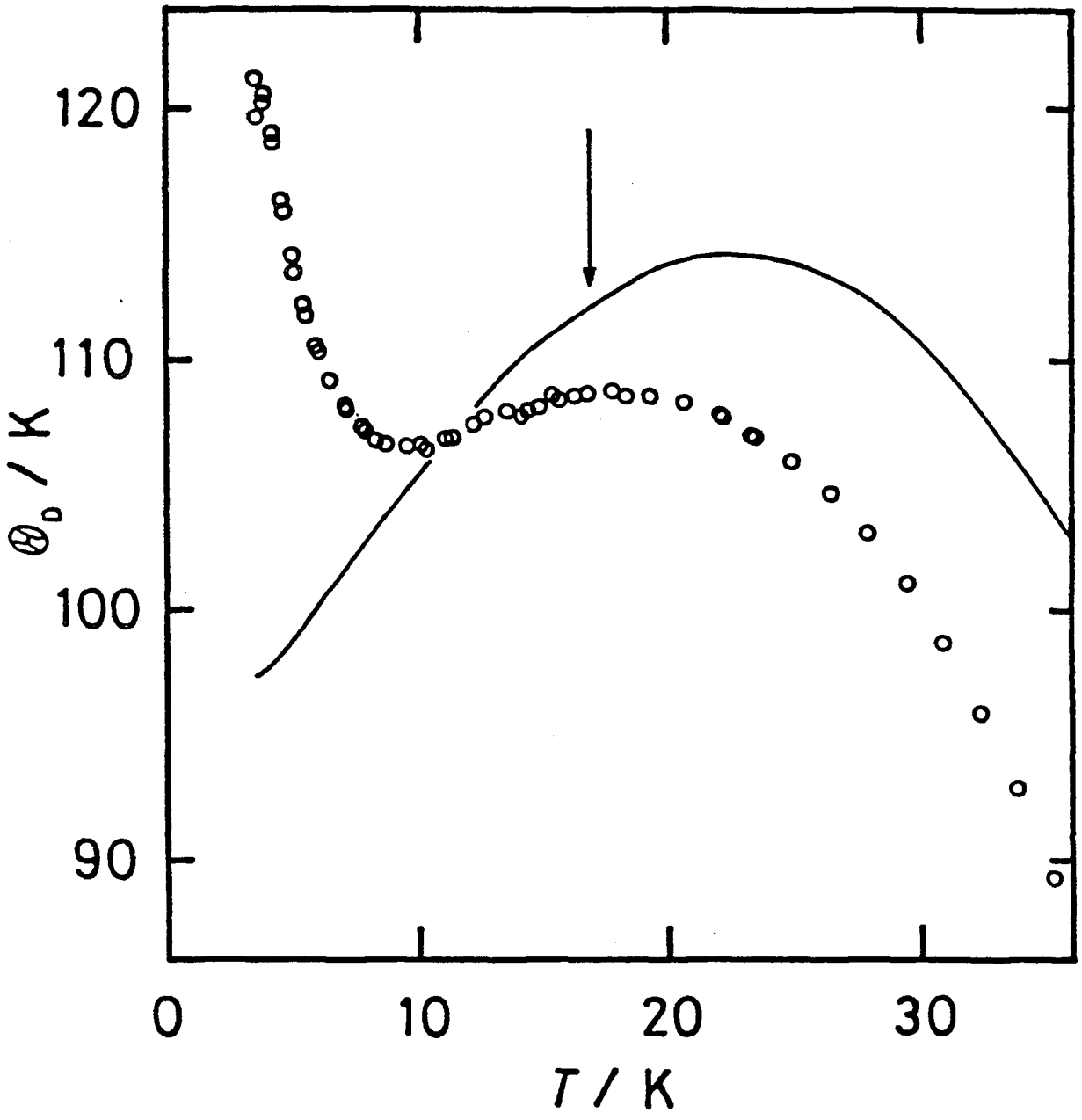

Figure IV-5. Debye characteristic temperatures corresponding to the measured heat capacities of biphenyl (solid curve) and 4,4'-difluorobiphenyl (open circle), assuming 6 degrees of freedom per molecule. The arrow indicates the location of the lock-in transition of biphenyl.

References to Chapter IV

1. I. Natkaniec, A. V. Belushkin and T. Wasiutyński, Phys. Status Solidi b, 105(1981), 413.
2. H. Takeuchi, S. Suzuki, A. J. Dianoux and G. Allen, Chem. Phys., 55(1981), 153.
3. A. V. Belushkin, I. Natkaniec, J. Wasicki and T. Zaleski, Phys. Status Solidi b, 123(1984), K115.
4. E. Burgos, H. Bonadeo and E. D'Alessio, J. Chem. Phys., 65(1976), 2460.
5. H. Bonadeo and E. Burgos, Acta Cryst., A38(1982), 29.
6. N. M. Plakida, A. V. Belushkin, I. Natkaniec and T. Wasiutyński, Phys. Status Solidi b, 118(1983), 129.
7. P. J. L. Baudour, Y. Delugeard and H. Cailleau, Acta Cryst., B32(1976), 150.
8. P. J. L. Baudour, H. Cailleau and W. B. Yelon, Acta Cryst., B33(1977), 1773.
9. P. J. L. Baudour, Y. Delugeard and P. Rivet, Acta Cryst., B34(1978), 625.
10. H. Cailleau, F. Moussa and J. Mons, Solid State Commun., 31(1979), 521.
11. H. Cailleau, F. Moussa, C. M. E. Zeyen and J. Bouillot, to be published.
12. H. Cailleau, J. L. Baudour and C. M. E. Zeyen, Acta Cryst., B35(1979), 426.
13. J. L. Baudour and M. Sanquer, Acta Cryst., B39(1983), 75.

14. M. L. Boriack and A. W. Overhauser, Phys. Rev. B, 18(1978), 6454.

15. G. Taddei, H. Bonadeo, M. P. Marzocchi and S. Califano, J. Chem. Phys., 58(1971), 966.

16. G. Venkataraman and V. C. Sahni, Rev. Mod. Phys., 42(1970), 409.

Chapter V Possibility of phase transition in p-substituted biphenyls

V-1 Introduction

The crystals of the first three members of p-polyphenylene undergo phase transitions associated with a molecular conformation change,[1-13] which is a resultant of delicate balance between the inter- and the intramolecular interactions. However, their behavior around the phase transition is considerably different from one another. Biphenyl shows a phase transition (at 40.4 K) of a displacive type associated with the soft modes,[14-17] while p-terphenyl and p-quaterphenyl crystals undergo an order-disorder type transition[11,18] at much higher temperatures compared with biphenyl. Furthermore, the heat capacity anomalies of biphenyl and p-quaterphenyl is very broad but that of p-terphenyl is sharp.[19,20] It is possible qualitatively to understand the behavior of the three substances by considering the molecular symmetry and the potentials for the intramolecular twisting modes, as described in Section III-3.

If any substituents were introduced into the p-polyphenylene molecule, the intramolecular part of the potential curve for a twisting degree of freedom would be affected and the transition, if existed, would

reflect its contribution. Therefore, it is very important to study substituted p-polyphenylenes in order to understand the twist transition.

Information on crystal structures of symmetrically substituted biphenyls is tabulated in Table V-1. We can recognize the following characteristics. (1) Planar conformation may appear in the case that the atoms at the ortho positions are hydrogen. (2) The central C-C bond length does not depend strongly on the torsional angle between the two phenyl rings. (3) There may be a possibility of existence of the twist transition on cooling for the crystals of 4,4'-difluorobiphenyl and p,p'-biphenol (4,4'-dihydroxybiphenyl), as they have a planar conformation at room temperature.

The molecule of 4,4'-difluorobiphenyl in the gaseous state is twisted by about 40°.[30] The first determination of the structure of this substance by Dhar[31] showed that the crystal structure was the same as for the other known 4,4'-dihalogenobiphenyls (dichloro- and dibromobiphenyl); i.e. the molecule was twisted in the crystal.[22,23] On the other hand, spectroscopic studies[32,33] suggested that the molecule should be planar in the crystal at room temperature. Halstead et al.[21] recently reported the space group determination by X-ray diffraction (given in Table V-1), showing planar conformation, which is compatible with their results of high resolution NMR

Table V-1. Structures of symmetrically substituted biphenyls at room temperature.

	space group	θ^a / °	l^b /nm
biphenyl(BP)[6]	$P2_1/a$	0	0.1494
4,4'-difluoro-BP[21]	$P2_1/a$	0	
4,4'-dichloro-BP[22]	$P2_1/n$	39,42	0.1487,0.1578
4,4'-dibromo-BP[23]	$P2_1/n$	38,42	
4,4'-dimethyl-BP[24] (*p,p'*-bitolyl)	$P2_1/n$	36,40	0.1486,0.1459
4,4'-dinitro-BP[25]	Pc	33	0.1499
4,4'-dihydroxy-BP[26] (*p,p'*-biphenol)	$P2_1/a$	0	0.147
perfluoro-BP[27]	Fdd2	59.6	
perchloro-BP[28]	Pbcn	86.6	0.1522
2,2',4,4',6,6'-hexachloro-BP[29]	C2/c	87.3	0.1477

[a]Twisting angle. [b]Central C-C bond length.

experiments.[21,34]

4,4'-Difluorobiphenyl is a substituted biphenyl by fluorine atoms for hydrogen atoms at the 4 and 4' (p and p') positions. The substitution induces greater delocalization of π-electrons, as discussed in Section II-2. The planar conformation in 4,4'-difluorobiphenyl should be more favored than in biphenyl, and its twist transition might be at a lower temperature.

The crystal structure of p,p'-biphenol is now well known[26,35,36]; it is of biphenyl-type as shown in Figure V-1. The molecules occupy the inversion sites. Since the molecule has two hydroxyl groups surrounded with the four neighboring molecules, the hydrogen bonds form a two dimensional network and the "ice condition" should be applied to this system. The space group $P2_1/a$ does not require the symmetric, nor the disordered hydrogen bonds. Therefore, if there exists an order-disorder transition of hydrogen bonds, the space group can remain unchanged (an isomorphous transition).

Taking into consideration the intramolecular potential calculated in Section II-2, the molecule of p,p'-biphenol will be twisted in the gaseous and the liquid states, although no reports have been published on the molecular structure in the isolated state.

Since the intramolecular potential curves for the twisting motion calculated for 4,4'-difluorobiphenyl and p,p'-biphenol are very similar to each other as

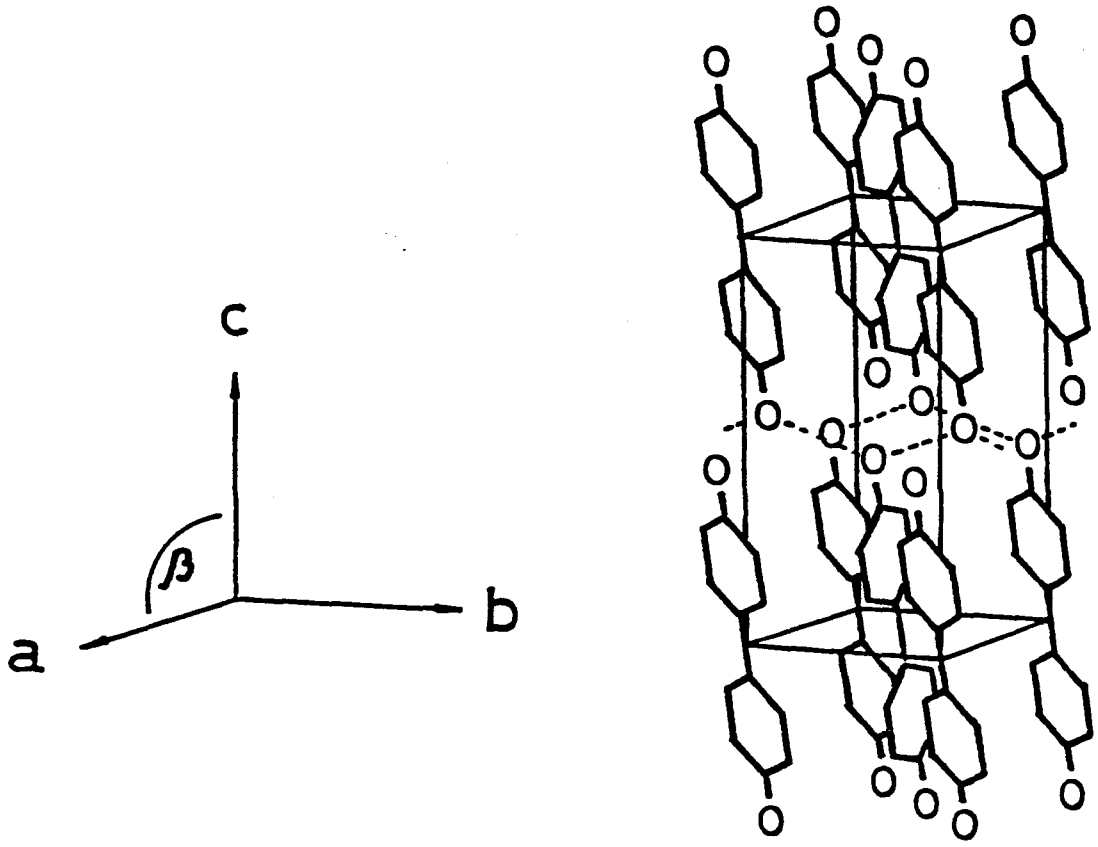

Figure V-1. Crystal structure of p,p'-biphenol at room temperature. Broken line represents hydrogen-bond.

described in Section II-2, a similar twist transition might be observed if the property of the transition was primarily determined by the intramolecular interaction. However, there exists a rather strong intermolecular interaction in p,p'-biphenol crystal, i.e. hydrogen bond. Therefore, it is very interesting to compare the properties of 4,4'-difluorobiphenyl and p,p'-biphenol.

In addition to the two substances described above, studies on p-phenylphenol (4-hydroxybiphenyl) were made as Brock and Haller[37] recently reported the possibility of existence of the phase transition similar to that of biphenyl. They made structure refinements on two polymorphs. The crystal grown from solution was reported to belong to the space group $P2_12_12_1$ with cell constants a = 1.5472 nm, b = 0.5469 nm, c = 2.0600 nm, and Z = 8 at room temperature. There were two independent, nearly planar molecules (θ = 2.3° and 2.0°) in an asymmetric unit (primitive unit cell). On the other hand, the crystal grown by sublimation under reduced pressure was reported to belong to the space group $P2_1/a$ with cell constants a = 0.8067 nm, b = 0.5449 nm, c = 2.0022 nm, β = 95.14°, and Z = 4 at room temperature. There was only one independent, nearly planar molecule in an asymmetric unit. In both polymorphs, the hydrogen bonds form one dimensional chain in contrast to the two dimensional network in crystalline p,p'-biphenol.[26,35,36] From the

consideration on the densities of two polymorphs, they suggested that the orthorhombic ($P2_12_12_1$) form was more stable at low temperatures. Satellite reflections were observed in the experiments on the monoclinic ($P2_1/a$) form at room temperature, which could be related to a structural modulation involving rotation about the long molecular axis. Thus, heat capacity measurements were made on the sublimed and the sublimed-melted specimens for the sake of comparison. The powder X-ray diffraction patterns and the Raman spectra of lattice modes were also recorded for both the specimens.

In this chapter, experimental results on the three substances, 4,4'-difluorobiphenyl, p,p'-biphenol and p-phenylphenol, are described in detail and discussed in the connection with the intra- and the intermolecular interactions.

V-2 Heat capacities of the p-substituted biphenyls

V-2-1 4,4'-Difluorobiphenyl

Experimental

4,4'-Difluorobiphenyl was purchased from ICN Pharmaceuticals, Inc. and purified by the method of fractional sublimation in vacuum at room temperature. In order to avoid possible formation of any metastable phases and to improve crystallinity, the specimen was

melted under a helium atmosphere (10^5 Pa), cooled gradually down to room temperature for recrystallization, and pulverized gently. The purity of the specimen used for the calorimetry was better than 99.9 moles per cent as confirmed by gas-chromatography. The powdered specimen was loaded into the calorimeter vessel, which was sealed after addition of a small amount of helium gas (6 kPa at room temperature) for heat exchange. The contribution of the helium to the heat capacity was negligibly small. The amount of the sample was 14.7851 g (0.0777378 mol) after the buoyancy correction had been applied. The contribution of the sample to the total heat capacity including that of the calorimeter vessel was 67 per cent at 10 K, which decreased to 39 per cent at 100 K and then increased to 52 per cent at 300 K as the temperature rose.

The working thermometers, and the apparatus and the operation of the adiabatic calorimeter were the same as described in Chapter III.

Results and Discussion

The measurements of the heat capacities were made between 3 and 300 K; the primary results are shown in Figure V-2 and tabulated in Table V-2 in chronological order. The temperature increment of each measurement may be deduced from the adjacent mean temperatures,

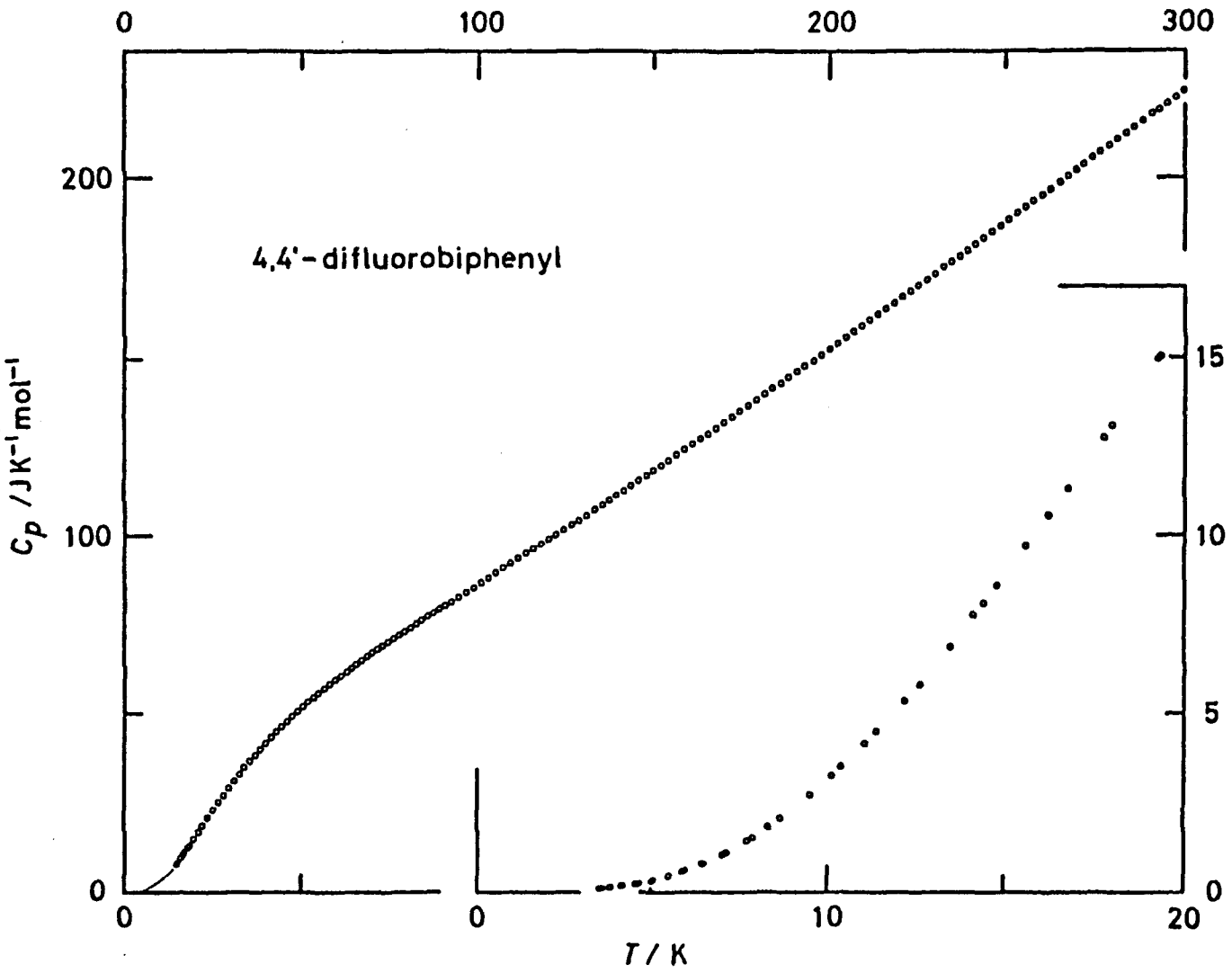

Figure V-2. Measured molar heat capacities of 4,4'-difluorobiphenyl.

Table V-2. Measured molar heat capacities of 4,4'-difluorobiphenyl.

T/K	C_p/J·K^{-1}·mol^{-1}	T/K	C_p/J·K^{-1}·mol^{-1}	T/K	C_p/J·K^{-1}·mol^{-1}	T/K	C_p/J·K^{-1}·mol^{-1}
Series 1		161.354	125.86	239.451	180.07	5.855	0.578
89.114	79.437	163.612	127.38	241.732	181.77	6.391	0.780
90.745	80.473	165.851	128.62	244.044	183.50	7.008	1.057
92.590	81.621	Series 2		246.384	185.14	7.697	1.432
94.634	82.921	168.069	130.13	248.710	186.82	Series 5	
96.772	84.242	170.347	131.75	251.021	188.46	3.478	0.092
98.947	85.572	172.648	133.32	253.317	190.18	3.780	0.121
101.138	86.899	174.974	134.85	255.599	191.94	4.183	0.170
103.296	88.222	177.279	136.49	257.901	193.54	4.621	0.246
105.419	89.576	179.566	138.06	260.223	195.15	5.039	0.340
107.548	90.938	181.837	139.58	262.532	196.88	5.472	0.456
109.684	92.309	184.134	141.22	Series 3		5.939	0.606
111.829	93.673	186.458	142.78	265.119	198.72	Series 6	
113.987	95.010	188.765	144.37	267.440	200.62	7.113	1.108
116.079	96.504	191.053	145.95	269.788	202.20	7.857	1.525
118.136	97.658	193.325	147.43	272.120	203.90	8.658	2.069
120.233	98.978	195.577	148.97	274.435	205.64	9.488	2.711
122.370	100.33	197.848	150.57	276.736	207.21	10.368	3.516
124.503	101.71	200.145	152.23	279.025	209.05	11.372	4.495
126.663	103.00	202.425	153.86	281.300	210.71	12.616	5.819
128.858	104.38	204.732	155.49	283.603	212.36	14.135	7.768
131.028	105.78	207.064	157.20	285.937	214.08	Series 7	
133.174	107.15	209.391	158.81	288.259	215.93	8.321	1.832
135.297	108.54	211.701	160.38	290.567	217.76	10.113	3.256
137.435	109.93	213.987	162.01	292.862	218.96	11.054	4.152
139.591	111.35	216.303	163.61	295.144	220.48	12.189	5.356
141.725	112.71	218.646	165.27	297.460	222.20	13.480	6.866
143.880	114.11	220.974	166.95	299.810	223.98	Series 8	
146.062	115.54	223.287	168.57	Series 4		14.788	8.586
148.222	116.94	225.585	170.16	3.553	0.102	16.232	10.541
150.361	118.34	227.870	171.73	3.792	0.121	17.791	12.754
152.522	119.78	230.183	173.45	4.134	0.163	19.343	15.046
154.663	121.25	232.522	175.42	4.535	0.230	Series 9	
156.820	122.77	234.845	176.92	4.949	0.317	14.411	8.096
159.076	124.34	237.155	178.42	5.381	0.429	15.608	9.685

Table V-2. (continued).

T/K	C_p/J·K^{-1}·mol^{-1}	T/K	C_p/J·K^{-1}·mol^{-1}	T/K	C_p/J·K^{-1}·mol^{-1}	T/K	C_p/J·K^{-1}·mol^{-1}
16.796	11.332	30.847	31.416	50.370	52.391	70.273	67.446
18.011	13.087	32.302	33.326	51.832	53.634	71.804	68.480
19.291	14.973	33.750	35.136	53.328	54.909	73.326	69.468
20.641	16.966	35.233	36.932	54.885	56.172	74.841	70.483
22.036	19.025	36.737	38.717	56.497	57.454	76.361	71.449
23.455	21.133	38.245	40.419	58.111	58.729	77.883	72.448
Series 10		39.767	42.071	59.675	59.919	79.460	73.472
21.951	18.893	41.285	43.689	61.193	61.023	81.093	74.471
23.392	21.041	42.775	45.211	62.696	62.112	82.736	75.537
24.880	23.211	44.273	46.712	64.189	63.210	84.375	76.590
26.378	25.336	45.808	48.175	65.670	64.286	86.004	77.566
27.865	27.387	47.350	49.619	67.196	65.305	87.638	78.610
29.358	29.421	48.878	51.049	68.739	66.405	89.272	79.669

Table V-3. Molar thermodynamic functions of 4,4'-difluorobiphenyl.

T / K	C_p / J·K^{-1}·mol^{-1}	$\{H(T)-H(0)\}/T$ / J·K^{-1}·mol^{-1}	$S(T)-S(0)$ / J·K^{-1}·mol^{-1}	$-\{G(T)-H(0)\}/T$ / J·K^{-1}·mol^{-1}
5	0.329	0.077	0.098	0.021
10	3.16	0.76	0.99	0.22
20	16.02	4.93	6.78	1.85
30	30.28	11.05	16.02	4.97
40	42.32	17.42	26.45	9.03
50	52.06	23.40	36.97	13.57
60	60.13	28.87	47.20	18.33
70	67.27	33.86	57.01	23.16
80	73.78	38.44	66.42	27.98
90	80.02	42.72	75.48	32.76
100	86.21	46.76	84.23	37.47
110	92.49	50.63	92.74	42.11
120	98.82	54.38	101.06	46.68
130	105.12	58.04	109.21	51.17
140	111.59	61.64	117.24	55.61
150	118.09	65.18	125.16	59.98
160	124.95	68.70	133.00	64.30
170	131.53	72.20	140.77	68.57
180	138.34	75.69	148.48	72.79
190	145.16	79.16	156.14	76.98
200	152.11	82.64	163.76	81.13
210	159.21	86.11	171.36	85.24
220	166.21	89.60	178.93	89.33
230	173.30	93.08	186.47	93.39
240	180.52	96.57	194.00	97.43
250	187.74	100.07	201.51	101.44
260	195.04	103.59	209.02	105.43
270	202.38	107.11	216.52	109.41
280	209.73	110.64	224.01	113.37
290	216.95	114.19	231.50	117.31
300	224.10	117.73	238.97	121.24
298.15	222.77	117.07	237.59	120.52

Table V-4. Third law entropy of 4,4'-difluorobiphenyl.

	S / J·K^{-1}·mol^{-1}
0 to 3 K (smooth extrapolation)	0.019
3 to 298.15 K (graphical)	273.59
sublimation[a]	305.
entropy of real gas at 298.15 K	543.
compression and correction to ideal gas[a,b]	-101.3
$S°$(4,4'-difluorobiphenyl, 298.15 K, g, P = 100000 Pa)	441.

[a] $\Delta_{vap}H$ = 91200 J·mol^{-1} and P = 0.5092 Pa at 298.15 K.[38]

[b] Using Berthelot's equation of state.

which is small enough to neglect the curvature correction in comparison with the experimental precision. After each energy input was over, thermal equilibrium within the calorimeter vessel was attained within 1 min below 30 K, in 5 min at 50 K, 15 min at 70 K, 25 min between 80 and 180 K, and 20 min above 200 K.

Some thermodynamic functions calculated from the present results are given for rounded temperatures in Table V-3, in which small contributions below 4 K were estimated by smooth extrapolation from the higher temperature side. The third law entropy of ideal-gas 4,4'-difluorobiphenyl, which involved previous vapor pressure data,[38] was calculated as summarized in Table V-4.

As seen in Figure V-2, no apparent thermal anomaly exists in the temperature range covered in this study. The measured heat capacities in the low temperature region were converted to the equivalent Debye characteristic temperatures as shown in Figure V-3, assuming that there are 6 degrees of freedom per molecule. The Debye temperature curve does not show any anomaly either, in contrast to the case of solid biphenyl in which there is a broad, shallow minimum in the Debye temperatures centered at 16.8 K (see Section III-2-1). Therefore, it is concluded that there is no phase transition in 4,4'-difluorobiphenyl crystal between 4 and 300 K; if there were any, its entropy of transition would be smaller than about

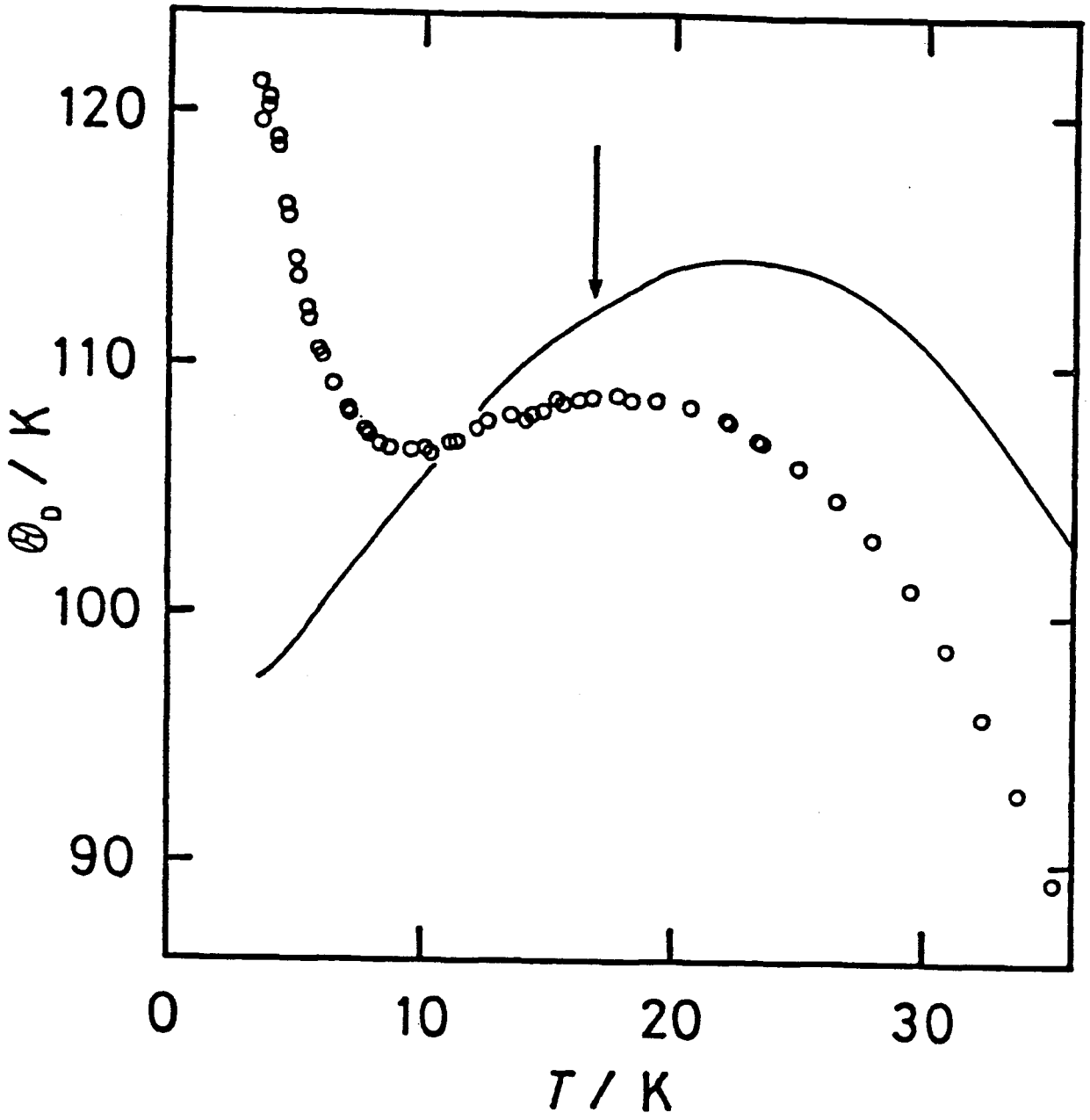

Figure V-3. Debye characteristic temperatures corresponding to the measured heat capacities of biphenyl (solid curve) and 4,4'-difluorobiphenyl (open circle), assuming 6 degrees of freedom per molecule. The arrow indicates the location of the lock-in transition of biphenyl.

0.005 $J \cdot K^{-1} \cdot mol^{-1}$.

It was anticipated that the fluorine substitution would enhance the π-conjugation across the central C-C bond, and displacing the twist transition to a lower temperature than for biphenyl. Now, as no phase transition was found in 4,4'-difluorobiphenyl, there remain several possibilities as to what occurs in 4,4'-difluorobiphenyl. It is improbable to believe that the twist transition in 4,4'-difluorobiphenyl exists below the lowest temperature of the present study for the following reason. Figure V-3 shows that the heat capacity of 4,4'-difluorobiphenyl becomes smaller than that of biphenyl below about 11 K in spite of the greater mass. This means that, in the crystal, the molecule of 4,4'-difluorobiphenyl is harder and therefore the potential barrier hindering the twisting motion is steeper than that of biphenyl in contrast to isolated states (see Section II-2).

The question then remains as to whether the potential in the crystal has a double or a single minimum. The double-minimum potential model is not consistent with experimental results and the argument given above; double-minimum potential would give rise to a phase transition.

We are therefore led to the conclusion that the molecule of 4,4'-difluorobiphenyl in the crystal has a single, steep minimum in the potential that hinders

twisting of the central C-C bond all the way from 0 K through room temperature. The structure shown in Table V-1 for this molecule may not be then the result of a statistical average but may be a fixed conformation, although there still remains the possibility that the molecule is twisted[31] at all temperatures as in other 4,4'-dihalogenobiphenyls.[22,23] This point will be analyzed in detail in Section V-3.

V-2-2 p,p'-Biphenol

Experimental

A sample of p,p'-biphenol was purchased from Tokyo Kasei Kogyo Co., Ltd., and purified by fractional sublimation at about 450 K in vacuum. The mass percentages of C and H were 77.41 (calculated 77.40) and 5.41 (5.41), respectively for the purified sample as determined by chemical analysis. The amount of the sample used for heat capacity measurements was 13.5333 g (0.0726776 mol) after buoyancy correction, which contributed 52 per cent to the total heat capacity including that of the calorimeter vessel at 10 K, 36 per cent at 100 K, 43 per cent at 200 K, and 51 per cent at 300 K. A small amount of helium gas (7 kPa at room temperature) was also put into the calorimeter vessel for heat exchange, and its contribution to the total heat capacity was negligibly small.

The working thermometers, and the apparatus and the operation of the adiabatic calorimeter were the same as described in Chapter III.

Results and Discussion

The measured heat capacities of p,p'-biphenol from 3 K to 310 K are shown in Figure V-4 and tabulated in Table V-5 in chronological order. After each heat input was over, thermal equilibrium within the calorimeter vessel was attained within 1 min between 7 and 30 K, in 7 min at 50 K, 25 min at 100 K, and 15 min above 200 K. However, below 6 K the time needed for equilibration was long as 7 min; it will be described in detail in the following.

Some thermodynamic functions obtained through manipulation of the measured values are tabulated in Table V-6, where the small contributions below 4 K were estimated by smooth extrapolation from the higher temperature side.

The Debye characteristic temperatures corresponding to the measured heat capacities in the low temperature region are shown in Figure V-5 assuming 9 degrees of freedom per molecule. As seen in Figures V-4 and V-5, no anomalous behavior of heat capacity was observed in the temperature region covered in this study. Therefore, it is concluded that there is no phase transition in p,p'-biphenol crystal between 4 and

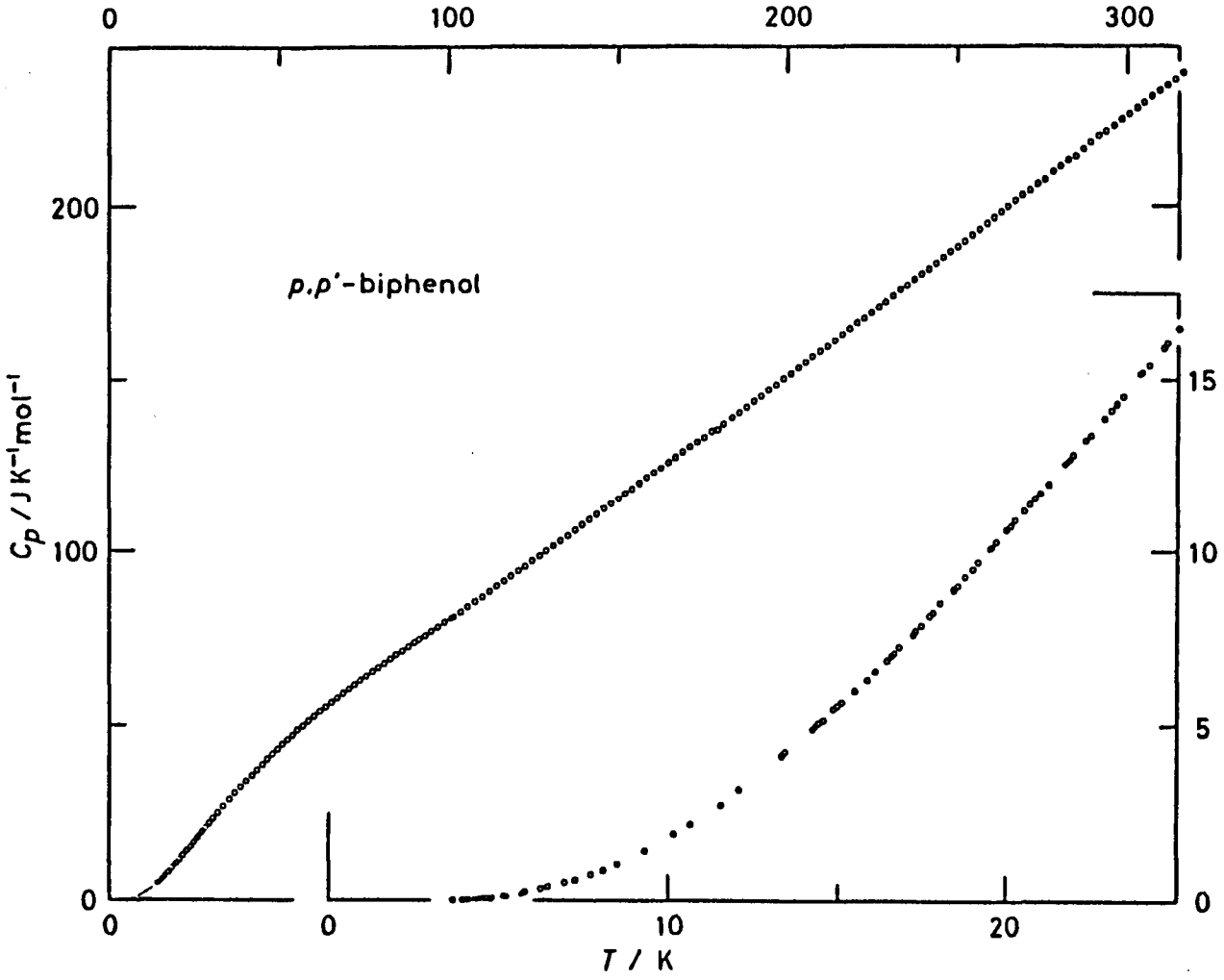

Figure V-4. Measured molar heat capacities of p,p'-biphenol.

Table V-5. Measured molar heat capacities of *p,p'*-biphenol.

T / K	C_p / J·K^{-1}·mol^{-1}	T / K	C_p / J·K^{-1}·mol^{-1}	T / K	C_p / J·K^{-1}·mol^{-1}	T / K	C_p / J·K^{-1}·mol^{-1}
Series 1		9.332	1.409	52.637	45.994	26.392	18.049
90.126	73.610	10.180	1.896	54.121	47.310	27.499	19.355
91.474	74.643	Series 7		55.667	48.622	28.596	20.652
93.191	75.806	10.659	2.179	57.252	49.996	29.678	21.937
94.987	77.011	12.112	3.185	58.884	51.348	30.738	23.207
96.875	78.266	13.359	4.145	60.564	52.698	Series 12	
98.832	79.567	Series 8		62.248	53.990	101.657	81.274
100.826	80.878	14.987	5.562	63.913	55.315	103.711	82.605
Series 2		16.827	7.253	65.581	56.600	105.805	84.117
3.641	0.038	18.453	8.935	67.265	57.847	107.944	85.619
4.001	0.054	20.018	10.631	68.969	59.125	110.089	87.109
4.412	0.071	Series 9		70.677	60.372	112.197	88.588
4.786	0.095	14.455	5.083	72.403	61.638	114.293	90.000
5.219	0.146	16.120	6.578	74.156	62.871	116.384	91.422
5.768	0.258	17.721	8.151	75.921	64.118	118.464	92.885
Series 3		19.163	9.693	77.702	65.367	120.565	94.373
7.249	0.584	20.527	11.187	79.486	66.600	122.666	95.809
8.077	0.890	21.865	12.699	81.261	67.788	124.752	97.236
Series 4		23.219	14.285	83.026	69.025	126.833	98.692
3.931	0.045	24.608	15.929	84.785	70.212	128.911	100.12
4.290	0.057	Series 10		86.540	71.371	131.006	101.64
4.656	0.102	25.748	17.279	88.292	72.575	133.091	103.13
5.156	0.164	27.294	19.106	90.048	73.780	135.172	104.64
5.762	0.263	29.655	21.921	Series 11		137.272	106.22
6.451	0.409	32.090	24.810	12.733	3.576	139.392	107.73
7.255	0.601	33.765	26.748	13.698	4.385	141.521	109.27
8.081	0.868	35.432	28.647	14.594	5.169	143.651	110.76
Series 5		37.106	30.538	15.497	5.994	145.803	112.37
4.104	0.052	38.753	32.321	16.456	6.863	147.960	113.89
4.519	0.101	40.372	34.062	17.469	7.877	150.119	115.40
Series 6		41.967	35.708	18.559	9.031	152.269	117.02
5.241	0.130	43.558	37.394	19.710	10.279	154.402	118.32
5.693	0.226	45.107	38.901	20.858	11.553	156.515	119.92
6.248	0.352	46.622	40.358	21.976	12.826	158.597	121.47
6.943	0.519	48.151	41.877	23.077	14.116	160.690	122.96
7.716	0.748	49.664	43.326	24.174	15.421	162.817	124.50
8.514	1.041	51.161	44.675	25.279	16.726	164.944	126.06

Table V-5. (continued).

T/K	C_p/J·K^{-1}·mol^{-1}	T/K	C_p/J·K^{-1}·mol^{-1}	T/K	C_p/J·K^{-1}·mol^{-1}	T/K	C_p/J·K^{-1}·mol^{-1}
167.051	127.58	230.988	174.40	295.904	222.64	29.075	21.227
169.168	129.08	233.125	176.24	298.140	224.33	29.789	22.062
171.285	130.52	235.246	177.47	300.383	225.97	Series 16	
173.384	132.00	237.377	179.06	302.616	227.59	14.258	4.919
175.496	133.44	239.519	180.66	304.832	229.23	14.885	5.469
177.613	135.06	241.647	182.10	307.051	230.89	15.504	6.005
Series 13		243.783	183.81	309.279	232.52	16.097	6.547
179.581	135.56	245.937	185.43	311.517	234.07	16.671	7.084
181.681	137.21	248.074	187.04	313.762	235.76	17.243	7.630
183.108	139.03	250.188	188.58	315.995	237.53	17.832	8.251
185.955	140.55	252.314	190.03	Series 15		18.424	8.874
188.803	142.16	254.450	191.72	14.332	4.979	19.006	9.493
190.251	143.75	256.591	193.38	15.126	5.674	19.580	10.120
192.401	145.30	258.738	195.06	15.886	6.358	20.145	10.742
194.561	146.98	260.874	196.70	16.606	7.030	20.703	11.378
196.730	148.50	262.946	198.29	17.315	7.730	21.253	11.967
198.883	150.17	265.025	199.89	18.039	8.523	21.797	12.617
201.023	151.79	267.168	201.48	18.782	9.274	22.337	13.249
203.166	153.40	269.299	202.93	19.531	10.093	22.873	13.880
205.301	155.07	Series 14		20.272	10.914	23.412	14.522
207.444	156.72	271.476	204.36	21.007	11.721	23.955	15.175
209.596	158.24	273.634	206.13	21.739	12.554	24.504	15.815
211.746	159.78	275.818	207.51	22.479	13.413	25.059	16.475
213.914	161.34	278.034	209.67	23.232	14.293	25.622	17.138
216.077	163.05	280.258	211.28	23.976	15.219	26.177	17.803
218.222	164.76	282.488	212.94	24.710	16.056	26.727	18.449
220.351	166.35	284.727	213.98	25.442	16.933	27.292	19.131
222.470	167.84	286.957	216.53	26.171	17.784	27.866	19.797
224.600	169.50	289.194	218.42	26.897	18.656	28.447	20.485
226.735	171.09	291.440	219.77	27.626	19.506	29.036	21.209
228.858	172.76	293.677	221.00	28.354	20.372	29.628	21.898
						30.208	22.576

Table V-6. Molar thermodynamic functions of *p,p'*-biphenol.

T / K	C_p / J·K^{-1}·mol^{-1}	$\{H(T)-H(0)\}/T$ / J·K^{-1}·mol^{-1}	$S(T)-S(0)$ / J·K^{-1}·mol^{-1}	$-\{G(T)-H(0)\}/T$ / J·K^{-1}·mol^{-1}
5	0.134	0.026	0.032	0.006
10	1.78	0.403	0.507	0.104
20	10.60	3.09	4.15	1.07
30	22.32	7.53	10.65	3.12
40	33.66	12.68	18.65	5.98
50	43.62	17.89	27.26	9.37
60	52.24	22.92	35.99	13.08
70	59.87	27.66	44.63	16.97
80	66.93	32.13	53.09	20.96
90	73.70	36.38	61.36	24.99
100	80.31	40.44	69.47	29.03
110	87.03	44.36	77.44	33.07
120	93.95	48.21	85.31	37.10
130	100.93	51.99	93.10	41.11
140	108.13	55.75	100.85	45.10
150	115.29	59.48	108.55	49.07
160	122.37	63.19	116.22	53.03
170	129.45	66.88	123.85	56.97
180	136.32	70.54	131.44	60.90
190	143.56	74.19	139.01	64.81
200	151.03	77.85	146.56	68.71
210	158.53	81.51	154.11	72.60
220	166.03	85.19	161.66	76.47
230	173.61	88.87	169.20	80.34
240	181.02	92.55	176.75	84.20
250	188.44	96.24	184.29	88.05
260	196.02	99.93	191.83	91.90
270	203.46	103.63	199.37	95.74
280	211.09	107.33	206.90	99.58
290	218.33	111.03	214.44	103.41
300	225.68	114.73	221.96	107.23
310	233.02	118.43	229.40	111.05
298.15	224.31	114.05	220.57	106.52

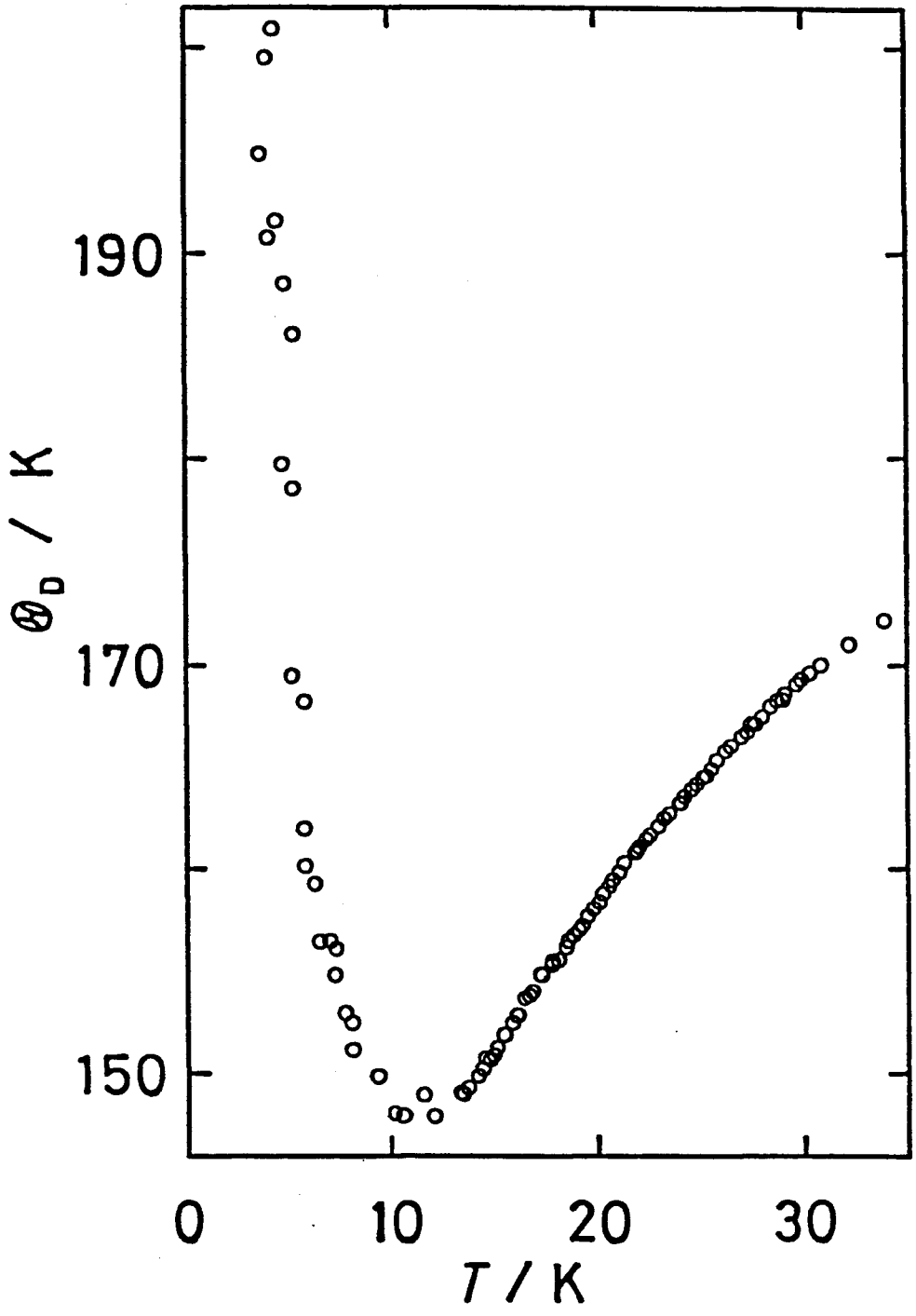

Figure V-5. Debye characteristic temperatures corresponding to measured heat capacities of p,p'-biphenol assuming 9 degrees of freedom per molecule.

315 K; if there were any, its entropy of transition would be smaller than about 0.005 $J \cdot K^{-1} \cdot mol^{-1}$.

It was expected that the substitution with hydroxyl groups would enhance the π-conjugation across the central C-C bond, thus displacing the twist transition to a lower temperature than for biphenyl. Now, since no phase transition was found in p,p'-biphenol as in 4,4'-difluorobiphenyl, the same discussion about the twist transition should be applied to the case of p,p'-biphenol and the same conclusion is drawn concerning the molecular structure and the potential hindering the twisting motion in the crystal.

Although there was nothing unusual in the heat capacity measurements above 10 K, slow thermal relaxation was encountered in the lower temperature region. The approach of the thermometer reading to a steady drift is shown in Figure V-6. As the thermal equilibrium is usually attained within a few tens of seconds, it seems that there may be some slow mechanism of the heat flow in this crystal lattice. It can be considered that the crystal consists of sub-systems, the "lattice" and the other systems. A few min is needed for the heat flow between the "lattice" and the other sub-system, or for the thermal equilibration within the sub-system. It is interesting that the Debye characteristic temperature decreases rapidly in this temperature region as the temperature increases (see Figure V-5). In view that such a

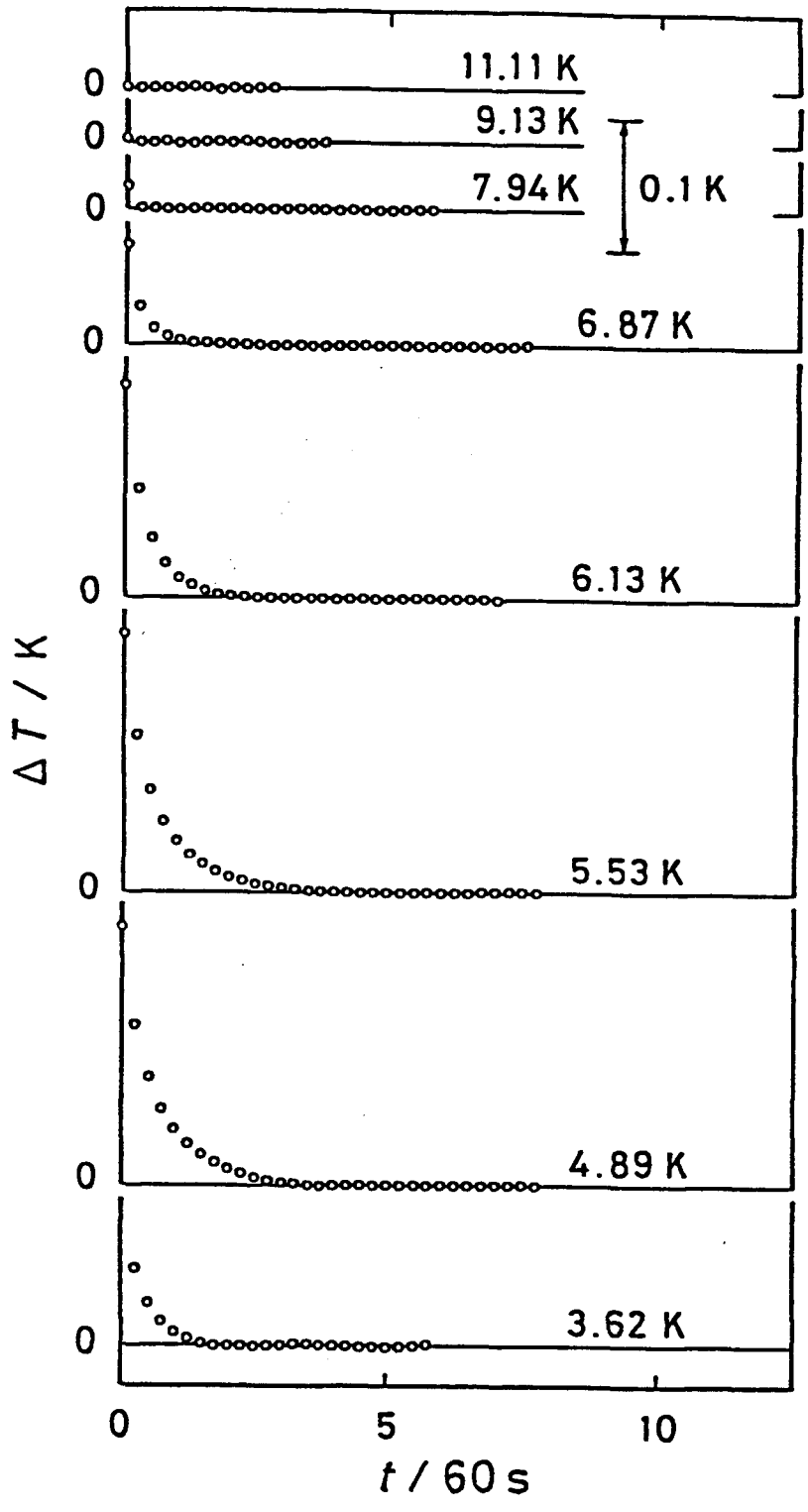

Figure V-6. Temperature drift under adiabatic conditions after each energy input in p,p'-biphenol.

phenomenon is not observed in the other substances without hydrogen-bond but in p-phenylphenol (see the next section), the hydrogen-bond may play an important role in this slow process.

V-2-3 p-Phenylphenol

Experimental

The sample of p-phenylphenol was purchased from Tokyo Kasei Kogyo Co., Ltd., nominal purity; better than 99 moles per cent and purified by fractional sublimation at about 360 K in vacuum. Gas-chromatographic analysis showed no detectable impurities. A part of the sublimed specimen weighed 18.9334 g (0.111235 mol) in vacuum was used for the adiabatic calorimetry without any further sample treatment, and this sample is denominated the sample A here after. The rest of the sublimed specimen was melted under the helium atmosphere (10^5 Pa), and gradually cooled down to room temperature for recrystallization. The sample was then pulverized gently. The amount of the melted-pulverized sample used for the calorimetry was 15.2147 g (0.089388 mol) after buoyancy correction; this sample is denominated the sample B. Each of the samples was put into the calorimeter vessel with a small amount of helium gas (7

kPa at room temperature) for heat exchange; its contribution to the total heat capacity was negligibly small. The contribution of the sample to the total heat capacity including that of the calorimeter vessel was 70 per cent in the case of the sample A (65 per cent in the case of the sample B) at 20 K. It decreased to 46 per cent (40 per cent) at 100 K as the temperature increased, however, it recovered again to 60 per cent (54 per cent) at 300 K.

The working thermometers, and the apparatus and the operation of the adiabatic calorimeter were the same as described in Chapter III.

The Raman spectra in the lattice vibration region were recorded for both the samples at liquid nitrogen and room temperatures. The laser Raman spectrometer (model R750, Japan spectroscopic Co., Ltd.) was used with the laser excitation of argon ion of 514.5 nm.

Results and Discussion

Measured molar heat capacities of the sample A are shown in Figure V-7. The measured values of the samples A and B, are tabulated in chronological order in Tables V-7 and V-8. The temperature increment due to each measurement may be deduced from the adjacent mean temperatures, which is small enough to ignore the curvature correction in comparison with the experimental precision. The heat capacities of the

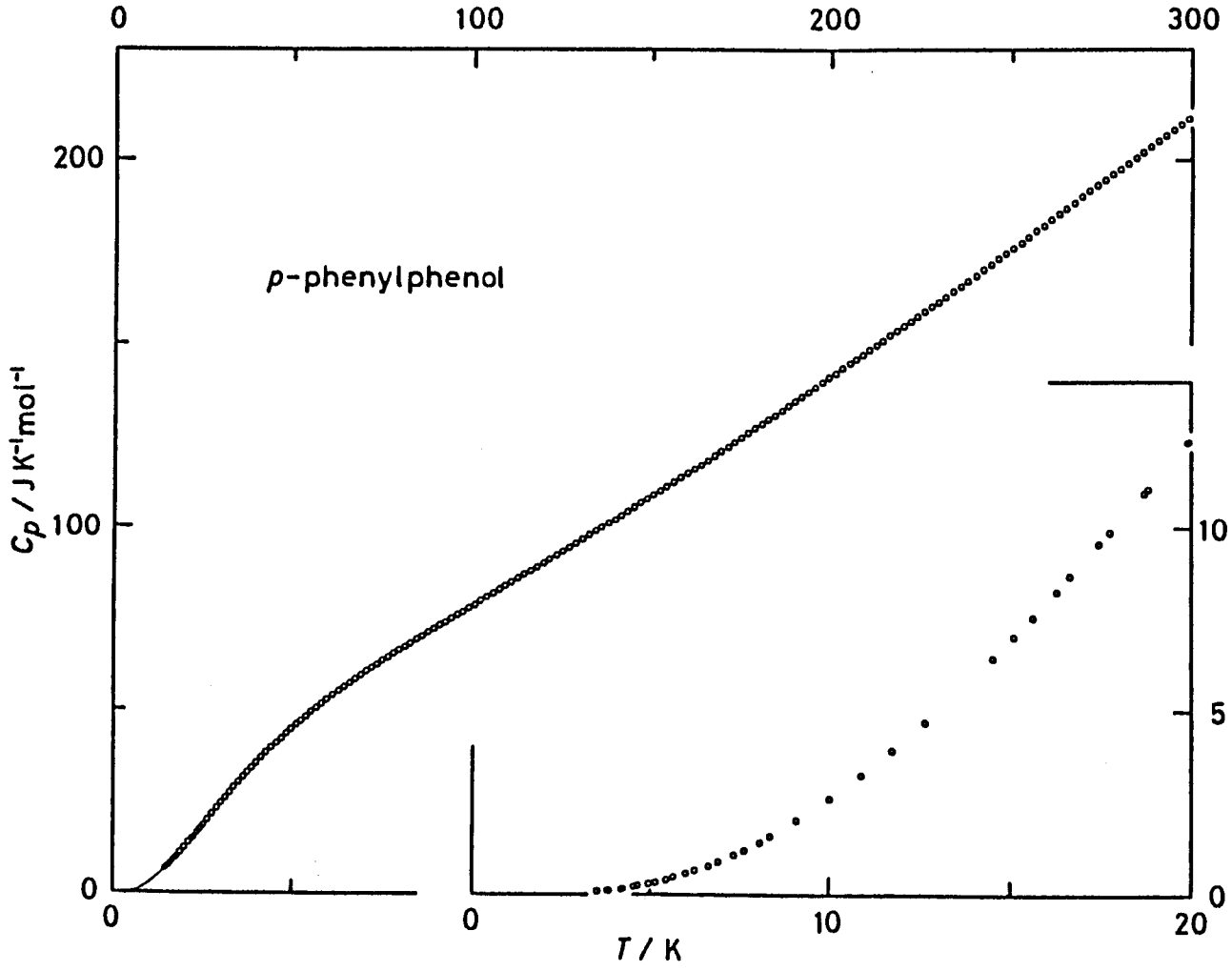

Figure V-7. Measured molar heat capacities of sublimed p-phenylphenol (sample A).

Table V-7. Measured molar heat capacities of sublimed *p*-phenylphenol (sample A).

T / K	C_p / J·K^{-1}·mol^{-1}	T / K	C_p / J·K^{-1}·mol^{-1}	T / K	C_p / J·K^{-1}·mol^{-1}	T / K	C_p / J·K^{-1}·mol^{-1}
Series 1		Series 5		53.864	48.096	107.454	82.616
3.856	0.118	15.085	6.995	55.305	49.269	109.169	83.590
4.172	0.159	16.264	8.241	56.780	50.404	110.886	84.617
4.533	0.216	17.473	9.565	58.258	51.524	112.637	85.641
4.947	0.298	18.704	10.955	59.743	52.679	114.409	86.705
5.431	0.415	19.919	12.382	61.372	53.876	116.190	87.692
5.992	0.571	21.106	13.773	63.048	55.067	117.965	88.807
6.618	0.784	22.280	15.186	64.610	56.138	119.737	89.864
7.314	1.064	23.476	16.640	66.144	57.182	121.518	90.912
8.051	1.411	24.699	18.108	67.664	58.216	123.311	91.981
Series 2		Series 6		69.184	59.279	125.115	93.030
3.500	0.084	22.523	15.501	70.711	60.250	126.947	94.151
3.824	0.116	23.740	16.980	72.227	61.265	128.790	95.260
4.217	0.165	24.970	18.453	73.737	62.242	130.616	96.377
4.646	0.237	26.212	19.965	75.256	63.215	132.424	97.476
5.130	0.338	27.463	21.456	76.783	64.171	134.214	98.559
5.652	0.472	28.721	22.976	78.291	65.186	136.035	99.634
6.229	0.645	29.976	24.431	79.818	66.113	137.887	100.75
6.889	0.884	31.224	25.904	81.391	67.106	139.720	101.83
7.619	1.200	32.459	27.314	82.975	68.066	141.536	102.96
8.357	1.580	33.684	28.770	84.571	69.037	143.338	104.04
9.096	2.013	34.908	30.113	86.166	69.991	145.126	105.18
Series 3		36.136	31.489	87.763	70.904	146.944	106.37
10.006	2.609	37.380	32.761	89.362	71.916	148.791	107.47
10.873	3.237	38.640	34.137	90.951	72.874	150.638	108.59
11.741	3.910	39.910	35.422	92.544	73.830	152.500	109.78
12.635	4.660	41.216	36.770	94.142	74.816	154.378	110.94
13.532	5.383	42.587	38.124	95.771	75.795	156.272	112.14
Series 4		43.980	39.449	Series 7		158.166	113.33
14.512	6.428	45.376	40.767	97.219	76.597	160.045	114.56
15.608	7.539	46.798	42.053	98.913	77.608	161.926	115.71
16.684	8.683	48.225	43.365	100.609	78.574	163.808	116.92
17.748	9.874	49.640	44.602	102.311	79.603	165.676	118.11
18.813	11.068	51.051	45.784	104.018	80.606	167.544	119.39
19.902	12.342	52.458	46.935	105.732	81.556		

Table V-7. (continued).

T/K	C_p/J·K^{-1}·mol^{-1}	T/K	C_p/J·K^{-1}·mol^{-1}	T/K	C_p/J·K^{-1}·mol^{-1}	T/K	C_p/J·K^{-1}·mol^{-1}
Series 8		199.632	140.72	231.803	162.85	265.175	186.73
169.418	120.57	201.514	141.92	233.855	164.38	267.347	188.29
171.291	121.72	203.383	143.17	Series 9		269.505	189.96
173.167	122.99	205.239	144.56	235.914	165.79	271.650	191.50
175.045	124.26	207.085	145.78	238.010	167.24	273.780	192.95
176.926	125.51	208.919	146.92	240.129	168.81	275.898	194.45
178.811	126.76	210.774	148.30	242.236	170.32	278.003	195.96
180.699	127.97	212.667	149.60	244.330	171.79	280.097	197.47
182.573	129.17	214.565	150.87	246.410	173.23	282.177	198.94
184.450	130.39	216.468	152.20	248.479	174.73	284.245	200.46
186.331	131.63	218.376	153.51	250.535	176.20	286.336	201.98
188.199	132.98	220.290	154.78	252.578	177.65	288.454	203.47
190.072	134.20	222.208	156.07	254.643	179.21	290.557	205.06
191.982	135.49	224.115	157.52	256.732	180.65	292.665	206.53
193.914	136.75	226.013	158.87	258.826	182.13	294.779	208.05
195.822	138.04	227.915	160.21	260.925	183.83	296.880	209.62
197.739	139.41	229.823	161.46	263.029	185.24	298.986	211.13

Table V-8. Measured molar heat capacities of melt-frozen *p*-phenylphenol (sample B).

T / K	C_p / J·K^{-1}·mol^{-1}	T / K	C_p / J·K^{-1}·mol^{-1}	T / K	C_p / J·K^{-1}·mol^{-1}	T / K	C_p / J·K^{-1}·mol^{-1}
Series 1		23.842	17.353	66.745	57.598	122.403	91.330
4.313	0.099	25.044	18.806	68.345	58.727	124.255	92.368
4.476	0.225	26.259	20.294	69.931	59.775	126.169	93.461
Series 2		27.556	21.848	71.527	60.783	128.063	94.648
4.891	0.158	28.869	23.402	73.139	61.798	129.939	95.800
5.186	0.248	30.142	24.911	74.755	62.831	131.798	96.947
Series 3		31.429	26.379	76.364	63.843	133.639	98.027
6.232	0.703	32.709	27.892	77.967	64.826	135.464	99.172
6.674	0.867	33.972	29.315	79.566	65.798	137.272	100.25
7.249	1.110	35.192	30.713	81.162	66.829	139.063	101.35
7.958	1.461	36.393	31.980	82.756	67.823	140.839	102.48
Series 4		37.634	33.353	84.364	68.787	142.619	103.45
4.920	0.193	38.902	34.580	85.986	69.771	144.460	104.67
5.251	0.254	40.175	35.944	87.609	70.692	146.362	105.89
5.601	0.474	41.471	37.210	89.233	71.753	148.264	107.09
6.020	0.622	42.760	38.464	Series 9		150.152	108.10
6.504	0.802	44.045	39.712	89.594	72.076	152.034	109.24
7.071	1.038	45.393	40.916	91.255	73.087	153.919	110.52
Series 5		46.733	42.208	92.945	74.087	155.793	111.74
8.334	1.683	48.009	43.353	94.652	75.080	157.668	112.88
9.060	2.133	49.274	44.427	96.362	76.082	159.545	114.10
9.786	2.655	50.587	45.543	98.076	77.021	161.425	115.25
10.550	3.227	Series 7		99.794	78.058	163.324	116.46
11.412	3.899	51.955	46.642	101.519	79.075	Series 10	
12.338	4.701	53.336	47.778	103.236	80.021	165.246	117.67
13.278	5.515	54.712	48.861	104.994	81.084	167.184	118.92
Series 6		Series 8		106.792	82.118	169.125	120.14
14.360	6.561	54.517	48.742	108.567	83.144	171.052	121.35
15.493	7.700	55.946	49.876	110.321	84.189	172.964	122.68
16.621	8.860	57.417	51.021	112.054	85.201	174.864	123.90
17.769	10.147	58.938	52.156	113.769	86.183	176.767	125.13
18.966	11.530	60.485	53.276	115.465	87.184	178.674	126.39
20.193	12.973	62.034	54.374	117.150	88.247	180.586	127.60
21.422	14.452	63.591	55.444	118.869	89.260	182.502	128.95
22.639	15.901	65.154	56.537	120.629	90.242	184.430	130.14

Table V-8. (continued).

T/K	C_p/J·K^{-1}·mol^{-1}	T/K	C_p/J·K^{-1}·mol^{-1}	T/K	C_p/J·K^{-1}·mol^{-1}	T/K	C_p/J·K^{-1}·mol^{-1}
186.370	131.37	229.006	160.28	269.643	189.33	7.166	1.097
188.299	132.70	230.910	161.88	271.604	190.68	7.943	1.482
190.266	133.93	Series 11		273.554	192.07	Series 13	
192.269	135.32	232.829	163.16	275.495	193.49	3.716	0.135
194.258	136.74	234.781	164.58	277.426	194.78	4.189	0.151
196.234	138.03	236.758	166.04	279.347	196.09	Series 14	
198.196	139.38	238.724	167.51	281.257	197.59	4.333	0.168
200.147	140.72	240.679	168.86	283.159	199.10	4.976	0.306
202.086	142.05	242.623	170.21	285.051	200.50	5.556	0.524
204.013	143.40	244.558	171.58	286.968	201.75	6.151	0.713
205.928	144.63	246.482	172.90	288.908	203.22	6.776	0.932
207.832	145.89	248.395	174.13	290.838	204.71	7.411	1.207
209.739	147.14	250.266	175.49	292.792	205.88	8.108	1.572
211.651	148.50	252.145	176.67	294.773	207.32	8.838	2.004
213.572	149.80	254.062	178.14	296.745	208.70	9.633	2.556
215.514	151.15	255.985	179.60	298.706	210.26	10.496	3.195
217.462	152.46	257.916	180.89	300.656	211.56	11.400	3.909
219.400	153.82	259.836	182.34	Series 12		12.385	4.729
221.326	155.21	261.745	183.65	4.695	0.334	13.513	5.725
223.240	156.50	263.697	185.00	5.136	0.515		
225.163	157.835	265.689	186.40	5.707	0.559		
227.089	159.11	267.671	187.82	6.404	0.792		

Table V-9. Molar thermodynamic functions of sublimed *p*-phenylphenol (sample A).

T / K	C_p / J·K^{-1}·mol^{-1}	$\{H(T)-H(0)\}/T$ / J·K^{-1}·mol^{-1}	$S(T)-S(0)$ / J·K^{-1}·mol^{-1}	$-\{G(T)-H(0)\}/T$ / J·K^{-1}·mol^{-1}
5	0.310	0.071	0.091	0.019
10	2.60	0.666	0.871	0.205
20	12.46	3.90	5.41	1.52
30	24.45	8.74	12.73	3.98
40	35.54	14.09	21.32	7.23
50	44.89	19.35	30.29	10.94
60	52.85	24.28	39.19	14.91
70	59.79	28.87	47.87	19.00
80	66.23	33.14	56.28	23.14
90	72.32	37.16	64.44	27.28
100	78.24	40.97	72.36	31.39
110	84.11	44.63	80.09	35.47
120	90.01	48.16	87.67	39.50
130	96.01	51.61	95.11	43.49
140	102.02	55.00	102.44	47.44
150	108.23	58.34	109.69	51.35
160	114.50	61.65	116.88	55.22
170	120.97	64.95	124.01	59.06
180	127.49	68.24	131.11	62.87
190	134.13	71.54	138.18	66.64
200	140.92	74.83	145.23	70.40
210	147.70	78.14	152.27	74.13
220	154.65	81.46	159.30	77.84
230	161.62	84.79	166.33	81.54
240	168.71	88.15	173.36	85.21
250	175.82	91.51	180.39	88.88
260	183.05	94.89	187.43	92.54
270	190.24	98.29	194.47	96.18
280	197.40	101.70	201.51	99.81
290	204.63	105.13	208.57	103.44
300	211.87	108.57	215.63	107.06
298.15	210.54	107.93	214.32	106.39

Table V-10. Molar thermodynamic functions of melt-frozen *p*-phenylphenol (sample B).

T / K	C_p / J·K^{-1}·mol^{-1}	$\{H(T)-H(0)\}/T$ / J·K^{-1}·mol^{-1}	$S(T)-S(0)$ / J·K^{-1}·mol^{-1}	$-\{G(T)-H(0)\}/T$ / J·K^{-1}·mol^{-1}
5	0.378	0.097	0.126	0.029
10	2.82	0.739	0.985	0.246
20	12.74	4.06	5.71	1.65
30	24.74	8.96	13.14	4.19
40	35.72	14.31	21.80	7.49
50	45.02	19.55	30.81	11.25
60	52.89	24.47	39.73	15.26
70	59.79	29.03	48.41	19.38
80	66.13	33.28	56.81	23.54
90	72.23	37.27	64.95	27.69
100	78.17	41.06	72.87	31.81
110	84.00	44.70	80.60	35.90
120	89.91	48.22	88.16	39.94
130	95.86	51.65	95.59	43.93
140	101.92	55.03	102.91	47.89
150	108.05	58.36	110.15	51.80
160	114.36	61.66	117.33	55.67
170	120.72	64.95	124.45	59.50
180	127.21	68.23	131.54	63.31
190	133.81	71.50	138.59	67.09
200	140.63	74.79	145.63	70.84
210	147.41	78.09	152.65	74.57
220	154.28	81.39	159.67	78.28
230	161.26	84.71	166.68	81.97
240	168.34	88.05	173.69	85.64
250	175.34	91.40	180.71	89.30
260	182.37	94.76	187.72	92.95
270	189.52	98.14	194.74	96.59
280	196.66	101.53	201.76	100.22
290	203.96	104.94	208.79	103.85
300	211.14	108.36	215.82	107.46
298.15	209.79	107.73	214.52	106.79

sample B is not shown in Figure V-7. Although the general feature of the heat capacities of both samples was similar, the small difference at the lowest and at room temperatures was observed. After each energy input was over, thermal equilibrium within the calorimeter vessel was attained within 2 min below 30 K, in 12 min at 50 K, 18 min at 100 K, 10 min at 200 K and 7 min at 300 K in measurements on the sample A. However, in the sample B, it took as long as 10 min at 4 K, decreased to 30 s at 14 K, then increased to 20 min at 100 K and decreased again to 7 min above 250 K as the temperature rose.

Some thermodynamic functions at rounded temperatures were calculated from the primary results and are given in Tables V-9 and V-10, in which small contributions below 5 K were evaluated by smooth extrapolation to 0 K.

The difference between the low temperature heat capacities of the two samples is shown in Figure V-8. The Debye characteristic temperatures of the two samples are also shown there. For the sample B, the reliable data could not be obtained below 5 K. The heat capacity of the sample B is larger than that of the sample A below 65 K. The fact that there is no apparent maximum in the difference curve suggests that the origin of the difference may be in the difference in crystal lattice itself or in the crystallinity. On

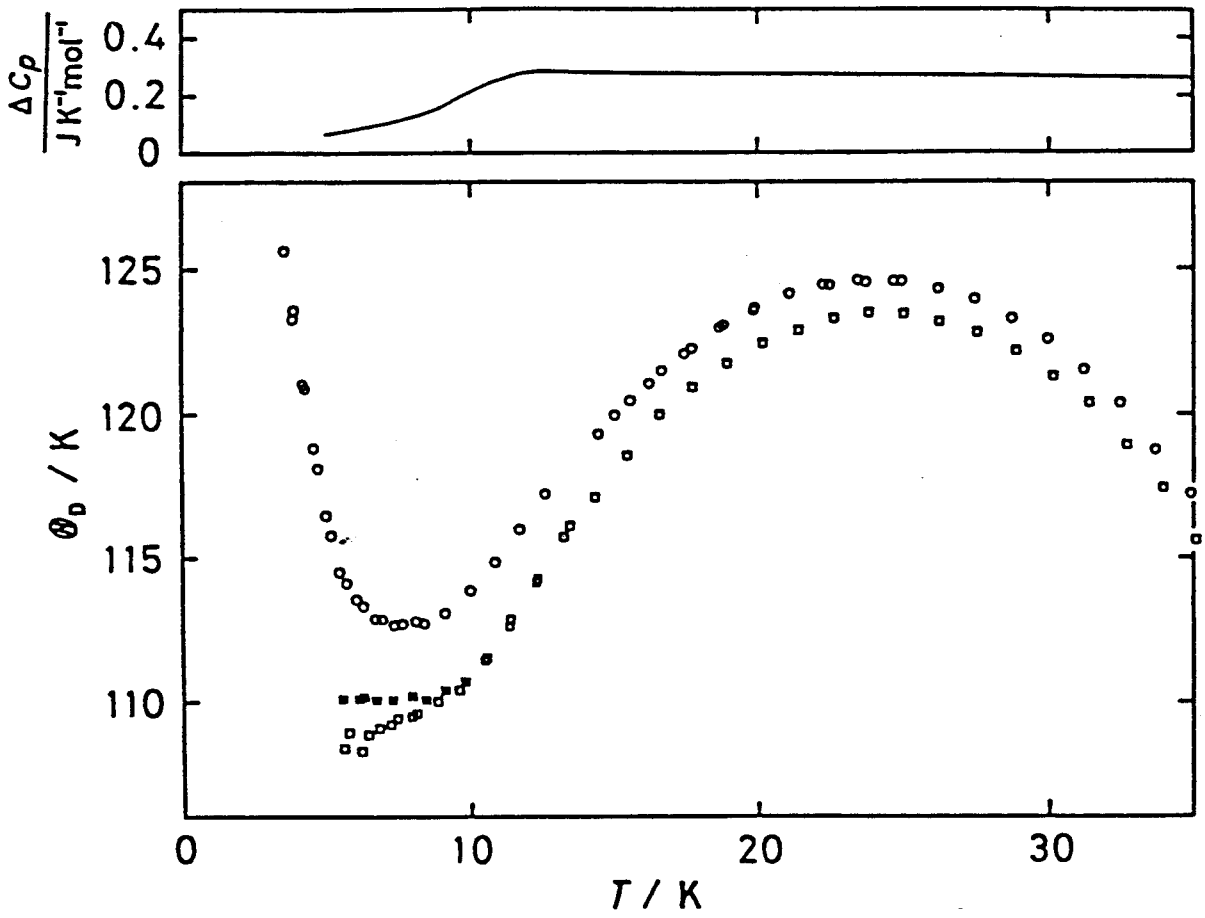

Figure V-8. Debye characteristic temperatures of sublimed (sample A, open circle) and melt-frozen (sample B, square) p-phenylphenol, assuming 6 degrees of freedom per molecule, and the heat capacity difference between the samples A and B. The filled squares correspond to the instantaneous heat capacities of the sample B.

the other hand, the higher temperature values of heat capacity of the sample A is slightly larger than that of the sample B (0.4 per cent at 300 K).

No anomalous heat capacity is seen in Figures V-7 and V-8. The powder X-ray diffraction patterns showed that both the samples were of $P2_1/a$ polymorph. Thus, it is concluded that there is no phase transition between 4 and 300 K in contrast to the suggestion given by Brock and Haller.[37)]

Slow relaxation observed at the lowest temperature region in the sample B is similar to that in p,p'-biphenol described in the preceding section. In view that such a phenomenon was not observed in the crystals without hydrogen bond, it may have some connection with hydrogen bond network and chain. The sample B was prepared by melting under helium atmosphere and gradual cooling for recrystallization, while the sample A by sublimation only. Thus, it is likely that the crystallinity of the samples is considerably different each other. The X-ray powder diffraction patterns of both samples, indeed, showed differences in intensity of diffraction lines but their locations agreed with each other within the experimental precision and they could be indexed by assuming the $P2_1/a$ polymorph.

The Raman spectra of both the samples are shown in Figure V-9. The spectra of both samples become well-resolved on cooling, and there are no anomalous

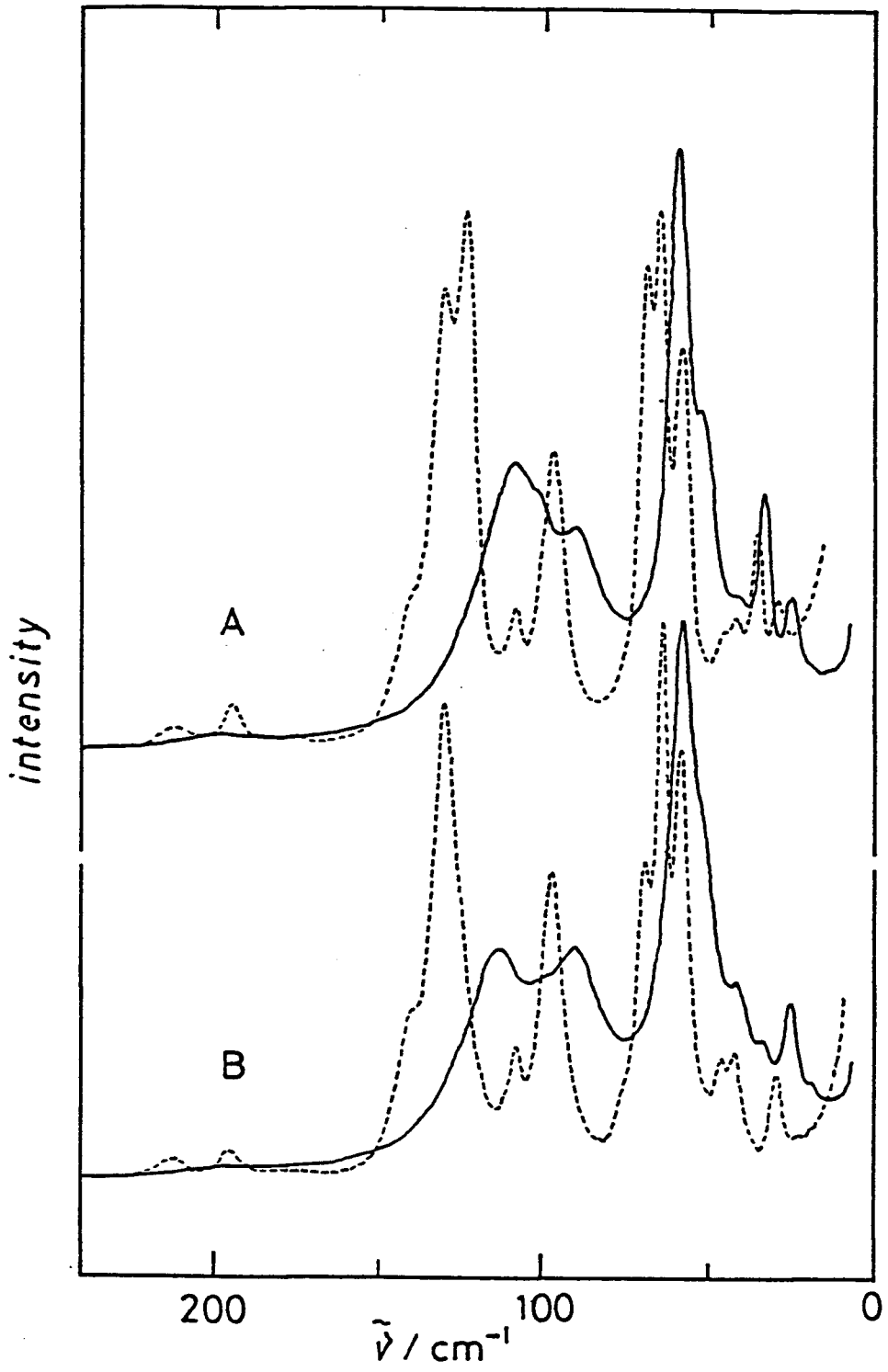

Figure V-9. Raman spectra of sublimed (sample A) and melt-frozen (sample B) p-phenylphenol at room temperature (solid curve) and at liquid nitrogen temperature (broken curve).

behavior in agreement with the results of heat capacity measurements. Taking into consideration the results of the X-ray diffraction experiments, the difference in the spectra between the samples A and B should be attributed to the different crystallinity of the samples.

Finally, the comparison of the heat capacities of biphenyl, p-phenylphenol and p,p'-biphenol is shown in Figure V-10. In spite of the smallest mass, below 100 K, biphenyl shows the largest value of the heat capacities, and p-phenylphenol shows larger heat capacities than p,p'-biphenol. On the other hand, the order of the heat capacity values at room temperature is reversed, i.e. biphenyl < p-phenylphenol < p,p'-biphenol. Their heat capacity values are , at low temperatures, primarily determined by the lattice stiffness; the hydrogen-bond makes the crystal lattice stiffer. At higher temperatures, the order of the heat capacity values can not be explained by the lattice properties such as its stiffness or mass effect since their lattice heat capacities already saturate to the classical value at room temperature. Thus, the order of the heat capacity values at room temperature must be determined by the difference of the number of degrees of freedom. The number of freedom per molecule increases by 3 per substitution with a hydroxyl group. The difference of about 13 $J \cdot K^{-1} \cdot mol^{-1}$ between biphenyl

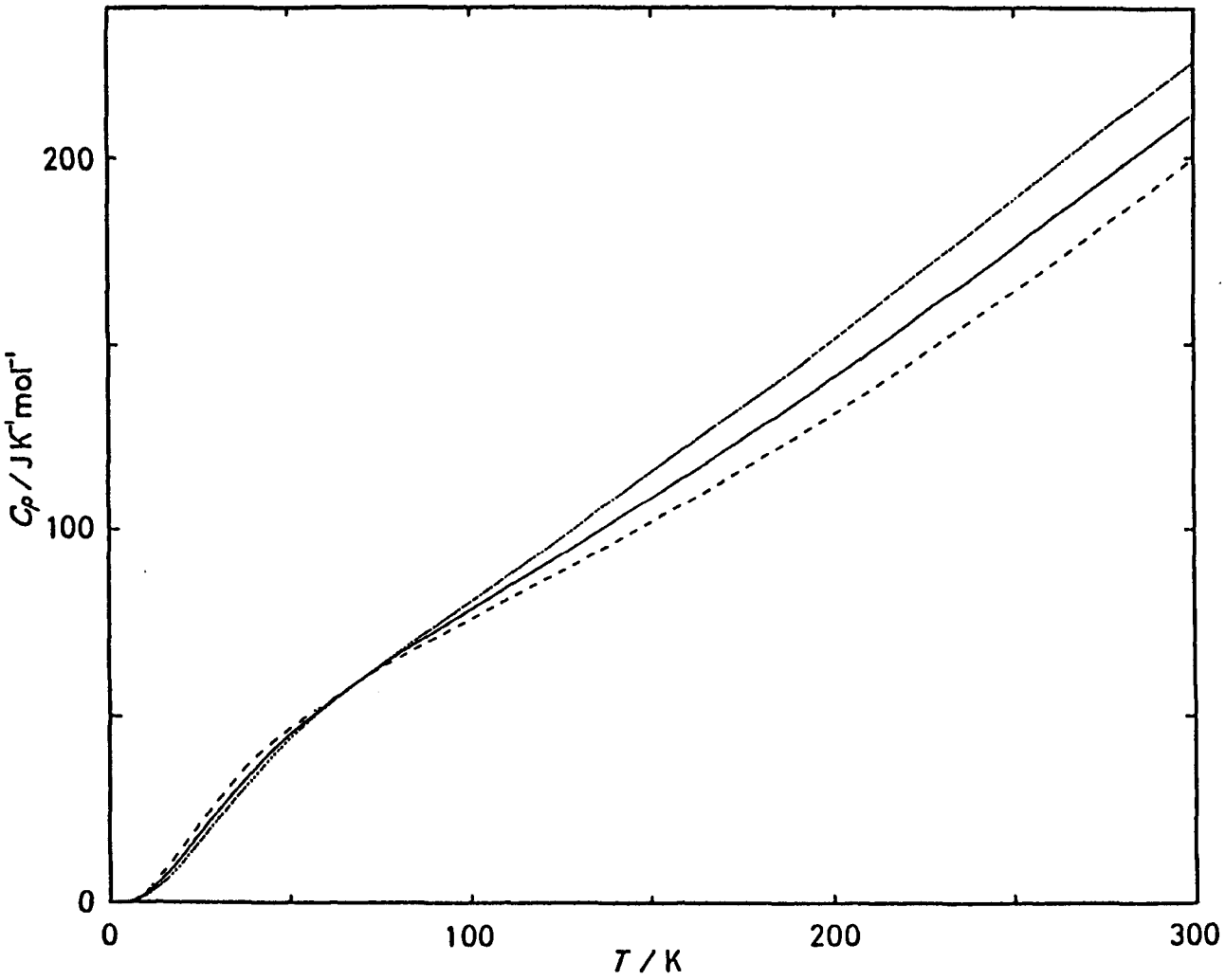

Figure V-10. Molar heat capacities of biphenyl (broken curve), p-phenylphenol (solid curve), and p,p'-biphenol (dotted curve).

and p-phenylphenol and between p-phenylphenol and p,p'-biphenol may be attributed to the C-O vibrations (bending and stretching) if the simple localized scheme of intramolecular vibration could be applied.

V-3 Stability of a planar molecular conformation in 4,4'-difluorobiphenyl and p,p'-biphenol crystals

As no anomaly was found in the heat capacity curve of 4,4'-difluorobiphenyl crystal in the temperature region where thermal motion plays an important role, it is meaningful to compare the static cohesive energy (i.e. lattice energy) of a crystal consisting of planar molecules with that of a crystal consisting of twisted molecules in order to discuss the stability of a planar conformation in the crystalline state.

Two probable crystal structures were considered. The structure of a crystal consisting of planar molecules was taken to be the same as that of biphenyl[21]; $P2_1/a$, $Z = 2$ (there is a half molecule in an asymmetric unit).[6] The structure consisting of twisted molecules was assumed to be the same as that of the other 4,4'-dihalogenobiphenyls[31] (dichloro- and dibromobiphenyl); $P2_1/n$, $Z = 8$ (there are two independent molecules in an asymmetric unit).[22,23]

The molecular geometry was fixed; the phenyl rings were assumed as a normal hexagon with the C-C bond

length of 0.140 nm. The central C-C bond length was 0.150 nm. The length of C-H and C-F bonds were 0.110 nm and 0.149 nm, respectively. The twist angle of the phenyl rings was 40° for 4,4'-dihalogenobiphenyl-type structure. Since this value of twist angle is observed in other crystalline 4,4'-dihalogenobiphenyls[22,23] and it is the same as for an isolated 4,4'-difluorobiphenyl molecule within the error of the experimental value[30], the first derivative of the intramolecular potential curve could be neglected in the minimization of the lattice energies. The twist angle for biphenyl-type structure was 0°.

Intermolecular interaction was represented by a sum of interatomic potentials of Buckigham type. Their parameters were taken from literature.[39,40]

Lattice energies of two crystal structures were calculated using the accelerated convergence method[41] and minimized with respect to the size and the shape of the unit cells, i.e. 7 and 16 variables for biphenyl-type and 4,4'-dohalogenobiphenyl-type structures, respectively, using the DAFLEP.[42]

Crystal structural parameters and lattice energies obtained are given in Table V-11 with probable experimental data for the sake of comparison. The discrepancies between the calculated and the "experimental" values in both cases are of the same order of magnitude as that reported for biphenyl

Table V-11. Calculated and "observed" lattice parameters of 4,4'-difluorobiphenyl.

		a / nm	*b* / nm	*c* / nm	β / °	(*V*/*Z*) / nm^3	*E* / $kJ \cdot mol^{-1}$
$P2_1/a$	calc.	0.7541	0.5535	0.9930	88.66	0.2072	-113
Z = 2	obs.[31]	0.776	0.581	0.996	92.6	0.2243	—
planar	Δ^a / %	-2.8	-4.7	-0.3	-4.3	-7.6	—
$P2_1/n$	calc.	1.500	1.270	0.948	94.91	0.2249	-96
Z = 8	obs.[21]	1.483	1.330	0.945	96.8	0.2313	—
twisted	Δ^a / %	1.1	-4.5	0.4	-2.0	-2.8	—

[a] $\Delta = 100 \cdot (\text{calc.} - \text{obs.})/\text{obs.}$

crystal.[43] However, the purpose of the calculation is to elucidate the relative stability of two crystal structures.

The final values of lattice energy was -96 kJ·mol^{-1} for the 4,4'-dihalogenobiphenyl-type of structure and -113 kJ·mol^{-1} for the biphenyl-type of structure. These values must be corrected further for the intramolecular energy difference between the planar and the twisted conformations. This difference is about 10 kJ·mol^{-1} in the case of biphenyl,[44] and it is smaller in 4,4'-difluorobiphenyl than in biphenyl due to greater π-conjugation through the central C-C bond; this was confirmed by the simple calculation by the Hückel model described in Section II-2. The difference in the resultant lattice energy between the two structures was thus derived as about 7 kJ·mol^{-1}. Therefore, the biphenyl-type structure is stable even at 0 K in contrast to the case of biphenyl crystal because of the stabilization of a planar conformation due to greater π-conjugation in 4,4'-difluorobiphenyl molecule.

A similar interpretation should be applied to the absence of the twist transition in p,p'-biphenol because of the following reasons. First, it must be pointed out that the intramolecular potential of p,p'-biphenol is very similar to that of 4,4'-difluorobiphenyl in spite of the different substituents as shown in Section II-2. Second, the intermolecular

interaction favoring a planar conformation has a two dimensional character as discussed in Section III-4 because the interatomic distance between 4 (4') position and the other positions of the neighboring molecule changes little on the twisting of the neighboring molecule. Thus, the part favoring a planar conformation in the interaction is expected to be similar in 4,4'-difluorobiphenyl and in p,p'-biphenol.

References to Chapter V

1. J. Trotter, Acta Cryst., 14(1961), 1135.
2. G. B. Robertson, Nature, 191(1961), 593.
3. A. Hargreaves and S. H. Rizvi, Acta Cryst., 15(1962), 365.
4. V. M. Kozhin and K. V. Mirskaya, Sov. Phys. Cryst., 14(1970), 938.
5. G. P. Charboneau and Y. Delugeard, Acta Cryst., B32(1976), 1420.
6. G. P. Charboneau and Y. Delugeard, Acta Cryst., B33(1977), 1586.
7. H. Cailleau, J. L. Baudour and C. M. E. Zeyen, Acta Cryst., B35(1979), 426.
8. J. L. Baudour and M. Sanquer, Acta Cryst., B39(1983), 75.
9. H. M. Rietvelt, E. N. Maslen and C. J. B. Clews, Acta Cryst., B26(1970), 693.
10. P. J. L. Baudour, Y. Delugeard and H. Cailleau, Acta Cryst., B32(1976), 150.
11. P. J. L. Baudour, H. Cailleau and W. B. Yelon., Acta Cryst., B33(1977), 1773.
12. Y. Delugeard, J. Desuche and J. L. Baudour, Acta Cryst., B32(1976), 702.
13. J. L. Baudour, Y. Delugeard and P. Rivet, Acta Cryst., B34(1978), 625.
14. A. Bree and M. Edelson, Chem. Phys. Lett., 46(1977), 500.

15. H. Cailleau, A. Girard, F. Moussa and C. M. E. Zeyen, Solid State Commun., 29(1979), 259.
16. M. Wada, A. Sawada and Y. Ishibashi, J. Phys. Soc. Jpn., 50(1981), 737.
17. N. M. Plakida, A. V. Belushkin, I. Natkaniec and T. Wasiutyński, Phys. Status Solidi b, 118(1983), 129.
18. B. A. Bolton and P. N. Prasad, Chem. Phys., 35(1978), 331.
19. H. Cailleau and A. Dworkin, Mol. Cryst. Liq. Cryst., 50(1979), 217.
20. S. S. Chang, J. Chem. Phys., 79(1983), 6229.
21. T. K. Halstead, H. W. Spiess and U. Haeberlen, Mol, Phys., 31(1976), 1569.
22. C. P. Brock, M. S. Kuo and H. A. Levy, Acta Cryst., B34(1978), 981.
23. P. Cronebusch, W. B. Gleason and D. Britton, Cryst. Struct. Commun., 5(1976), 839.
24. G. Casalone, C. Mariani, A. Mugnoli and M. Simonetta, Acta Cryst., B25(1969), 1741.
25. E. B. Boonstra, Acta Cryst., 16(1963), 816.
26. N. A. Akhmed, M. S. Farag and A. Amin, Zh. Strukt. Khim., 12(1971), 738.
27. W. B. Gleason and D. Britton, Cryst. Struct. Commun., 5(1976), 483.
28. B. F. Pedersen, Acta Cryst., B31(1975), 2931.
29. P. Singh and J. D. Mckinney, Acta Cryst., B35(1979), 259.

30. O. Bastiansen and L. Smedvik, Acta Chem. Scand., 8(1954), 1593.
31. J. Dhar, Indian J. Phys., 20(1946), 154.
32. R. M. Barrett and D. Steele, J. Mol. Struct., 11(1972), 105.
33. H. Michelsen, P. Kraeboe, G. Hagen and T. S. Hansen, Acta Chem. Scand., 26(1972), 1576.
34. T. K. Halstead, J. Tagenfeldt and U. Haeberlen, J. Chem. Soc. Faraday II, 77(1981), 1817.
35. S. C. Wallwork and H. M. Powell, Nature, 167(1951), 1072.
36. M. S. Farag and N. A. Kader, J. Chem. U. A. R., 3(1960), 1.
37. C. P. Brock and K. L. Haller, J. Phys. Chem., 88(1984), 3570.
38. N. K. Smith, G. Gorin, W. D. Good and J. P. McCullough, J. Phys. Chem., 68(1964), 940.
39. A. Gavezzotti and M. Simonetta, Acta Cryst., A32(1976), 645.
40. D. E. Williams, J. Chem. Phys., 47(1967), 4680.
41. D. E. Williams, Acta Cryst., A27(1971), 452.
42. "DAFLEP", the Program Library, Computer Center, Osaka University.
43. C. P. Brock, Mol. Cryst. Liq. Cryst., 52(1979), 157.
44. A. J. Grumadas, D. P. Poshkus and A. V. Kiselev, J. Chem. Soc. Faraday II, 75(1979), 1398.

Chapter VI Twisting motion in o-substituted biphenyls

VI-1 Introduction

Since the intramolecular potential for the twisting is a resultant of two opposite effects, delocalization of π-electrons and steric repulsion between ortho atoms, the twist angle of a free molecule increases from 42° in biphenyl[1,2] to 70° in perfluorobiphenyl (PFB)[3] as the atomic size at the ortho positions increases. In crystalline state, molecules of PFB and perchlorobiphenyl (PCB) are twisted about 60°[4-7] and 87°,[8] respectively. These values can be interpreted with the van der Waals radii of fluorine and chlorine atoms. The crystal packing force is balanced with repulsion between ortho atoms. This situation shows that in PFB and PCB crystals molecules are tightly packed and that the twisting degree of freedom is strongly suppressed.

Although the idealized symmetry D_2 of a twisted molecule gives non vanishing probability of the Raman process for the twisting vibration in contrast to the symmetry D_{2h} of a planar molecule, no direct observation has been reported so far.[9,10] Therefore, it was attempted to obtain some information about a twisting motion from low temperature heat capacities of PFB and PCB as in the case of biphenyl and p-terphenyl

(see Chapter III).

VI-2 Heat capacities of perfluorobiphenyl and perchlorobiphenyl

Experimental

Commercially available PFB (Alfa Division, Ventron Corporation) was purified by fractional sublimation in vacuum at room temperature. The powdered specimen (13.5159 g, 0.0404524 mol) was loaded into the calorimeter vessel. The calorimeter was evacuated and sealed after the addition of a small amount of helium gas for heat exchange (8 kPa at room temperature). The purity of the sample used for the calorimetry was better than 99.9 moles per cent as determined by gas-chromatography.

The PCB standard reagent (nominal purity; better than 99.0 moles per cent, gas-chromatography) for quantitative analysis of polychlorinated-biphenyls was purchased from Wako Pure Chemical Industries, Ltd., and purified further by fractional sublimation in vacuum at about 450 K. The powdered specimen (13.0809 g, 0.0262322 mol) was loaded into the calorimeter vessel with a small amount of helium gas (5 kPa at room temperature). The contribution of the sample to the total heat capacity including that of the calorimeter

vessel was 70 per cent in the measurements on PFB (73 per cent in PCB) at 10 K, 41 (37) per cent at 50 K, 36 (31) per cent at 100 K, and 45 (36) per cent at 300 K. The heat capacity of helium gas in the vessel was negligibly small with respect to both the total and the sample heat capacities.

The working thermometers, and the apparatus and the operation of the adiabatic calorimeter were the same as described in Chapter III.

Results and Discussion

Measured molar heat capacities of PFB and PCB are shown in Figure VI-1 and tabulated in Tables VI-1 and VI-2 in chronological order. The scatter of the present data is slightly larger than those of the other sample described previous chapters because of the smaller amount of the samples. No thermal anomaly is seen in both heat capacity curves. The temperature increment of each individual measurement, which may be deduced from the adjacent mean temperatures, is small enough to permit the curvature correction to be ignored in comparison with the experimental precision. After each heat input, thermal equilibration was reached within 2 min below 20 K, in 15 min at 60 K, 25 min at 100 K, 30 min at 150 K, and within 20 min above 200 K in the measurements on PCB. Almost the same was in PFB.

The comparison of the present results with the

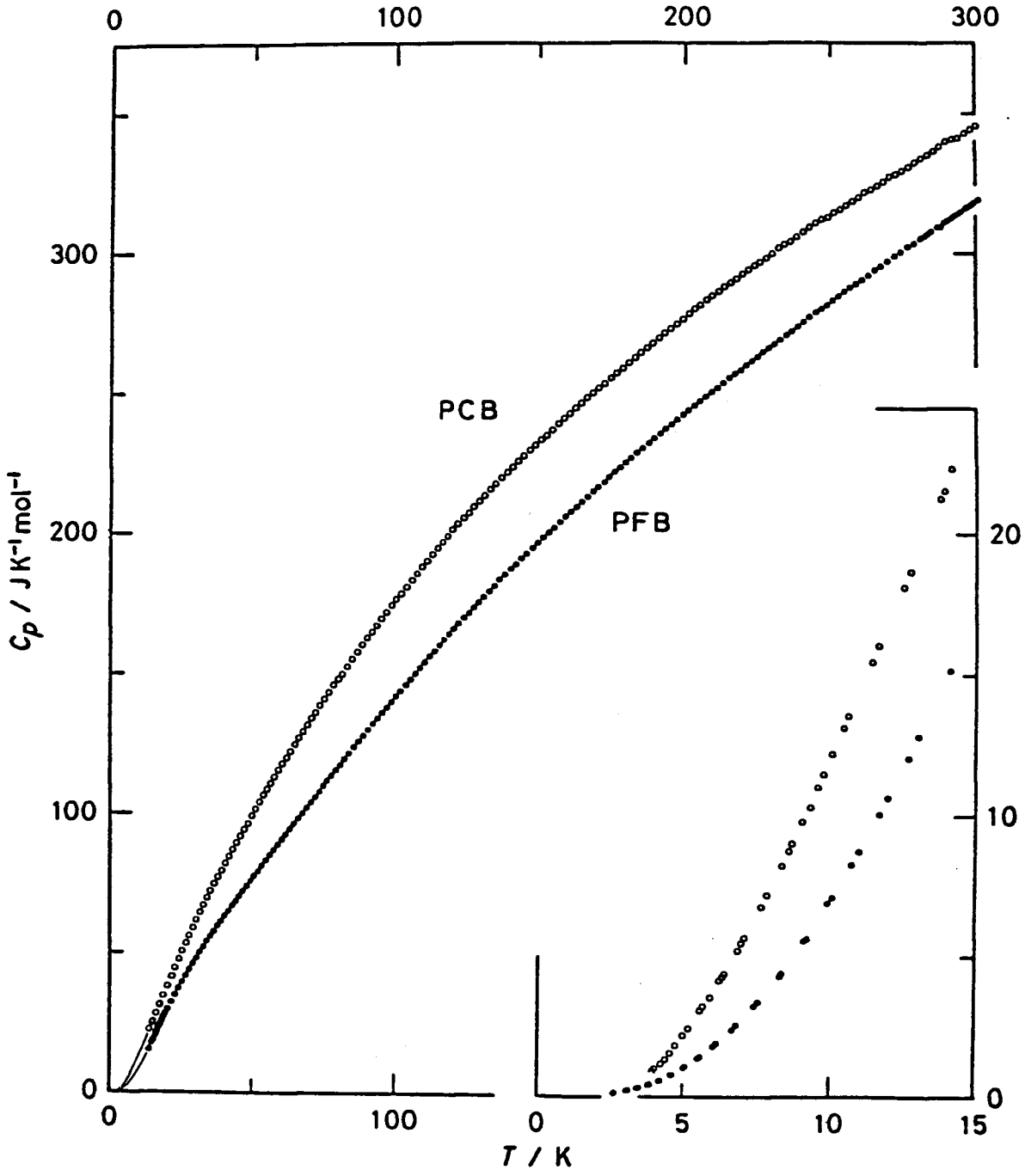

Figure VI-1. Measured molar heat capacities of perfluorobiphenyl (open circle) and perchlorobiphenyl (filled circle).

Table VI-1. Measured molar heat capacities of perfluorobiphenyl.

T/K	C_p/J·K^{-1}·mol^{-1}	T/K	C_p/J·K^{-1}·mol^{-1}	T/K	C_p/J·K^{-1}·mol^{-1}	T/K	C_p/J·K^{-1}·mol^{-1}
Series 1		Series 3		47.791	74.080	100.103	141.92
2.641	0.127	14.133	15.152	49.125	75.971	Series 6	
3.102	0.215	15.242	17.617	50.483	77.705	101.723	144.21
3.484	0.317	16.358	20.147	51.848	79.360	103.339	146.07
3.846	0.429	17.487	22.703	53.203	81.339	105.003	148.07
4.233	0.584	18.628	25.236	54.596	83.369	106.696	150.05
4.621	0.786	19.770	27.825	56.004	85.227	108.419	152.15
5.046	1.053	Series 4		57.386	87.048	110.160	154.01
5.516	1.377	15.786	18.835	58.769	88.871	111.892	156.15
6.042	1.806	16.912	21.395	60.141	90.732	113.618	158.05
6.660	2.376	18.091	24.044	61.522	92.531	115.337	160.12
7.418	3.219	19.322	26.858	62.942	94.478	117.052	162.11
8.276	4.269	20.586	29.547	64.384	96.360	118.774	164.09
9.111	5.552	21.844	32.207	65.829	98.228	120.521	166.04
9.920	6.909	23.059	34.705	67.281	100.10	122.278	167.97
10.757	8.283	24.266	37.121	68.741	101.96	124.018	169.96
11.705	10.057	25.486	39.464	70.188	103.94	125.742	171.88
12.706	12.038	Series 5		71.647	105.90	127.463	173.81
Series 2		26.700	41.728	73.140	107.81	129.183	175.66
3.116	0.219	27.911	43.821	74.609	109.91	130.902	177.65
3.454	0.302	29.135	46.114	76.075	111.79	132.650	179.56
3.820	0.425	30.365	48.002	77.550	113.66	134.440	181.41
4.189	0.573	31.587	50.149	79.038	115.50	136.270	183.51
4.596	0.787	32.806	52.092	80.560	117.33	138.112	185.35
5.071	1.075	34.028	54.103	82.120	119.44	139.940	187.27
5.583	1.432	35.252	56.037	83.718	121.47	141.753	189.09
6.142	1.890	36.475	57.871	85.332	123.78	143.611	191.11
6.792	2.505	37.701	59.775	86.965	125.83	145.512	193.17
7.536	3.350	38.935	61.449	88.635	127.84	147.399	195.08
8.352	4.393	40.177	63.382	90.315	130.03	149.271	196.80
9.200	5.624	41.436	65.074	91.966	132.12	151.128	198.76
10.083	7.115	42.698	66.940	93.605	134.12	152.974	200.54
11.002	8.747	43.945	68.563	95.245	136.14	154.851	202.42
11.987	10.627	45.194	70.472	96.874	138.04	156.761	204.31
13.049	12.802	46.477	72.224	98.492	140.00	158.657	206.19

Table VI-1. (continued).

T/K	C_p/J·K^{-1}·mol^{-1}	T/K	C_p/J·K^{-1}·mol^{-1}	T/K	C_p/J·K^{-1}·mol^{-1}	T/K	C_p/J·K^{-1}·mol^{-1}
160.541	207.91	196.777	240.97	236.009	272.43	278.516	303.60
162.413	209.66	198.702	242.65	238.036	274.12	280.827	305.39
164.273	211.47	200.648	244.33	240.089	275.76	283.168	306.98
166.136	213.30	202.617	245.91	242.167	277.41	Series 8	
168.003	215.12	204.578	247.55	244.235	279.11	287.860	309.54
169.860	216.87	206.532	249.20	246.295	280.28	290.170	311.69
171.706	218.55	208.507	250.86	248.348	281.65	292.468	313.59
173.541	220.52	210.505	252.41	250.392	283.30	294.760	314.98
175.389	222.17	212.494	254.16	252.428	284.75	297.077	316.66
177.277	223.82	214.472	255.83	254.457	286.41	299.423	318.29
179.184	225.61	216.441	257.40	256.479	287.97	Series 9	
181.080	227.22	218.402	258.83	258.472	289.28	282.156	306.32
Series 7		220.354	260.52	260.528	290.80	284.489	307.96
183.024	229.00	222.299	262.04	262.699	292.35	286.810	309.53
185.020	230.80	224.236	263.50	264.894	294.14	289.119	311.13
187.005	232.46	226.164	265.06	267.081	295.56	291.455	312.91
188.980	234.24	228.085	266.49	269.331	297.31	293.818	314.18
190.944	235.86	230.009	267.87	271.640	299.18	296.172	316.14
192.898	237.73	231.966	269.39	273.941	300.67	298.512	317.59
194.843	239.35	233.976	271.01	276.233	302.05	300.855	319.22

Table VI-2. Measured molar heat capacities of perchlorobiphenyl.

T/K	C_p/J·K^{-1}·mol^{-1}	T/K	C_p/J·K^{-1}·mol^{-1}	T/K	C_p/J·K^{-1}·mol^{-1}	T/K	C_p/J·K^{-1}·mol^{-1}
Series 1		142.608	226.19	211.085	286.65	283.241	334.77
81.037	149.96	144.545	228.13	213.153	288.39	285.389	336.32
82.825	152.68	146.468	230.13	215.213	289.62	287.533	337.87
84.605	155.31	148.407	231.98	217.267	291.12	289.687	339.85
86.350	157.78	150.363	233.89	219.312	292.81	291.848	340.60
88.064	160.35	Series 2		221.349	294.38	294.005	340.77
89.775	162.69	152.268	235.42	223.335	295.75	296.156	342.60
91.484	165.04	154.228	237.50	225.328	297.07	298.301	344.08
93.192	167.28	156.207	239.69	227.404	298.52	300.439	345.43
94.927	169.78	158.173	241.45	229.535	299.94	Series 4	
96.663	172.08	160.129	243.28	231.689	302.09	5.868	3.532
98.402	174.46	162.073	245.17	233.836	303.47	6.354	4.392
100.144	176.68	164.036	247.02	Series 3		6.946	5.465
101.888	178.68	166.048	248.77	235.927	304.09	7.620	6.776
103.663	181.04	168.078	250.62	238.057	305.88	8.313	8.255
105.470	183.57	170.097	252.35	240.179	307.76	9.017	9.843
107.280	185.86	172.136	253.89	242.326	309.60	9.733	11.491
109.096	188.23	174.194	255.87	244.498	311.25	Series 5	
110.918	190.37	176.242	257.57	246.662	312.40	4.068	1.019
112.749	192.75	178.278	259.36	248.819	313.01	4.366	1.323
114.587	194.95	180.303	261.25	250.970	314.62	4.729	1.825
116.406	197.20	182.351	263.00	253.115	315.72	5.163	2.432
118.235	199.42	184.420	264.91	255.253	317.26	5.646	3.208
120.074	201.05	186.478	266.55	257.401	318.77	6.203	4.131
121.895	203.68	188.527	268.21	259.559	320.05	6.807	5.205
123.728	205.66	190.566	269.96	261.710	321.78	Series 6	
125.574	207.54	192.595	271.75	263.855	322.85	3.938	0.930
127.405	209.86	194.646	273.27	265.993	324.17	4.219	1.166
129.217	211.72	196.719	274.91	268.142	325.53	4.538	1.568
131.050	213.87	198.783	276.64	270.301	327.17	4.975	2.175
132.934	216.02	200.838	278.57	272.453	328.13	5.562	3.064
134.859	218.09	202.885	280.35	274.599	329.32	6.284	4.262
136.797	220.30	204.924	281.82	276.757	330.67	7.048	5.670
138.719	222.21	206.954	283.51	278.925	332.27	7.808	7.204
140.656	224.17	209.008	285.17	281.086	333.57	8.551	8.769

Table VI-2. (continued).

T/K	C_p/J·K^{-1}·mol^{-1}	T/K	C_p/J·K^{-1}·mol^{-1}	T/K	C_p/J·K^{-1}·mol^{-1}	T/K	C_p/J·K^{-1}·mol^{-1}
9.284	10.312	20.316	38.076	32.829	67.372	57.680	113.39
10.036	12.215	Series 10		34.047	69.909	59.017	115.65
Series 7		14.133	22.371	35.269	72.412	60.373	117.89
8.659	9.047	15.298	25.313	36.494	74.976	61.765	120.09
9.534	11.048	16.481	28.233	37.733	77.446	63.194	122.54
10.432	13.141	17.677	31.305	38.971	79.781	64.643	124.85
11.399	15.497	18.866	34.325	40.229	82.261	66.097	127.17
12.497	18.109	20.055	37.333	41.540	84.736	67.555	129.51
13.744	21.279	21.259	40.280	42.865	87.285	68.999	131.79
Series 8		Series 11		44.196	89.572	70.430	134.18
10.593	13.559	21.739	41.567	45.532	92.022	71.890	136.28
11.623	16.056	22.963	44.650	46.873	94.448	73.416	138.73
12.719	18.664	24.207	47.737	48.228	96.941	75.011	141.11
13.872	21.575	25.446	50.714	49.582	99.418	76.615	143.62
Series 9		26.664	53.658	50.940	101.78	78.206	146.08
15.147	25.047	27.888	56.361	52.304	104.14	79.787	148.38
16.438	28.275	29.129	59.204	53.657	106.60		
17.665	31.352	30.364	61.983	55.003	108.81		
18.962	34.681	31.601	64.667	56.344	111.05		

Table VI-3. Molar thermodynamic functions of perfluorobiphenyl.

T / K	C_p / J·K^{-1}·mol^{-1}	$\{H(T)-H(0)\}/T$ / J·K^{-1}·mol^{-1}	$S(T)-S(0)$ / J·K^{-1}·mol^{-1}	$-\{G(T)-H(0)\}/T$ / J·K^{-1}·mol^{-1}
5	1.03	0.251	0.322	0.071
10	6.95	1.90	2.54	0.64
20	28.31	9.59	13.64	4.06
30	47.52	19.13	28.87	9.74
40	63.25	28.23	44.74	16.51
50	77.09	36.62	60.34	23.72
60	90.49	44.49	75.59	31.10
70	103.77	52.01	90.53	38.53
80	116.78	59.30	105.24	45.95
90	129.61	66.40	119.74	53.34
100	141.94	73.34	134.04	60.70
110	154.00	80.13	148.14	68.01
120	165.44	86.76	162.03	75.27
130	176.63	93.25	175.72	82.47
140	187.38	99.59	189.20	89.61
150	197.63	105.79	202.48	96.70
160	207.38	111.84	215.55	103.72
170	217.06	117.74	228.41	110.68
180	226.32	123.52	241.09	117.57
190	235.14	129.16	253.56	124.40
200	243.73	134.68	265.84	131.17
210	252.06	140.07	277.94	137.87
220	260.22	145.35	289.85	144.51
230	267.94	150.51	301.59	151.08
240	275.63	155.56	313.16	157.59
250	283.04	160.51	324.56	164.04
260	290.37	165.37	335.80	170.43
270	297.74	170.13	346.90	176.77
280	304.81	174.82	357.86	183.04
290	311.78	179.42	368.67	189.25
300	318.67	183.95	379.36	195.41
298.15	317.43	183.12	377.39	194.28

Table VI-4. Molar thermodynamic functions of perchlorobiphenyl.

T / K	C_p / J·K^{-1}·mol^{-1}	$\{H(T)-H(0)\}/T$ / J·K^{-1}·mol^{-1}	$S(T)-S(0)$ / J·K^{-1}·mol^{-1}	$-\{G(T)-H(0)\}/T$ / J·K^{-1}·mol^{-1}
5	2.21	0.506	0.638	0.133
10	12.13	3.65	4.93	1.29
20	37.26	14.11	20.94	6.84
30	61.21	25.90	40.68	14.78
40	81.81	37.36	61.18	23.82
50	100.12	48.10	81.42	33.32
60	117.26	58.20	101.19	42.99
70	133.42	67.80	120.49	52.69
80	148.54	76.96	139.31	62.35
90	162.95	85.73	157.65	71.92
100	176.47	94.14	175.53	81.39
110	189.27	102.21	192.95	90.75
120	201.45	109.98	209.95	99.97
130	212.72	117.45	226.52	109.07
140	223.56	124.65	242.69	118.04
150	233.55	131.58	258.46	126.88
160	243.19	138.25	273.84	135.59
170	252.25	144.70	288.86	144.16
180	260.96	150.91	303.52	152.61
190	269.51	156.93	317.86	160.93
200	277.81	162.77	331.90	169.13
210	285.84	168.44	345.65	177.21
220	293.29	173.95	359.12	185.17
230	300.63	179.30	372.32	193.02
240	307.36	184.50	385.26	200.77
250	313.83	189.54	397.94	208.40
260	320.40	194.45	410.38	215.93
270	326.61	199.23	422.59	223.36
280	332.87	203.89	434.58	230.69
290	338.85	208.44	446.36	237.92
300	345.16	212.89	457.95	245.06
298.15	343.96	212.07	455.82	243.75

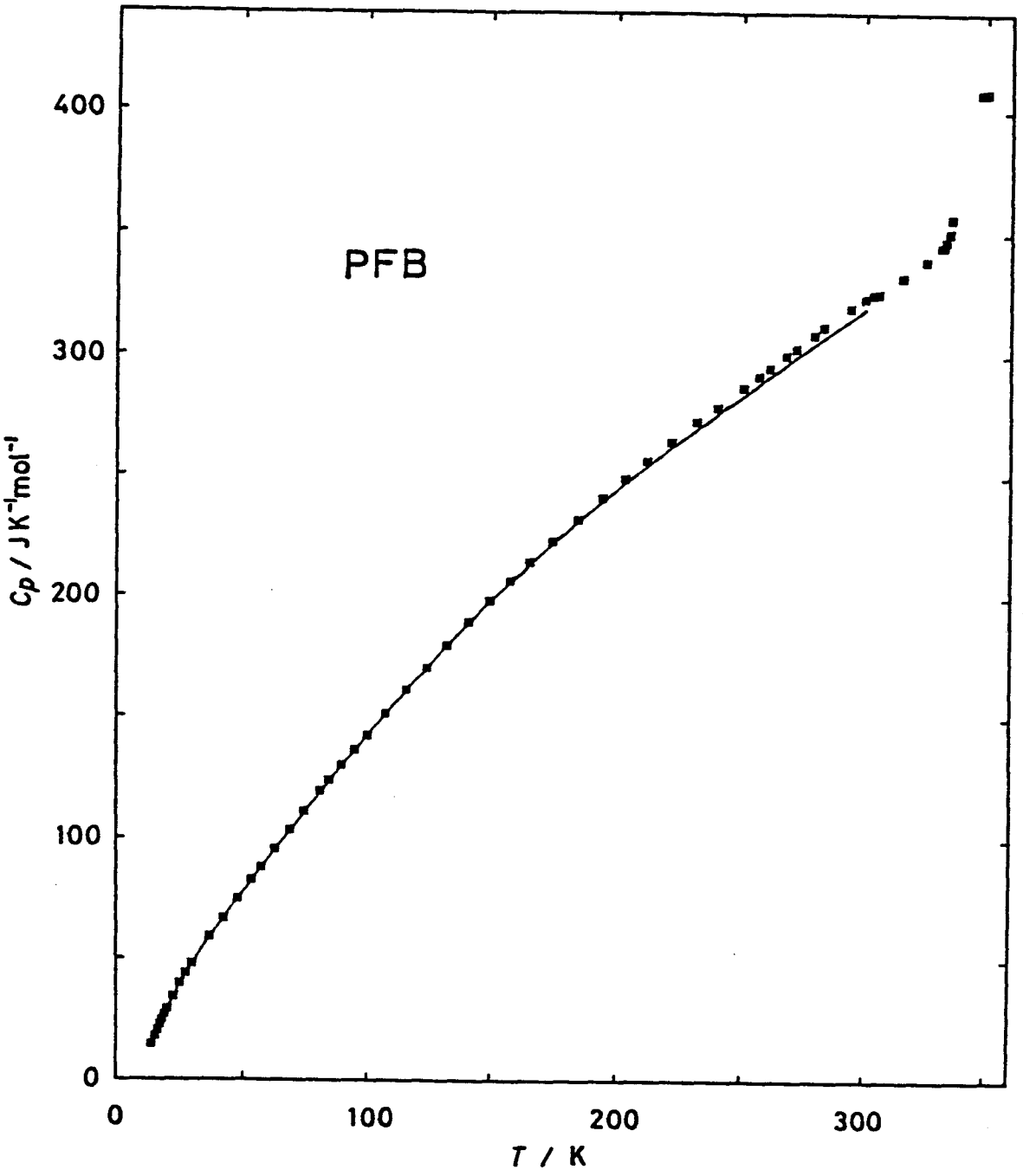

Figure VI-2. Comparison between the present data (solid curve) and the data reported by Paukov and Rakhmenkulov[11] (square).

previous data on PFB by Paukov and Pakhmenkulov[11] is shown in Figure VI-2. The present data is smaller than theirs by about 1 per cent in entire temperature region.

Some thermodynamic functions were calculated from the primary data and they are given for rounded temperatures in Tables VI-3 and VI-4, in which small contributions below 4 K were estimated by smooth extrapolation to 0 K (see also Figure VI-3).

The third law entropy may be calculated using the vapor pressure data of PFB.[12,13] Normal modes calculation and the assignment of Raman and IR spectra of the intramolecular vibration of PFB molecule were made by Steele.[10] However, the calculation of the third law and the statistical entropies and the comparison of them were not carried out because Steele assumed molecular symmetry to be D_{2h} of a planar conformation and did not take into account any steric effects. His assumption is unrealistic; the distance between two ortho fluorine atoms, 0.16 nm, is extremely shorter than the sum of van der Waals radii, 0.27 nm.

VI-3 Twisting vibration in crystal

In general, heat capacity of molecular crystal at low temperature comprises the relatively independent

three parts. The first part is the contribution of translational and librational lattice vibrations. Translational lattice heat capacity of three degrees of freedom per molecule is the largest in all the contributions at low temperatures because they vary as T^3 in contrast to exponential dependence on temperature of other contributions. The Debye theory is well applicable to translational lattice heat capacity and the characteristic temperature (Debye temperature) is proportional to $(k/M)^{1/2}$, where k is a isotropic intermolecular force-constant and M is molar mass. Therefore, the mass effect can be reduced by multiplying the Debye temperature by a square root of molar mass, and the information about the intermolecular force can be obtained also from such a plot. Librational lattice vibrations of three degrees of freedom give the second largest contribution at low temperatures. Their frequencies lie in the range from about 20 to about 100 cm^{-1}. They are well described by the Einstein theory or a quantum statistical formulation of a heat capacity of a harmonic oscillator, at low temperatures where anharmonicity does not play an important role. The characteristic temperature (Einstein temperature) is proportional to $(k'/I)^{1/2}$, where k' is a intermolecular force-constant for librational motion and I is a molecular moment of inertia.

The second part of low temperature heat capacity

of molecular crystal is the contribution of intramolecular vibrations, 60 degrees of freedom per molecule in both cases of PFB and PCB. They are also well described by the Einstein theory. The contributions of intramolecular vibrations can usually be neglected at sufficiently low temperatures because their frequencies are rather high above those of lattice vibrations. However, since the frequency of the twisting vibration is expected to be in the lattice-vibration frequency range,[14] it is the only intramolecular vibration that should be taken into account in the analysis of the low temperature heat capacities of PFB and PCB. The Einstein temperature of the twisting vibration is proportional to $(k''/I')^{1/2}$, where k" is the force-constant for the twisting motion and I' is the molecular reduced moment of inertia, which is a quarter of the moment of inertia of a whole molecule around the molecular figure axis.

The last part of low temperature heat capacity is the contribution of the work of volume expansion. However, this part can be neglected at sufficiently low temperatures because volume expansion comes from the anharmonicity of lattice vibrations.

Now, the heat capacities of PFB and PCB below 15 K is analyzed based on the discussion given above. The comparison between the heat capacities of PFB and PCB crystals is given in Figure VI-3 in terms of Debye

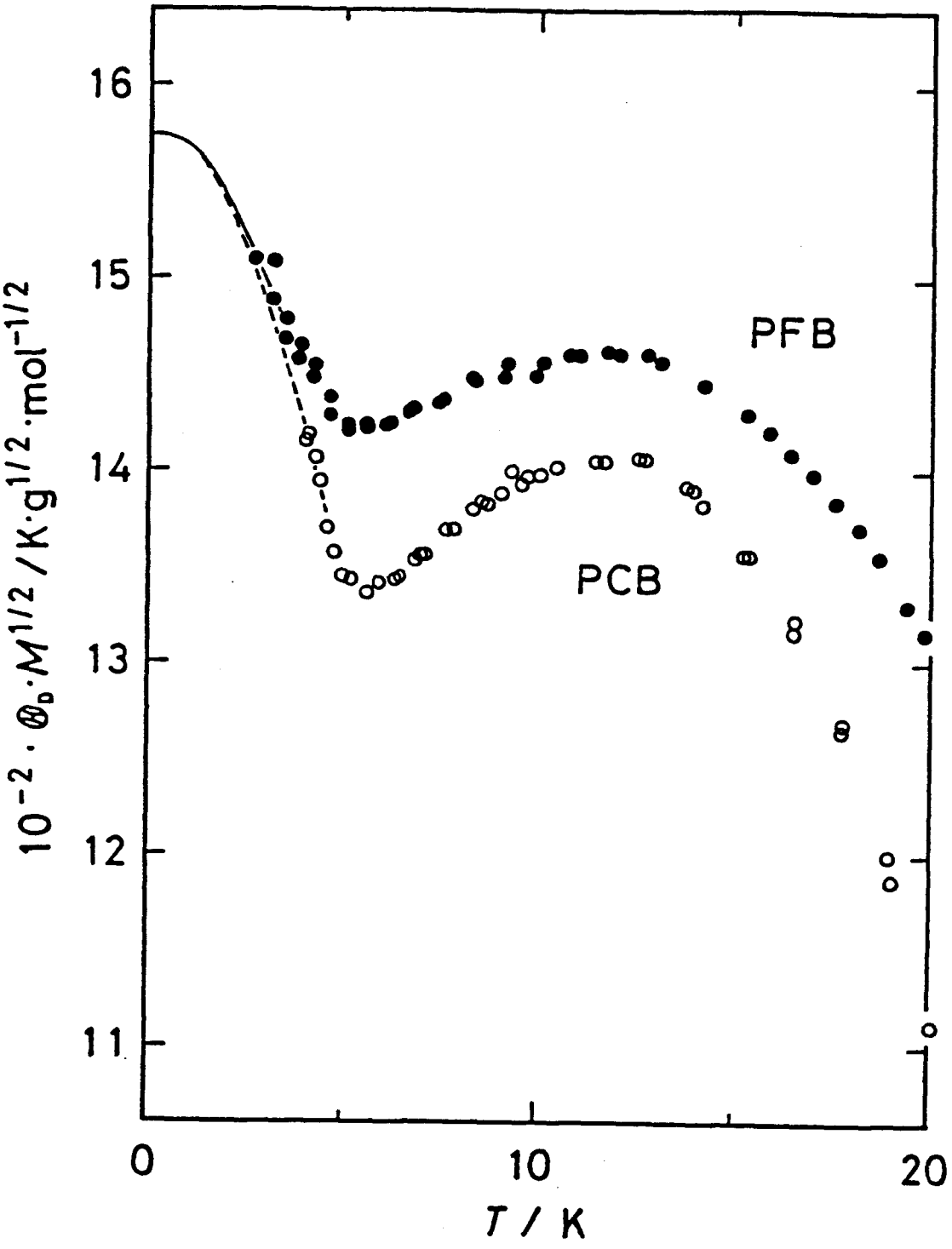

Figure VI-3. Debye characteristic temperatures multiplied with square roots of molar mass of perfluorobiphenyl (open circle) and perchlorobiphenyl (filled circle), assuming 6 degrees of freedom per molecule.

temperature multiplied by a square root of the molar mass assuming 6 degrees of freedom per molecule, where the value of the molar mass, M, was 334.12 $g \cdot mol^{-1}$ for PFB and 498.66 $g \cdot mol^{-1}$ for PCB. Smooth extrapolation to 0 K was made as shown in the figure by solid and broken curves. That both the extrapolation curves intersect the 0 K vertical line at the same point means that isotropic intermolecular force-constant is the same in both crystals. Obtained Debye temperatures at 0 K of the PFB and PCB crystals assuming 3 degrees of freedom per molecule are 68.35 K and 55.95 K, respectively. Thus, translational lattice heat capacities were subtracted from the measured heat capacities by using these Debye temperatures.

The remaining heat capacities is the sum of the contributions of librational lattice vibrations and the intramolecular twisting vibration. The contribution of volume expansion can be neglected because the temperature region considered here is sufficiently low compared with the Debye temperatures. The dependence of characteristic temperatures of librational and twisting vibrations on molecular parameters is the same, proportional to a square root of a molecular moment of inertia. Therefore, the effects of the differences of a moment of inertia can be corrected by multiplying Einstein temperatures by a square root of a moment of inertia. Moreover, since the isotropic intermolecular force-constants are the same in the PFB

and PCB crystals, the force-constant for librational motion is likely the same in both crystals. In this approximation, the correction for the difference in molecular moment of inertia makes it possible to compare immediately the twisting force-constants. Although, strictly speaking, Einstein temperature is defined to each vibrational mode and a moment of inertia relevant to each mode may be different to each other, a single Einstein temperature averaged over the librational and twisting vibrations through a heat capacity value of each crystal and a single value of a molecular moment of inertia defined by geometrical mean of three principal moments of inertia, 33.97 $g \cdot nm^2 \cdot mol^{-1}$ for PFB molecule and 65.38 $g \cdot nm^2 \cdot mol^{-1}$ for PCB molecule, were used.

The difference in the sum of the librational and twisting heat capacities between crystalline PFB and PCB after the correction for the value of the moment of inertia of PCB to that of PFB is shown in Figure VI-4, where the corrected heat capacity of PCB were subtracted from the uncorrected one of PFB. The difference has a plus sign and shows a maximum at about 14 K. Therefore, it is concluded that crystalline PFB shows relatively larger heat capacity of the intramolecular twisting vibration than PCB crystal. Namely, PFB molecules are softer than PCB molecules for the twisting motion and, therefore, molecular stiffness

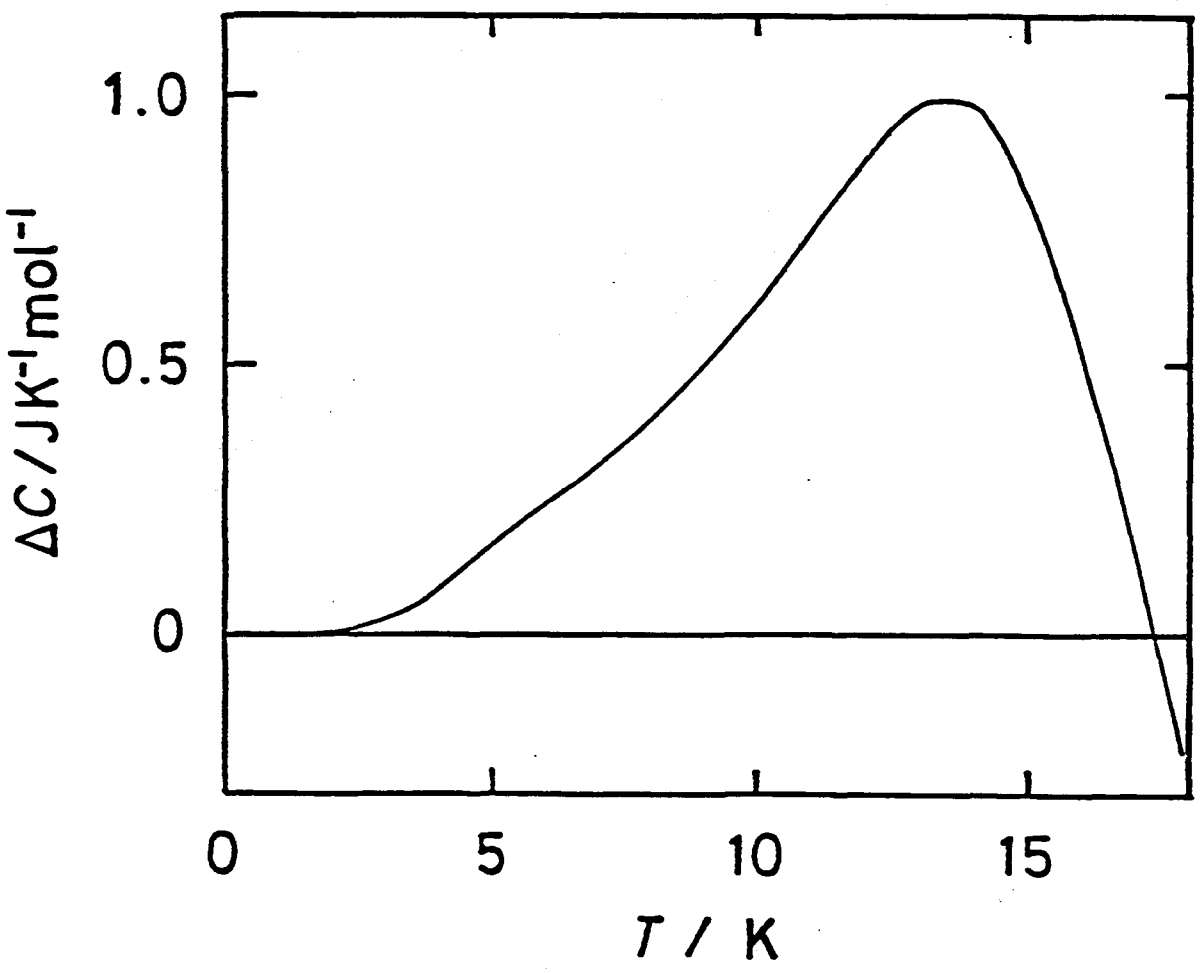

Figure VI-4. Difference between twisting heat capacities of perfluorobiphenyl and perchlorobiphenyl.

for the twisting motion increases as the size of ortho atoms becomes larger in biphenyl and its derivatives.

References to Chapter VI

1. O. Bastiansen, Acta Chem. Scand., 3(1949), 408.
2. H. Suzuki, Bull. Chem. Soc. Jpn., 32(1959), 1340.
3. A. Almenningen, A. O. Hartman and H. M. Seip, Acta Chem. Scand., 22(1968), 1013.
4. N. N. Neronova, Zh. Strukt. Khim., 9(1968), 147.
5. V. M. Kozhin and L. F. Kon'shina, Krystallografiya, 16(1971), 642.
6. G. A. Mackenzie, G. S. Pawley and O. W. Dietrich, Acta Cryst. A31(1975), 851.
7. W. B. Gleason and D. Britton, Cryst. Struct. Commun., 5(1976), 483.
8. B. F. Pedersen, Acta Cryst., B31(1975), 2931.
9. D. Steele, T. R. Nanney and E. R. Lippincott, Spectrochim. Acta, 22(1966), 849.
10. D. Steele, Spectrochim. Acta, 25A(1969), 959.
11. I. E. Paukov and F. S. Rakhmenkulov, Zh. Fiz. Khim., 45(1971), 1296.
12. L. G. Radchenko and A. I. Kitaigorodski, Zh. Fiz. Khim., 48(1974), 2702.
13. S. J. W. Price and H. J. Sapiano, Can. J. Chem., 57(1979), 1468.
14. J. W. Arthur and G. A. Mckenzie, J. Raman Spectrosc., 4(1976), 353.

Chapter VII Summary

Thermodynamic studies were carried out on the series of compounds having the intramolecular twisting degree(s) of freedom, i.e. biphenyl and its related substances. The special attention was paid to correlation of the intramolecular twisting degree(s) of freedom with the macroscopic properties. The heat capacities were measured by adiabatic calorimetry between 4 and 300 K and some thermodynamic functions were determined.

The twist transition of biphenyl was observed as a broad anomaly with the maximum at 40.4 K, and the entropy and the enthalpy of transition were determined to be 0.129 $J \cdot K^{-1} \cdot mol^{-1}$ and 5.02 $J \cdot mol^{-1}$, respectively; these values are consistent with the displacive nature of the transition associated with the soft modes. The lock-in transition was detected at 16.8 K by using the improved calorimeter vessel; the entropy and the enthalpy of transition were 0.009 $J \cdot K^{-1} \cdot mol^{-1}$ and 0.15 $J \cdot mol^{-1}$, respectively. The results on biphenyl-d_{10} were similar to those on biphenyl, but the temperature region of the two-dimensional incommensurate phase was narrower than biphenyl, i.e. between 20.2 and 36.8 K. The entropies of the corresponding phase transitions were the same as those of biphenyl, which implied the same mechanism of the transitions in the two compounds.

The twist phase transition of p-terphenyl was observed as a sharp λ-shaped anomaly with the maximum at 193.5 K; the entropy and the enthalpy of transition were 1.63 $J \cdot K^{-1} \cdot mol^{-1}$ and 304 $J \cdot mol^{-1}$, respectively. The critical exponent α of the heat capacity was determined as 0.13 for both the higher and the lower temperature sides of the transition. The results on p-terphenyl-d_{14} were similar to those on p-terphenyl, but the transition temperature was 180.3 K. The entropy of transition was the same as that of p-terphenyl, which implied the same mechanism of the transition in the two compounds.

The twist phase transition of p-quaterphenyl was observed as a broad anomaly with the maximum at 233.0 K; the entropy and the enthalpy of transition were 1.82 $J \cdot K^{-1} \cdot mol^{-1}$ and 414 $J \cdot mol^{-1}$, respectively.

The properties of the twist phase transitions of the p-polyphenylenes were compared with one another and discussed in relation to the internal flexibility. The change of the nature of the transition from a displacive type to an order-disorder type was attributed to the increase in barrier height hindering rotation of the phenyl rings. On the other hand, the broad anomaly in p-quaterphenyl was interpreted in terms of molecular symmetry, i.e. the existence of the softer twisting A_u mode.

The two-dimensionality in the inter-"spin"

interaction in p-terphenyl crystal was demonstrated by calculating the interaction using the atom-atom potentials of Buckingham type. The Ising type theory was developed and compared well with the experimental results on p-terphenyl.

As the temperature decreased, the heat capacity of biphenyl decreased less steeply than those of p-terphenyl and p-quaterphenyl, and the heat capacity curve of biphenyl crossed that of p-terphenyl at 12 K and that of p-quaterphenyl at 6 K. The crossover was attributed to the greater twisting flexibility of phenyl rings in biphenyl by lattice dynamics calculation. The role of the incommensurability in the crossover phenomena was pointed out by comparing the low temperature heat capacities of biphenyl and 4,4'-difluorobiphenyl.

No phase transition was observed in 4,4'-difluorobiphenyl, p,p'-biphenol and p-phenylphenol. The reason of the absence of any phase transition was interpreted through comparison between their intramolecular potential curves and that of biphenyl. The calculation of static lattice energies showed that the twist phase transition of 4,4'-difluorobiphenyl and p,p'-biphenol shifted below 0 K and a planar conformation was stable above 0 K because of the stabilization of a planar molecular conformation due to the greater π-conjugation.

No thermal anomaly was observed in

perfluorobiphenyl and perchlorobiphenyl. The analysis of their low temperature heat capacities showed that perfluorobiphenyl molecule was softer than perchlorobiphenyl in terms of the force-constant for the twisting motion.

List of publications

1. T. Atake, K. Saito and H. Chihara,
"Low Temperature Heat Capacities of Biphenyl and Biphenyl-d_{10}"
Chem. Lett., 1983, 493-496.

2. K. Saito, T. Atake and H. Chihara,
"Crossover of the Low Temperature Heat Capacities of Biphenyl and p-Terphenyl"
Chem. Lett., 1984, 521-524.

3. K. Saito, T. Atake and H. Chihara,
"Molar Heat Capacity and Thermodynamic Properties of p-Quaterphenyl"
J. Chem. Thermodyn., 17(1985), 539-548.

4. K. Saito, H. Chihara, T. Atake and Y. Saito,
"Thermodynamic Studies on Incommensurate Biphenyl and Related Substances"
Jpn. J. Appl. Phys., 24(1985), Suppl. 24-2, 772-774.

5. K. Saito, T. Atake and H. Chihara,
"Thermodynamic Studies of p-Polyphenyls: Heat Capacity of 4,4'-Difluorobiphenyl"
J. Chem. Thermodyn., 18(1986), in press.

6. K. Saito, T. Atake and H. Chihara,
"Stability of a Planar Molecular Conformation in 4,4'-Difluorobiphenyl"
(in preparation)

7. K. Saito, T. Atake and H. Chihara,
"Perfluorobiphenyl and Perchlorobiphenyl: Heat Capacities and Intramolecular Twisting Vibrations"
(in preparation)

8. K. Saito, T. Atake and H. Chihara,
"Incommensurate Phase Transitions and Anomalous Lattice Heat Capacity of Biphenyl"
(in preparation)

9. T. Atake, K. Saito and H. Chihara,
"Thermodynamic Studies on Successive Phase Transitions of Crystalline Biphenyl-d_{10}"
(in preparation)

10. K. Saito, T. Atake and H. Chihara,
"Thermodynamic Studies on an Order-Disorder Phase Transition of p-Terphenyl at 193.5 K"
(in preparation)

11. T. Atake, K. Saito and H. Chihara,
"Molar Heat Capacities and Thermodynamic Properties of Crystalline p-Terphenyl-d_{14}"
(in preparation)

12. K. Saito, T. Atake and H. Chihara,
"Thermodynamic Studies of p-Polyphenyls: Heat Capacity of p,p'-Biphenol"
(in preparation)

13. K. Saito, T. Atake and H. Chihara,
"Molar Heat Capacities of p-Phenylphenol"
(in preparation)

Appendix Program for the heat capacity measurements

```
5 'CpMAIN Ver. 1.03    08/08/84
10 WIDTH 80,25
20 CONSOLE 0,25,0,0
30 ON KEY GOSUB *ENDING,*HEATOFF,*EQUILIBRIUM,*RESTART,*NLSCHANGE,*NTIMEMAXCHANGE,*IN
TERVALOFHEATINGCHANGE
40 KEY(1) ON:KEY(2) ON:KEY(3) OFF:KEY(4) OFF:KEY(5) OFF:KEY(6) OFF:KEY(7) OFF
50 CLS 3
60 IENDING=0
70 LPRINT DATE$:LPRINT
80 PRINT "Welcome to the Calorimeter II"
90 LPRINT "Welcome to the Calorimeter II"
100 THERMOMETER$="Gamma Pt thermometer"
110 LPRINT "Thermometer : ";THERMOMETER$
120 PRINT "Thermometer : ";THERMOMETER$
130 DEFDBL A-H,O-Z
140 DEFINT I-N
150 DIM TL$(14),DAT$(11),DA$(6),CDAT$(5),RMAP(150),RR(33),TEMP(200),CE$(16),CC(33),R$
(16),T1(100),T2(100)
160 PRINT
170 LPRINT
180 INPUT "SAMPLE NAME ";SAMPLE$
190 LPRINT " Sample : ";SAMPLE$;
200 SNAME$=LEFT$(SAMPLE$+"      ",6)
210 OPEN "2:TITLE" AS #5
220 FIELD #5,18AS TL$(1),18AS TL$(2),18AS TL$(3),18AS TL$(4),18AS TL$(5),18AS TL$(6),
18AS TL$(7),18AS TL$(8),18AS TL$(9),18AS TL$(10),18AS TL$(11),18AS TL$(12),18AS TL$(1
3),18AS TL$(14),4AS DUMMY1$
230 ILO=LOF(5)
240 IF ILO=0 THEN 320
250 FOR I=1 TO ILO
260 GET #5,I
270 FOR J=1 TO 14
280 IF SNAME$=LEFT$(TL$(J),6) THEN 420
290 IF SNAME$=MID$(TL$(J),10,6) THEN 420
300 NEXT J
310 NEXT I
320 NUMBEROFSERIES=1:NUMBEROFDATA=0
330 GOSUB *FILEINITIALIZE
340 PRINT USING "The heat capacity of &        & has";LEFT$(SAMPLE$,10);
350 PRINT " not been measured yet."
360 LSET TL$(1)=SNAME$+"DAT          "
370 FOR I=2 TO 14
380 LSET TL$(I)="                    "
390 NEXT I
400 PUT #5,1
410 GOTO 800
420 OPEN "2:"+SNAME$+"DAT" AS #2
430 FIELD #2,48AS DAT$(1),48AS DAT$(2),48AS DAT$(3),48AS DAT$(4),48 AS DAT$(5),16AS D
UMMY2$
440 IEND=LOF(2)
450 GET #2,IEND
460 FOR I=5 TO 1 STEP -1
470 IF CVI(LEFT$(DAT$(I),2))>0 THEN 490
480 NEXT I
490 NUMBEROFSERIES=1+CVI(LEFT$(DAT$(I),2))
500 NUMBEROFDATA=CVI(MID$(DAT$(I),3,2))
510 T2(CVI(LEFT$(DAT$(I),2)))=CVD(MID$(DAT$(I),21,8))
520 IF IEND=2 THEN 540
530 GET #2,2
540 T1(1)=CVD(MID$(DAT$(1),9,8))
550 II=1
560 FOR I=2 TO IEND
570 GET #2,I
580 FOR J=1 TO 5
590 DA$(J)=DAT$(J)
600 NEXT J
610 IF I=IEND THEN 640
620 GET #2,I+1
630 DA$(6)=DAT$(1)
640 FOR J=2 TO 6
650 IJ=CVI(LEFT$(DA$(J),2))
660 IF IJ=0 AND I=IEND THEN 730
```

```
670 IF IJ=II OR IJ=0 OR IJ>99 THEN 710
680 T1(IJ)=CVD(MID$(DA$(J),9,8))
690 T2(IJ-1)=CVD(MID$(DA$(J-1),21,8))
700 II=IJ
710 NEXT J
720 NEXT I
730 CLOSE #2
740 PRINT USING "The heat capacity of &        & has";LEFT$(SAMPLE$,10);
750 PRINT " been already measured ;"
760 FOR I=1 TO NUMBEROFSERIES-1
770 PRINT USING "                                                                    ###.## K
 - ###.## K";T1(I),T2(I)
780 NEXT I
790 GOSUB *FILEINITIALIZE
800 PRINT:INPUT "Platinum region or Germanium region ";REGION$
810 LPRINT USING "     #.######## mol";AMOUNTOFSAMPLE
820 LPRINT COMMENT1$
830 LPRINT :LPRINT USING " series number ###";NUMBEROFSERIES
840 LPRINT "      ";COMMENT2$
850 IF LEFT$(REGION$,1)="G" THEN *GERMANIUM ELSE IF LEFT$(REGION$,1)="g" THEN *GERMAN
IUM
860 OPEN "TableP" AS #6
870 FIELD #6,248 AS DUMMY3$,8AS RM$
880 IEOFTABLEP=LOF(6)
890 FOR I=2 TO IEOFTABLEP-1
900 GET #6,I
910 RMAP(I-1)=CVD(RM$)
920 NEXT I
930 CLOSE #6
940 GET #5,LOF(5)
950 FOR I=1 TO 14
960 IF LEFT$(TL$(I),9)="          " THEN LSET TL$(I)=NEWTITLE$+"          ":GOTO 1030
970 IF RIGHT$(TL$(I),9)="          " THEN RSET TL$(I)=NEWTITLE$:GOTO 1030
980 NEXT I
990 LSET TL$(1)=NEWTITLE$+"                    "
1000 NF=LOF(5)+1
1010 I=1
1020 GOTO 1040
1030 NF=LOF(5)
1040 FOR J=I+1 TO 14
1050 LSET TL$(J)="                          "
1060 NEXT J
1070 PUT #5,NF
1080 CLOSE #5
1090 INPUT "Automatic or Manual                  ";MODE$
1100 D$=LEFT$(MODE$,1)
1110 IF D$="A" THEN *AUTOMATIC ELSE IF D$="a" THEN *AUTOMATIC
1120 IF D$="M" THEN *MANUAL ELSE IF D$="m" THEN *MANUAL
1130 PRINT "AGAIN !":BEEP:GOTO 1090
1140 *AUTOMATIC
1150 PRINT
1160 INPUT "Rref / ohm for Heater                              ";RREF
1170 LPRINT :LPRINT USING "Rref for Heater = ###.##### ohm";RREF
1180 INPUT "Final temperature / K of this series               ";TMAX
1190 'INPUT "delta T / K                                        ";DELTAT
1200 INPUT "Maximum time / min for temperature measurement ";AMIN
1210 NTIMEMIN=FIX(AMIN*2)
1220 INPUT "Initial interval / min for Least Square Fit     ";ALS
1230 LPRINT USING "Minimum time / min for Least Square          ## min";ALS
1240 NLS=FIX(ALS*2)
1250 INPUT "Initial time / min for temperature measurement ";AMAX
1260 NTIMEMAX=FIX(AMAX*2)
1270 INPUT "Initial heating interval / min                  ";AHI
1280 INTERVALOFHEATING=FIX(AHI*60)
1290 'INPUT "Maximum heating interval / min                  ";AHMAX
1300 'INTERVALOFHEATINGMAX=FIX(AHMAX*2)
1310 ISET IFC
1320 ISET REN
1330 SRQ OFF
1340 ON SRQ GOSUB *GPIB
1350 PRINT @4;"M01,TR2,SI003T1,RN0,S0"
1360 PRINT @4;"M00,18G"
1370 PRINT @4;"M01,19G"
1380 PRINT @4;"FP00,LP01,RI030T1"
1390 PRINT @5;"F5,G0,S1"
1400 PRINT @6;"F1,R0,AC1,RE1,M2,S0"
```

```
1410 PRINT @4;"DI,00G"
1420 CMD DELIM=1
1430 PRINT @3;"AUTO"
1440 PRINT @3;"I1.0"
1450 CMD DELIM=0
1460 POLL 4,SP4
1470 POLL 6,SP6
1480 TM0=0#
1490 NUMBERINSERIES=0
1500 INPUT "Initial data number                                    ";ND
1510 IF ND<>0 THEN NUMBEROFDATA=ND-1
1520 *MAINLOOP
1530 KEY(6) ON
1540 GOSUB *TEMPERATUREMEASUREMENT
1550 IF NUMBERINSERIES=1 THEN TI=AF*(NTIME+(10#+INTERVALOFHEATING)/60#)+BF:AI=AF
1560 IF NUMBERINSERIES>1 THEN GOSUB *CP
1570 IF TF>=TMAX THEN *ENDING
1580 IF INTERVALOFHEATING=0 THEN *ENDING
1590 GOSUB *HEATER
1600 KEY(6) OFF
1610 GOTO *MAINLOOP
1620 *FILEINITIALIZE
1630 IF NUMBEROFSERIES=1 THEN INPUT "Comment on this sample (<170 Bite) ";COMMENT1$
1640 INPUT "Amount of sample / mol              ";AMOUNTOFSAMPLE
1650 IF AMOUNTOFSAMPLE<>0 THEN 1730
1660 OPEN "2:"+SNAME$+RIGHT$("00"+STR$(NUMBEROFSERIES-1),3) AS #1
1670 FIELD #1,18AS DUMMY1$,8AS AM$,230 AS DUMMY12$
1680 GET #1,1
1690 AMOUNT$=AM$
1700 CLOSE #1
1710 AMOUNTOFSAMPLE=CVD(AMOUNT$)
1720 GOTO 1740
1730 AMOUNT$=MKD$(AMOUNTOFSAMPLE)
1740 INPUT "Comment on this series (<170 Bite) ";COMMENT2$
1750 OPEN "TableP" AS #3
1760 FIELD #3,20AS THERM$,8AS TO$,8AS DT$,220AS DUMMY3$
1770 GET #3,1
1780 TOP=CVD(TO$):DTP=CVD(DT$)
1790 THERMOMETER1$=THERM$
1800 CLOSE #3
1810 OPEN "TableG" AS #3
1820 FIELD #3,20AS THERM$,8AS TO$,8AS DT$,220AS DUMMY3$
1830 GET #3,1
1840 TOG=CVD(TO$):DTG=CVD(DT$)
1850 THERMOMETER2$=THERM$
1860 CLOSE #3
1870 NEWTITLE$=SNAME$+RIGHT$("00"+STR$(NUMBEROFSERIES),3)
1880 OPEN "2:"+NEWTITLE$ AS #1
1890 FIELD #1,10AS SAN$,8AS DATD$,8AS AMS$,20AS TH1$,20AS TH2$,170AS COMM$
1900 LSET SAN$=LEFT$(SAMPLE$,10)
1910 LSET DATD$=DATE$
1920 LSET AMS$=AMOUNT$
1930 LSET TH1$=THERMOMETER1$
1940 LSET TH2$=THERMOMETER2$
1950 LSET COMM$=COMMENT2$
1960 PUT #1,1
1970 CLOSE #1
1980 IF NUMBEROFSERIES >1 THEN 2090
1990 OPEN "2:"+SNAME$+"DAT" AS #1
2000 FIELD #1,10AS SAN$,8AS DATD$,8AS AMS$,20AS TH1$,20AS TH2$,170AS COMM$
2010 LSET SAN$=LEFT$(SAMPLE$,10)
2020 LSET TH1$=THERMOMETER1$
2030 LSET DATD$=DATE$
2040 LSET AMS$=AMOUNT$
2050 LSET TH2$=THERMOMETER2$
2060 LSET COMM$=COMMENT1$
2070 PUT #1,1
2080 CLOSE #1
2090 OPEN "2:"+SNAME$+"DAT" AS #1
2100 FIELD #1,48AS CDAT$(1),48AS CDAT$(2),48AS CDAT$(3),48AS CDAT$(4),48AS CDAT$(0),6
AS DUMMY1$
2110 OPEN "2:"+NEWTITLE$ AS #2
2120 FIELD #2,2AS ND$,23AS DAT$(1),23AS DAT$(2),23AS DAT$(3),23AS DAT$(4),23AS DAT$(5
),23AS DAT$(6),23AS DAT$(7),23AS DAT$(8),23AS DAT$(9),23AS DAT$(10),23AS DAT$(0),1AS
DUMMY2$
2130 OPEN "TableP" AS #3
```

```
2140 FIELD #3,16AS R$(1),16AS R$(2),16AS R$(3),16AS R$(4),16AS R$(5),16AS R$(6),16AS
R$(7),16AS R$(8),16AS R$(9),16AS R$(10),16AS R$(11),16AS R$(12),16AS R$(13),16AS R$(1
4),16AS R$(15),16AS R$(16)
2150 OPEN "Ccell" AS #4
2160 FIELD #4,16AS CE$(1),16AS CE$(2),16AS CE$(3),16AS CE$(4),16AS CE$(5),16AS CE$(6)
,16AS CE$(7),16AS CE$(8),16AS CE$(9),16AS CE$(10),16AS CE$(11),16AS CE$(12),16AS CE$(
13),16AS CE$(14),16AS CE$(15),16AS CE$(16)
2170 RETURN
2180 *TEMPERATUREMEASUREMENT
2190 NDATAFILE=0:LPRINT
2200 CLS 3:SCREEN 2,,0,1
2210 VIEW (0,40)-(639,399)
2220 WINDOW (0,0)-(NTIMEMAX,.05)
2230 LINE (0,.05)-(NTIMEMAX,.05)
2240 LINE (0,0)-(0,.05)
2250 FOR JIKU=10 TO NTIMEMAX STEP 10
2260 LINE (JIKU,.049)-(JIKU,.05)
2270 NEXT JIKU
2280 LINE (NTIMEMAX*.7,.01)-(NTIMEMAX*.7,.02)
2290 LOCATE 58,9:PRINT "0.01 K"
2300 NUMBEROFDATA=NUMBEROFDATA+1
2310 NUMBERINSERIES=NUMBERINSERIES+1
2320 KEY(4) ON
2330 NTIME=-1
2340 CMD DELIM=1
2350 IBRIDGE=1
2360 GOSUB *BRIDGE
2370 IH=0:IM=0:IS=30
2380 GOSUB *TIME
2390 ON TIME$=TT$ GOSUB *BRIDGE
2400 TIME$ ON
2410 IBRIDGE=0
2420 SUMR=R
2430 FOR ITEMP=1 TO 50 :NEXT ITEMP
2440 GOSUB *BRIDGE
2450 SUMR=SUMR+R
2460 FOR ITEMP=1 TO 100:NEXT ITEMP
2470 GOSUB *BRIDGE
2480 R=(SUMR+R)/3#
2490 NTIME=NTIME+1
2500 GOSUB *TEMPERATURE
2510 IF NTIME=0 THEN TORIGIN=T+.1#
2520 CIRCLE (NTIME,.0001*((TORIGIN-T)*10000 MOD 500)),.004*NTIMEMAX
2530 LOCATE 0,0:PRINT USING "T = ###.##### K
          ### ### ###";T,INTERVALOFHEATING¥60,NTIMEMAX¥2,NLS¥2
2540 IF NTIME MOD 2=1 THEN LPRINT USING "      &      &     R = ##.###### ohm     T =
 ###.##### K";DATATIME$,R,T:GOTO 2560
2550 LPRINT USING "                          &      &     R = ##.###### ohm     T = ###
.##### K";DATATIME$,R,T;
2560 IEQUILIBRATION=0
2570 IDENT$="T"
2580 GOSUB *DATAFILE
2590 FOR IT=1 TO NTIMEMIN-1
2600 TEMP(IT)=TEMP(IT+1)
2610 NEXT IT
2620 TEMP(NTIMEMIN)=T
2630 IF NTIME>=NLS THEN GOSUB *EQUILIBRATION
2640 IF NTIME=NTIMEMAX THEN IEQUILIBRATION=1
2650 IF IEQUILIBRATION=1 THEN 2700
2660 IRES=0
2670 IBRIDGE=1
2680 KEY(3) ON:KEY(5) ON:KEY(7) ON
2690 IF IBRIDGE=2 THEN 2370 ELSE IF IRES=1 THEN 2200 ELSE IF IEQUILIBRATION<>1 THEN 2
690
2700 CMD DELIM=0
2710 KEY(3) OFF:KEY(4) OFF:KEY(5) OFF:KEY(7) OFF
2720 RETURN
2730 *BRIDGE
2740 INPUT @3;RO$
2750 IF IBRIDGE=1 THEN DATATIME$=TIME$:IBRIDGE=2
2760 R=VAL(LEFT$(RIGHT$(RO$,12),9))
2770 RETURN
2780 *TEMPERATURE
2790 FOR I=1 TO IEOFTABLEP-1
2800 IF R<RMAP(I) THEN 2830
2810 NEXT I
```

```
2820 I=IEOFTABLEP
2830 IF I=ITABLE THEN 2900
2840 GET #3,I+1
2850 FOR K=1 TO 16
2860 RR(2*K)=CVD(LEFT$(R$(K),8))
2870 RR(2*K+1)=CVD(RIGHT$(R$(K),8))
2880 NEXT K
2890 RR(1)=RMAP(I-1)
2900 FOR J=2 TO 33
2910 IF R<RR(J) THEN 2930
2920 NEXT J
2930 TD=(R-RR(J-1))/(RR(J)-RR(J-1))*DTP
2940 T=TD+DTP*(J-2)+TOP+(I-1)*DTP*32#
2950 ITABLE=I
2960 RETURN
2970 *TIME
2980 TIMET$=TIME$
2990 IHH=VAL(LEFT$(TIMET$,2))
3000 IMM=VAL(MID$(TIMET$,4,2))
3010 ISS=VAL(RIGHT$(TIMET$,2))
3020 ISS=ISS+IS:IMM=IMM+IM:IHH=IHH+IH
3030 FOR ITIME=1 TO 2
3040 IMM=IMM+ISS¥60:ISS=ISS MOD 60
3050 IHH=IHH+IMM¥60:IMM=IMM MOD 60
3060 IDD=IDD+IHH¥24:IHH=IHH MOD 24
3070 NEXT ITIME
3080 IF IHH>9 THEN HT$=RIGHT$(STR$(IHH),2) ELSE HT$="0"+RIGHT$(STR$(IHH),1)
3090 IF IMM>9 THEN MT$=RIGHT$(STR$(IMM),2) ELSE MT$="0"+RIGHT$(STR$(IMM),1)
3100 IF ISS>9 THEN ST$=RIGHT$(STR$(ISS),2) ELSE ST$="0"+RIGHT$(STR$(ISS),1)
3110 TT$=HT$+":"+MT$+":"+ST$
3120 RETURN
3130 *CP
3140 TIME$ OFF
3150 DT=TF-TI
3160 C=DE/DT
3170 TM=(TI+TF)*.5#
3180 GOSUB *EMPTYCELL
3190 CP=(DE-CELL)/DT/AMOUNTOFSAMPLE
3200 PRINT USING "data number ###    T1 = ###.##### K  T2 = ###.##### K  delta T = #.
##### K";NUMBEROFDATA-1,TI,TF,DT
3210 PRINT USING "                   delta E = #.######^^^^ J      C = #.#####^^^^ J"
;DE,C
3220 PRINT USING "                   Tm = ###.### K    Cp = ####.#### J/(K·mol)";TM,C
P
3230 LPRINT:IF NTIME MOD 2=0 THEN LPRINT
3240 LPRINT USING "data number ###  T1 = ###.##### K T2 = ###.##### K delta T = #.###
## K delta E = #.######^^^^ J  Tm = ###.### K Cp = ####.#### J/(K·mol)";NUMBEROFDATA-
1,TI,TF,DT,DE,TM,CP
3250 GOSUB *CPDATAFILE
3260 IF NUMBERINSERIES=2 THEN CO=C
3270 'INTERVALOFHEATING=INTERVALOFHEATING*(.5#*(C-CO)*(DT+DELTAT)/(TM-TMO)+C)*DELTAT/
DE
3280 'IF INTERVALOFHEATING>INTERVALOFHEATINGMAX THEN INTERVALOFHEATING=INTERVALOFHEAT
INGMAX
3290 CO=C
3300 TMO=TM
3310 TI=AF*(NTIME+(10#+INTERVALOFHEATING)/60#)+BF
3320 AI=AF
3330 RETURN
3340 *EMPTYCELL
3350 TEM=TI
3360 GOSUB *ENTHALPY
3370 ECELL=CELL
3380 TEM=TF
3390 GOSUB *ENTHALPY
3400 CELL=CELL-ECELL
3410 RETURN
3420 *ENTHALPY
3430 IF TEM<1.9# THEN 3550 ELSE IF TEM<24.9# THEN 3590 ELSE IF TEM<149.75# THEN 3670
ELSE IF TEM>=315.5# THEN 3550
3440 KTM=FIX((TEM-149.5#)/32#)
3450 GET #4,KTM+13
3460 GOSUB 3750
3470 IF KTM<4 THEN 3500
3480 CC(33)=0#
3490 GOTO 3520
```

```
3500 GET #4,KTM+14
3510 CC(33)=CVD(LEFT$(CE$(1),8))
3520 LTM=FIX(TEM-149.5#-KTM*32#)
3530 CELL=CC(LTM+1)+(TEM-KTM*32#-149.5#-LTM)*(CC(LTM+2)-CC(LTM+1))
3540 RETURN
3550 BEEP
3560 LPRINT "Temperature is out of renge !"
3570 CELL=0#
3580 RETURN
3590 KTM=FIX((TEM-1.9#)/6.4#)
3600 GET #4,KTM+1
3610 GOSUB 3750
3620 GET #4,KTM+2
3630 CC(33)=CVD(LEFT$(CE$(1),8))
3640 LTM=FIX(5#*(TEM-KTM*6.4#-1.9#))
3650 CELL=CC(LTM+1)+5#*(TEM-KTM*6.4#-1.9#-LTM*.2#)*(CC(LTM+2)-CC(LTM+1))
3660 RETURN
3670 KTM=FIX((TEM-24.75#)/16#)
3680 GET #4,KTM+5
3690 GOSUB 3750
3700 GET #4,KTM+6
3710 CC(33)=CVD(LEFT$(CE$(1),8))
3720 LTM=FIX(2#*(TEM-KTM*16#-24.75#))
3730 CELL=CC(LTM+1)+2#*(TEM-KTM*16#-24.75#-LTM*.5#)*(CC(LTM+2)-CC(LTM+1))
3740 RETURN
3750 FOR L=1 TO 16
3760 CC(2*L-1)=CVD(LEFT$(CE$(L),8))
3770 CC(2*L)=CVD(RIGHT$(CE$(L),8))
3780 NEXT L
3790 RETURN
3800 *HEATER
3810 CLS 3
3820 LPRINT
3830 IF NTIME MOD 2=1 THEN LPRINT
3840 LPRINT USING "data number ###          ";NUMBEROFDATA
3850 IH=0:IM=0
3860 ISCAN=INTERVALOFHEATING¥30
3870 IS=(INTERVALOFHEATING-(ISCAN-1)*30)¥2
3880 SRQ OFF
3890 DE=0#
3900 THEATON$=TIME$
3910 PRINT @4;"DI,01G"
3920 ISCANING=0
3930 GOSUB *TIME
3940 ON TIME$=TT$ GOSUB *SCAN
3950 TIME$ OFF
3960 PRINT USING "heating now                                                    started at &
     & ";THEATON$:IDVM=0
3970 CONSOLE 1,24
3980 POLL 4,SP4
3990 POLL 6,SP6
4000 IIS=INTERVALOFHEATING-IS
4010 IS=IIS MOD 60
4020 IM=(IIS¥60) MOD 60
4030 IH=((IIS¥60)¥60) MOD 24
4040 IDUMMY=0
4050 TIME$ ON
4060 IF IDUMMY=0 THEN 4060
4070 GOSUB *TIME
4080 ON TIME$=TT$ GOSUB *HEATOFF
4090 TIME$ ON
4100 SRQ ON
4110 IDUMMY=0
4120 IF IDUMMY=0 THEN 4120
4130 DE=ABS(DE)*HEATINGINTERVAL/ISCANING/RREF
4140 PRINT USING "Heating interval = #####.### sec   delta E = #.######^^^^ J";HEATIN
GINTERVAL,DE
4150 IF ISCANING MOD 4<>0 THEN LPRINT
4160 LPRINT USING "                          heating start at &      &     heating end
at &      &";THEATON$,THEATOFF$
4170 LPRINT USING "                          Heating interval = ####.### sec     delta
E = #.######^^^^ J";HEATINGINTERVAL,DE
4180 POLL 4,SP4
4190 GOSUB *DATAFILE
4200 RETURN
4210 *SCAN
```

```
4220 IPOWER=1
4230 IDVM=0
4240 SRQ OFF
4250 PRINT @4;"E"
4260 IDUMMY=1
4270 RETURN
4280 *HEATOFF
4290 SRQ OFF
4300 PRINT @4;"H"
4310 PRINT @4;"DI,00G"
4320 THEATOFF$=TIME$
4330 IPOWER=0
4340 POLL 4,SP4
4350 GOSUB *COUNTER
4360 CONSOLE 0,25
4370 IDUMMY=1
4380 RETURN
4390 *GPIB
4400 POLL 6,SP6;4,SP4
4410 IF IEEE(4)<>65 THEN *GPIBERROR
4420 ON IEEE(5)-3 GOTO *SCANNER,*COUNTER,*DMM
4430 *GPIBERROR
4440 LPRINT "ERROR in GP-IB":BEEP
4450 PRINT @4;"H"
4460 PRINT @4;"DI,00G"
4470 RETURN 1540
4480 *SCANNER
4490 IF IPOWER<>1 THEN SRQ ON:RETURN
4500 IDVM=IDVM+1
4510 PRINT @6;"E":TE$(IDVM MOD 2)=TIME$
4520 POLL 4,SP4
4530 SRQ ON
4540 RETURN
4550 *DMM
4560 IF IPOWER<>1 THEN 4790
4570 IF IDVM=0 THEN 4790
4580 INPUT @6;E$
4590 IF LEFT$(E$,3)<>"DV " THEN PRINT @6;"E" ELSE GOTO 4620
4600 FOR ID=1 TO 100 :NEXT ID
4610 INPUT @6;E$:GOTO 4590
4620 POLL 6,SP6
4630 IF SP6=65 THEN PRINT @6;"E":INPUT @6;E$;POLL 6,SP6:GOTO 4630
4640 MID$(E$,14,1)="D"
4650 E(IDVM MOD 2)=VAL(RIGHT$(E$,13))
4660 IDENT$="D"
4670 GOSUB *DATAFILE
4680 IF IDVM MOD 2=1 THEN SRQ ON:RETURN
4690 PRINT USING "&      &    E8 = #.######^^^^ V   E9 = #.######^^^^ V";TE$(1),E(1),
E(0)
4700 IF IDVM MOD 4=2 THEN LPRINT USING "                              &      &   E8 = #.###
###^^^^ V   E9 = #.######^^^^ V    ";TE$(1),E(1),E(0);:GOTO 4720
4710 LPRINT USING "&      &    E8 = #.######^^^^ V   E9 = #.######^^^^ V";TE$(1),E(1)
,E(0)
4720 DE=DE+E(1)*E(0)
4730 ISCANING=ISCANING+1
4740 IF ISCANING=ISCAN THEN PRINT @4;"H"
4750 FOR ISC=1 TO 100 :NEXT ISC
4760 POLL 4,SP4
4770 SRQ ON
4780 RETURN
4790 INPUT @6;DUMMYE$:SRQ ON:RETURN
4800 *COUNTER
4810 IF IPOWER<>0 THEN *COUNTERERROR
4820 INPUT @5;HEATING$
4830 IF LEFT$(HEATING$,1)<>"S" THEN *GPIBERROR
4840 MID$(HEATING$,13,1)="D"
4850 HEATINGINTERVAL=VAL(MID$(HEATING$,3,14))
4860 IDENT$="E"
4870 HEATINGINTERVAL=1000#*CINT((INTERVALOFHEATING-HEATINGINTERVAL)/1000#)+HEATINGINT
ERVAL
4880 RETURN
4890 *COUNTERERROR
4900 THEATOFF$=TIME$
4910 PRINT @4;"DI,00G"
4920 HON=VAL(LEFT$(THEATON$,2))
4930 HOF=VAL(LEFT$(THEATOFF$,2))
```

```
4940 IF HOF<HON THEN HOF=HOF+24#
4950 MON=VAL(MID$(THEATON$,4,2))
4960 MOF=VAL(MID$(THEATOFF$,4,2))
4970 SON=VAL(RIGHT$(THEATON$,2))
4980 SOF=VAL(RIGHT$(THEATOFF$,2))
4990 HEATINGINTERVAL=3600#*(HOF-HON)+60#*(MOF-MON)+SOF-SON
5000 IDENT$="CE"
5010 RETURN
5020 *DATAFILE
5030 NDATAFILE=NDATAFILE+1
5040 NMO11=NDATAFILE MOD 11
5050 IF NMO11=1 THEN LSET ND$=MKI$(NUMBEROFDATA)
5060 IF IDENT$="E" THEN LSET DAT$(NMO11)=IDENT$+"      "+MKD$(HEATINGINTERVAL)+MKD$(D
E):GOTO 5110
5070 IF IDENT$="CE" THEN LSET DAT$(NMO11)=IDENT$+"RROR "+MKD$(HEATINGINTERVAL)+MKD$(D
E):GOTO 5110
5080 IF IDENT$="T" THEN LSET DAT$(NMO11)=IDENT$+LEFT$(DATATIME$,2)+MID$(DATATIME$,4,2
)+RIGHT$(DATATIME$,2)+MKD$(R)+MKD$(T)
5090 IF IDENT$="D" THEN LSET DAT$(NMO11)=IDENT$+LEFT$(TE$(1),2)+MID$(TE$(1),4,2)+RIGH
T$(TE$(1),2)+MKD$(E(1))+MKD$(E(0))
5100 IF NMO11<>0 THEN RETURN
5110 PUT #2,LOF(2)+1
5120 RETURN
5130 *CPDATAFILE
5140 IF IENDING=1 THEN 5240
5150 NMO5=(NUMBEROFDATA-1) MOD 5
5160 IF NMO5=1 THEN 5180 ELSE IF NUMBERINSERIES<>2 THEN 5180
5170 GET #1,LOF(1)
5180 LSET CDAT$(NMO5)=MKI$(NUMBEROFSERIES)+MKI$(NUMBEROFDATA-1)+MKS$(CP)+MKD$(TI)+MKS
$(AI*2!)+MKD$(TF)+MKS$(AF*2!)+MKD$(HEATINGINTERVAL)+MKD$(DE)
5190 IF NMO5=0 THEN 5240
5200 FOR ICP=NMO5+1 TO 5
5210 LSET CDAT$(ICP MOD 5)=MKI$(0)+MKI$(0)+"
          "
5220 NEXT ICP
5230 RETURN
5240 NFCP=FIX((NUMBEROFDATA-2)/5)+2
5250 PUT #1,NFCP
5260 RETURN
5270 *EQUILIBRATION
5280 SN=0#
5290 SNN=0#
5300 SNT=0#
5310 STT=0#
5320 ST=0#
5330 NTIMEO=NTIME-NLS
5340 FOR IIS=NTIMEMIN-NLS+1 TO NTIMEMIN
5350 ST=ST+TEMP(IIS)
5360 SNT=SNT+TEMP(IIS)*(IIS+NTIME-NTIMEMIN)
5370 STT=STT+TEMP(IIS)^2
5380 NEXT IIS
5390 SN=(NTIME*(NTIME+1#)-NTIMEO*(NTIMEO+1#))*.5#
5400 SNN=(NTIME*(NTIME+1#)*(2#*NTIME+1#)-NTIMEO*(NTIMEO+1#)*(2#*NTIMEO+1#))*.16666666
66666667#
5410 SXX=SNN-SN^2/NLS
5420 AMEANN=(NTIME+NTIMEO+1#)*.5#
5430 AMEANT=ST/NLS
5440 SXY=SNT-NLS*AMEANN*AMEANT
5450 AF=SXY/SXX
5460 BF=AMEANT-AF*AMEANN
5470 TF=AF*(6#-HEATINGINTERVAL)/60#+BF
5480 LOCATE 0,1:PRINT USING "Drift = #.##^^^^ K/min";2*AF
5490 RETURN
5500 *ENDING
5510 SRQ OFF
5520 PRINT @4;"H"
5530 PRINT @4;"DI,02G"
5540 IF NDATAFILE MOD 11=0 THEN 5580
5550 NDATAFILE=-1
5560 IDENT$=" "
5570 GOSUB *DATAFILE
5580 IF (NUMBEROFDATA-1) MOD 5=0 THEN 5610
5590 IENDING=1
5600 GOSUB *CPDATAFILE
5610 CLOSE
5620 KEY OFF:TIME$ OFF
```

```
5630 END
5640 *EQUILIBRIUM
5650 IEQUILIBRATION=1
5660 RETURN
5670 *RESTART
5680 NUMBEROFDATA=NUMBEROFDATA-1
5690 NUMBERINSERIES=NUMBERINSERIES-1
5700 IRES=1
5710 RETURN
5720 *NLSCHANGE
5730 INPUT "fitting interval / min for Least Square     ";ALS
5740 NLS=FIX(ALS*2)
5750 IF NLS>NTIMEMIN THEN NLS=NTIMEMIN
5760 RETURN
5770 *NTIMEMAXCHANGE
5780 LPRINT
5790 INPUT "Maximum time / min for temperature measurement ";AMAX
5800 LPRINT USING "Maximum time for temperature measurement     ## min";AMAX
5810 NTIMEMAX=FIX(AMAX*2)
5820 RETURN
5830 *INTERVALOFHEATINGCHANGE
5840 INPUT "Heating interval / min    ";AHI
5850 INTERVALOFHEATING=FIX(60*AHI)
5860 RETURN
```